Author:
Cramphorn, Luke P

Title:
A Touchy Subject

Development and Exploration of Tactile Sensing for Perception and Manipulation

A Touchy Subject

Development and Exploration of Tactile Sensing for Perception and Manipulation

By

LUKE PAUL CRAMPHORN

Department of Engineering Mathematics
UNIVERSITY OF BRISTOL

A dissertation submitted to the University of Bristol in accordance with the requirements of the degree of DOCTOR OF PHILOSOPHY in the Faculty of Engineering.

JANUARY 2019

Abstract

Demand for robotic solutions to problems in every area of society has been rapidly increasing. Some notable examples include providing independence and care to the elderly, managing degrading farm land, and reducing the risk to human life with agile robots for search and rescue. Many of these areas will require robots to either work alongside humans, or in environments that are unstructured. For these an artificial sense of touch will be crucial.

Tactile sensing is a young field of research when compared to other sensing fields like computer vision. But just like computer vision, tactile sensing will open up important doors for robotics systems. Tactile provides an active sense for robots, allowing contact level perception on its influence on the world. It is this sensing and understanding of environmental influence that can be utilised for manipulation.

This thesis presents novel developments in tactile sensing hardware, perception, and deployment. The work demonstrates the development of the TacTip tactile sensor to be better suited to rapid prototyping and complex morphologies. This is achieved by redeveloping the TacTip technology to be bot modular and 3D printable in a multi-material printer. Ultimately this allowed the for exploration the effects of biomimetic fingerprints on tactile perception of varies spatial scales. Demonstrating improvements in acuity of location perception with its inclusion.

An investigation into using active perception algorithms for active manipulation is explored. Where the principle that existing algorithms that provide control for perception can be used such that perception for control is achieved. The work demonstrated the successful rolling of a cylinder on a table top using only tactile sensing, and highlights that the methods have a trade off between accuracy and reaction time.

To improve the generality of the TacTip sensors tactile sensing, I present the development of a novel method for inferring a third dimension to the sensor data. This method deploys the mathematical principle of voronoi tessellation to the point data outputted from the sensor. This tessellation creates cells around each point, the areas of which can be interpolated to crate a 3D surface representation of the data. Ultimately, along with exploration of the raw point data, tactile features such as shear, pressure, and contact locations could be inferred with out the use of data intensive machine learning techniques.

Lastly, this thesis present a fully tactile seven degree of freedom hand, fully equipped with the new TacTip developments and generalised feature inference. The hand was designed to be highly tactile, dexterous and relatively inexpensive tool. The hand is benchmarked on the YCB objectset with a closed loop adaptive grasp controller which demonstrates its viability for starting to explore tactile dexterous manipulation.

Overall this thesis demonstrates developments in tactile sensing with accurate location perception, feature perception, simple manipulations, and grasp adaptation. All of these are components necessary for reaching the ultimate goal and bigger challenge of complex dexterous tactile manipulation.

Dedication and acknowledgements

It is difficult to express my gratitude towards everyone who has assisted me in my doctoral journey in a little block of text. The experience has been the most interesting and challenging of my life so far. During which I have had the luxury of dabbling in extremely interesting robotics research with a team of equally interesting and genuinely fantastic individuals.

Firstly, I want to say a massive thank-you to Nathan Lepora for is supervision over the last four years. I believe that everything I have learnt from his guidance will serve me extremely well in carving out the rest of my future. Working with the tactile robotics team has always created opportunities, solutions, and discussions that have made the Bristol Robotics Lab (BRL) an exhilarating place to work. In particular, I want to thank Benjamin Ward-Cherrier, Nicolas Pestell, Jasper James, John Lloyd, and Kirsty Aquilina for their insight, assistance, grounding, and laughs throughout the recent years.

I am massively grateful to my cousin, Biddy, who gave up her bank holiday to proof read this document on short notice.

It goes without saying that the research presented here has benefited from the expertise of BRLs fantastic technicians, with particular thanks to Gareth Griffiths and Andrew Stinchcombe for their assistance and hard work.

It will come to no surprise to anyone who has either been through a PhD themselves, or is close to someone who has, when I say that the challenges it poses extended well beyond the academic and into the emotional. With many points of the process (not least the writing of this thesis) weighing heavily on my mental health. Thus, the completion of this doctorate couldn't have been achieved without the emotional support of my loving family and friends.

So I want to say a last couple of thanks to my parents and my sister, Leila, for always being on the other end of the phone, supporting me and believing in me. To my magical friends Ben, Tom, and Chanelle for keeping the laughs coming and stopping me tapping out when I've drawn a bad hand. And to my amazing partner, Charlie, for being unwavering in her support and belief of me through the last, and most critical year of this process.

AUTHOR'S DECLARATION

I declare that the work in this dissertation was carried out in accordance with the requirements of the University's Regulations and Code of Practice for Research Degree Programmes and that it has not been submitted for any other academic award. Except where indicated by specific reference in the text, the work is the candidate's own work. Work done in collaboration with, or with the assistance of, others, is indicated as such. Any views expressed in the dissertation are those of the author.

SIGNED: ..... DATE: .....

TABLE OF CONTENTS

List of Tables

Table **Page**

List of Figures

CHAPTER 1

INTRODUCTION

This thesis will present the findings of the author's doctoral studies. The focus of the studies was on developing and exploring tactile sensing for the purposes of perception and ultimately manipulation. During this time aspects of tactile sensing were researched, such as: biomimetic and morphological hardware for enhanced perceptual accuracy; active perception of a stimulus to perform rolling; algorithms for inferring tactile features; and the design, construction, and programming of a tactile hand to further explore the field.

This chapter will outline the research aims and questions that each chapter and the thesis will address. It will also present the motivations behind the topic and the author's scientific contributions and publications. The chapter closes with a short summary of the document's structure.

1.1 Research Aims and Questions

This thesis sets out to address an overall research aim...

'To develop hardware and methods for the purpose of improving understanding, and conducting exploration, of tactile perception and tactile manipulation.'

Which the author addresses by proposing four research questions that cover and connect the research areas of tactile sensing, manipulation, and biomimetics.

- **Question 1:** 'Can developments and improvements in the TacTip hardware lead to gains in its tactile sensing capabilities and new directions in which the sensor can be utilised?'

- **Question 2:** 'Can tactile sensing be used to provide the necessary information and feedback for performing basic manipulation of an object based solely on the state of contact?'
- **Question 3:** 'What key features can be identified from tactile data without training black-box methods like classifiers or regressors and will this enable greater versatility and generality of tactile sensing?'
- **Question 4:** 'Can the integration of tactile sensing into multifingered system provide data to improve dexterous capabilities?'

1.2 Motivation

Something about humans that really awes me, is our impact on geological records, with millennia worth of tools, constructs, and dramatic changes to the landscape all left by our ancestors. This is so much the case that the present geological epoch, the Holocene (-11,650 calendar years - present) is predominately defined by our impact and influence. No single species in the history of Earth has had such influence over our planet; for better or for worse.

Being this influential over our world cannot be put down to any one physical attribute. But the role our hands have played is by no means a supporting one. They are our main gateway between observing the world and interacting with it. Allowing us to turn the elements around us into tools for building homes, cities, and monuments that have stood for thousands of years.

As our hands are clearly a powerful and fundamental tool in our species progression, it is a logical step to assume that hands can have revolutionary influence on the progression of robotics. It is this potential for elevating some areas of robotics from science fiction to science fact, that is at the core of the motivation behind the work in this thesis. There is one aspect of hands that I believe can have a particular impact on robotics and that is the capabilities of tactile sensing.

The sense of touch is highly developed in humans and provides large quantities of crucial data that supplement our dexterous capabilities. In addition to providing the same for robotics [1], it could also play an important role in human-robot interaction and assisted living [25, 26]. As a relatively immature area of sensing, compared to vision and audition, tactile sensing has a lot of variety in both sensor technologies and interpretive algorithms. This variety comes as a result to the fact that there is no particular technology that can provide the quality and variety of features in one package as the human finger tip dose [8]. As the need for operating robots in unstructured environments increases so dose the need for a tactile sensor that can cover a wider portion of the desirables features for tactile sensing. To this end, it is clear that the continued development of tactile sensing hardware and software towards a more capable sensing tool will benefit the future of robotics.

The outputs of tactile sensing are both the interaction between sensor and environment, and the feedback for control to move and gain further information. In short this modality of sensing

is *'active'* [27]. It is this active nature of tactile sensing that makes it crucial that the a hand exist that incorporates the sensing into its dexterous capabilities.

Due to the clear role hands play in interacting with the environment, its no surprise that there is a host of designs for robotic hands commercially and in scientific literature. However these hands tend to fall into two categories. The first category are the Human inspired anthropomorphic hands which boast high degrees of dexterity, but in-turn makes the hand equally challenging to control. The second category is made up of simple non-anthropomorphic hands that use under-actuation to adaptivity and robustly grasp, although they mostly lack the dexterity for more complex interactions. It is also the case that many of these hands have limited to no coverage of tactile sensing. This leaves a gap in research for a moderately dexterous hand with high tactile sensor coverage that could provide a platform for exploring robotic tactile manipulation.

Over all tactile sensing and manipulation are challenging areas of robotics which have inspired great interest from the scientific communities due to the potential benefits value to many areas of robotics. The motivation is also true for the work in this thesis, and with continued research into the field we could one day soon find the key for robots to interact with the world as dynamically as we do.

1.3 Contributions

In the pursuit of this thesis's research aim a number of novel contributions to the fields of tactile and manipulation can be claimed. Each of these are discussed in full detail in this thesis, and briefly summarised here.

- Developments of the TacTip tactile sensor, including multi-material 3D printing and improved modularity, to increase the speed at which the sensor can be modified, expanded, and explored (Chapter 3).
- Demonstration that the inclusion of a biomimetic fingerprint to the TacTip improves tactile spatial perception (Chapter 3).
- Presentation of a rolling manipulation primitive, set to follow a goal trajectory, by using Bayesian perception for control (Chapter 4).
- Expansion of the rolling manipulation primitive to a more complicated platform in the form of a tactile integrated GRAB Lab Model M2 (Chapter 4).
- Introduction of a novel method for inferring tactile features directly from TacTip data by generating a third data dimension through Voronoi tessellation (Chapter 5).
- Demonstrated re-orientation of integrated tactile sensors, with a shadow moulder grasper, to optimise centre of pressure and contact area (Chapter 6).

- Designed and programmed a 3D printed, seven degree of freedom, robotic hand equipped with six TacTip sensors and demonstrated its grasping and sensing capabilities (Chapter 6).

1.4 Publications

First Authored

- L. Cramphorn, B. Ward-Cherrier, and N. F. Lepora, "Tactile manipulation with biomimetic active touch," in *Proceedings - IEEE International Conference on Robotics and Automation*, vol. 2016-June, pp. 123–129, IEEE, may 2016

- L. Cramphorn, B. Ward-Cherrier, and N. F. Lepora, "Addition of a Biomimetic Fingerprint on an Artificial Fingertip Enhances Tactile Spatial Acuity," *IEEE Robotics and Automation Letters*, vol. 2, no. 3, pp. 1336–1343, 2017

- L. Cramphorn, B. Ward-Cherrier, and N. F. Lepora, "A Biomimetic Fingerprint Improves Spatial Tactile Perception," pp. 418–423, Springer, Cham, 2016

- L. Cramphorn, J. Lloyd, and N. F. Lepora, "Voronoi Features for Tactile Sensing: Direct Inference of Pressure, Shear, and Contact Locations," in *IEEE International Conference on Intelligent Robots and Systems*, pp. 2752–2757, IEEE, may 2018

- L. Cramphorn, J. James, N. Pestell, A. Church, and N. F. Lepora, "The Tac-Manipulator: A tactile robotic hand with the tools for manipulation at its fingertips," *Not Submitted*, 2019

Co-Authored

- B. Ward-Cherrier, L. Cramphorn, and N. F. Lepora, "Tactile Manipulation With a TacThumb Integrated on the Open-Hand M2 Gripper," *IEEE Robotics and Automation Letters*, vol. 1, no. 1, pp. 169–175, 2016

- B. Ward-Cherrier, L. Cramphorn, and N. F. Lepora, "Exploiting symmetry to generalize biomimetic touch," in *Lecture Notes in Computer Science (including subseries Lecture Notes in Artificial Intelligence and Lecture Notes in Bioinformatics)*, vol. 9793, pp. 540–544, 2016

- N. Pestell, B. Ward-Cherrier, L. Cramphorn, and N. F. Lepora, "Tactile exploration by contour following using a biomimetic fingertip," in *Lecture Notes in Computer Science (including subseries Lecture Notes in Artificial Intelligence and Lecture Notes in Bioinformatics)*, vol. 9793, pp. 485–489, 2016

- N. F. Lepora, K. Aquilina, and L. Cramphorn, "Exploratory Tactile Servoing With Active Touch," *IEEE Robotics and Automation Letters*, vol. 2, no. 2, pp. 1156–1163, 2017

- B. Ward-Cherrier, L. Cramphorn, and N. F. Lepora, "Exploiting Sensor Symmetry for Generalized Tactile Perception in Biomimetic Touch," *IEEE Robotics and Automation Letters*, vol. 2, no. 2, pp. 1218–1225, 2017

- B. Ward-Cherrier, N. Pestell, L. Cramphorn, B. Winstone, M. E. Giannaccini, J. Rossiter, and N. F. Lepora, "The TacTip Family: Soft Optical Tactile Sensors with 3D-Printed Biomimetic Morphologies," *Soft Robotics*, p. soro.2017.0052, 2018

- N. F. Lepora, K. Aquilina, and L. Cramphorn, "Exploratory Tactile Servoing With Active Touch," *IEEE Robotics and Automation Letters*, vol. 2, no. 2, pp. 1156–1163, 2017

- N. Lepora, M. Pearson, and L. Cramphorn, "TacWhiskers: Biomimetic optical tactile whiskered robots," *IEEE International Conference on Intelligent Robots and Systems (IROS)*, 2018

- N. F. Lepora, N. Burnus, Y. Tao, and L. Cramphorn, "Active Touch with a Biomimetic 3D-Printed Whiskered Robot," in *Conference on Biomimetic and Biohybrid Systems*, pp. 263–275, Springer, Cham, 2018

- N. Pestell, L. Cramphorn, F. Papadopoulos, and N. F. Lepora, "A Sense of Touch for the Shadow Modular Grasper," *IEEE Robotics and Automation Letters*, vol. 4, pp. 2220–2226, apr 2019

1.5 Thesis Structure

This thesis is formatted as a compilation of the author's work published (and submitted) during the period of doctoral studies, with each publication being presented as the main material in Chapters three through six. This is summarised below:

- **Chapter 2** presents a literature search on the background and existing research relevant to addressing the thesis research goal and subsequent questions. The main topics covered in this review are biomimetics, tactile sensing, and robotic hands and dexterous manipulation.

- **Chapter 3** will describe the TacTip Tactile sensor and present the changes and improvements made to the sensor for improved development speed. Additionally the chapter will discuss how these changes allowed for the exploration of adding a biomimetic fingerprint to the sensor along with the outcomes of this.

- **Chapter 4** contains the work on an initial venture into robotic tactile manipulation. Presenting a method for performing a rolling manipulation primitive along a desired trajectory by utilising Bayesian perception for control. The chapter will also discuss some continuation of this method onto the more complex platform of a robotic gripper.

- **Chapter 5** provides an introduction to a novel method for inferring tactile features directly from optical tactile data by devising a third dimension via Voronoi tessellation.
- **Chapter 6** presents research into TacTip integrated robotic hands. Showing a method for orientating the sensors on the digits to be flat against an object and presenting a new design of 3D printed robotic hand with increased degrees of freedom, and a full set of tactile sensors, aimed at being a platform for further exploration of tactile manipulation.
- **Chapter 7** summarises and discusses the findings and contributions of the thesis. It also presents the main conclusion and thoughts for future work.

CHAPTER 2

LITERATURE REVIEW

Robotics is a vast research field, covering a massive range of disciplines and skills such as: computer science, psychology, physics, mathematics, biology, medicine, chemistry, and various engineering disciplines. This breadth of knowledge and expertise has created robotics systems that comfort the elderly with dementia [42], explore the unknowns of the Arctic ocean that is permanently covered in ice [43], and humanoid robots doing back-flips (because why not) [44]. As interesting and exciting as the field of robotics is, it is necessary, for the purpose of this thesis, to focus on one region. The region of interest here will be that of tactile robotics and manipulation, with interest in a biomimetic methodology and a goal of tactile dexterous manipulation.

In this chapter I present a review of relevant literature to the proposed thesis research aim. The chapter will be structured via outlining the scope of the search, details on the findings of the search, and a summary of the literature review.

2.1 Scope

This review is the presented findings of a literature search within the scope of three fields, focusing on research that overlaps these fields. The chosen fields have been selected so as to cover a sufficient portion of existing literature related to the thesis aim and research questions. These fields are: Biomimetics, Tactile Sensing, Robotic Hands and Dexterous Manipulation.

2.2 Biomimetics

The principle of imitating elements or systems within nature for the purpose of solving complex human problems: The term '***biomimetic***' was coined by Otto Schmitt in the 1950s, while attempt-

ing to develop a physical device that mimicked the electrical action of nerves [45, 46]. Although relatively young as a specific research field, the concept of taking inspiration from nature is potentially 3,000 or more years old. This is unsurprising when you consider that life has had at least 3.5 billion years of natural selection and evolution to solve complex chemical, engineering, and computational problems. The result of this time is a natural encyclopaedia of solutions to many human problems that we have yet to solve, or could have a better solution for [47]. A few examples of nature's solutions that surpass current engineering are: muscles which are compliant, light, and powerful; self reproduction, allowing the conversion of resources into more of itself; and self repair, where limited damage is reversed for continued existence.

One requirement on life is that it must be able to perform automated and complex tasks in unstructured, dynamic, and hazardous environments. This statement can also be applied to many of the goals for the future of robotic systems. To this end the method and principles of biomimetics have great value in the development of more advanced and versatile robots. This is reflected in the recently gained popularity of the term 'biomimetic', with an almost exponential increase in the use of it in academic publications in recent years [48]. Existing work implementing aspects and inspirations of nature's solutions to engineering problems has resulted in a variety of robotic systems that demonstrate improvements in task performance and provide better understanding of the biological systems. For example insect size flying robots [14, 49], soft robots with multiple gaits [50], bipedal humanoid robots [15, 51], robotic hands [52], swarming systems [53], whiskered robots [13], and neural networks inspired by the functions of the human brain [54] (see Figure 2.1).

The biomimetic principle and many of the systems that implement them, has resulted in the consideration of embodied intelligence [55] and morphological computation [56, 57], where focus is placed on the interactions between body and environment. The way the body facilitates computation of control and sensing can reduce energy consumption and improve the intelligent behaviours of the system [58].

The two other areas of robotics that will be discussed in this literature review are tactile and manipulation, both of which have, and will continue to, benefit from the use of biomimetic principles. This is because the best known tactile sensors, dexterous hands, and respective

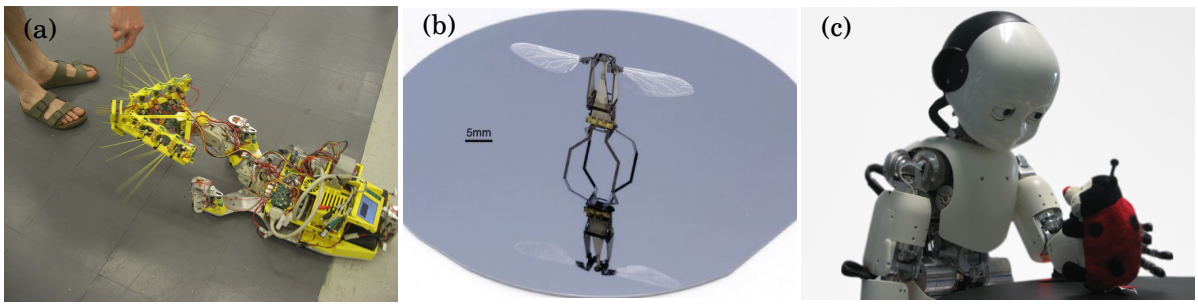

Figure 2.1: (a) ScrarchBot whiskered robot [13] *Source: Bristol Robotics Laboratory*; (b) RoboBee [14] *Source:[14]*; (c) iCub humanoid robot [15] *Source: icub.org*.

controllers are the human sensory network, hands, and brain, respectively. Thus this review will also discuss and consider the human parallels to these robotic fields.

2.3 Tactile Sensing

2.3.1 Human Touch

We as a species have managed to not only survive in every corner of Earth, but change the landscape to accommodate our needs. One of the main enablers of our successes is our ability to build and wield tools. This ability is made possible by a combination of evolutionary traits, such as opposable thumbs, dexterous hands, a sophisticated brain, and a versatile sense of touch. The human sense of touch is part of a complex network of sensory neurons and pathways that respond to changes at the surface or inside the body. This system, known as the somatosensory system, perceives external stimuli through a large number of receptors; mechanoreceptors for mechanical stimuli like pressure and vibration, thermoreceptors for temperature, and nocioceptors that detect and transmit pain and damage [59]. The distribution of this network is not even, with areas of high density located in highly tactile regions of the body, such as the tongue, lips, and hands. This distribution is often represented by a sensory cortical homunculus, where the human body is displayed proportioned to this system (Figure 2.2)[60].

The skin on the hands is known as glabrous skin, characterised by its smoothness and absence of hair. Glabrous skin is of interest in tactile sensing due to the high concentration of somatosensory cells that it contains, and by extension, its role in human tactile exploration,

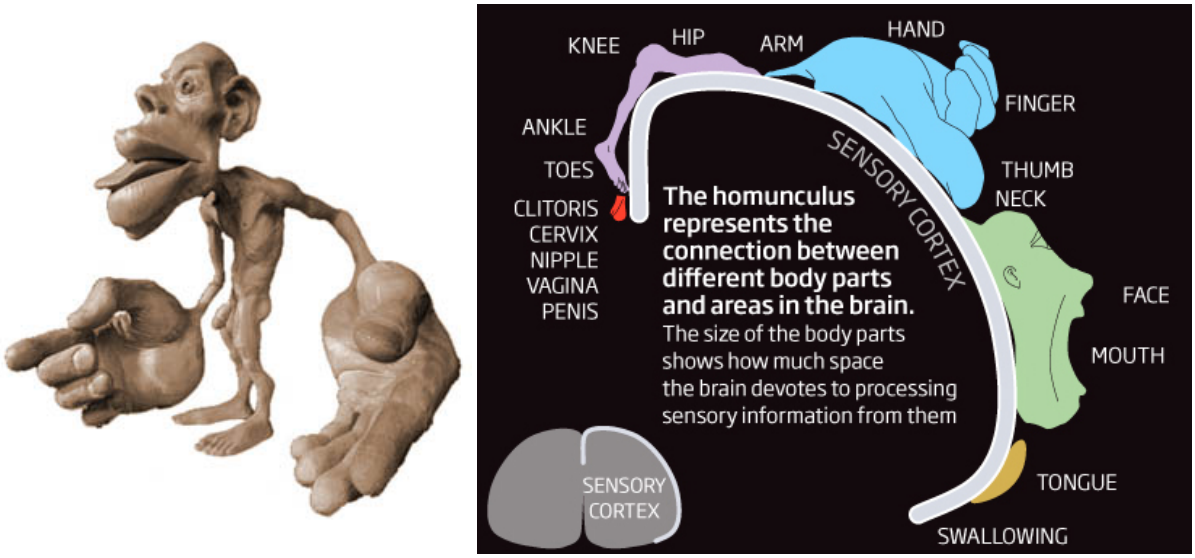

Figure 2.2: Sensory Cortical Homunculus: Showing a human proportioned to match the dedication of regions of the cortex to the somatosensory system. *LEFT: 3D homunculus (Source - University of Calgary [16]) RIGHT: 2D homunculus mapped to cortex (Source - new scientist [17])*

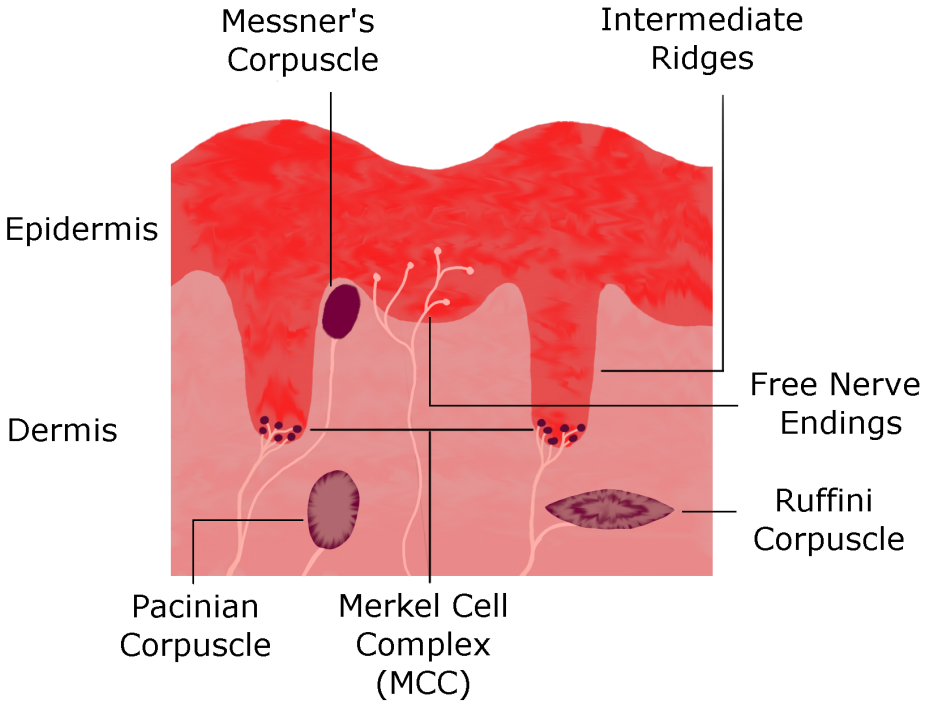

Figure 2.3: Diagram showing a cross sectional representation of human glabrous skin.

grasping, and dexterous manipulation. There are four primary mechanoreceptors in glabrous skin responsible for tactile sensing each with varied spiking frequency, spatial acuity, adaptation rate, location in the skin, and overall function. These primary receptors are Merkal Cells (SA-I), Meissner's Corpuscle (FA-I), Ruffini Corpuscle (SA-II), and Pacinian Corpuscles (FA-II); where SA is slow adapting and FA is fast adapting (Figure 2.3). In addition to the primary mechanoreceptors, there are free nerve endings known as tactile C fibres, responsible for sensual touch [61], although mostly located in hairy skin so will not be discussed further here.

The adaptation rate of a mechanoreceptor determines the duration of time before it stops responding to a present stimulus and influences the function of the receptor cells. FA receptors react to the onset and offset of a stimulus, adjusting to its presence quickly and not producing a signal until a change occurs. In contrast, SA receptors do not adjust to the presence of a stimulus quickly and continually send sensory signals throughout the duration of the stimulus. This means that FA type mechanoreceptors respond to temporal changes in skin deformation such as vibrations and the onset and offset of contact for grasp control. Whereas SA type receptors respond to sustained pressures and spatial deformations useful for grasp stability and shape perception.

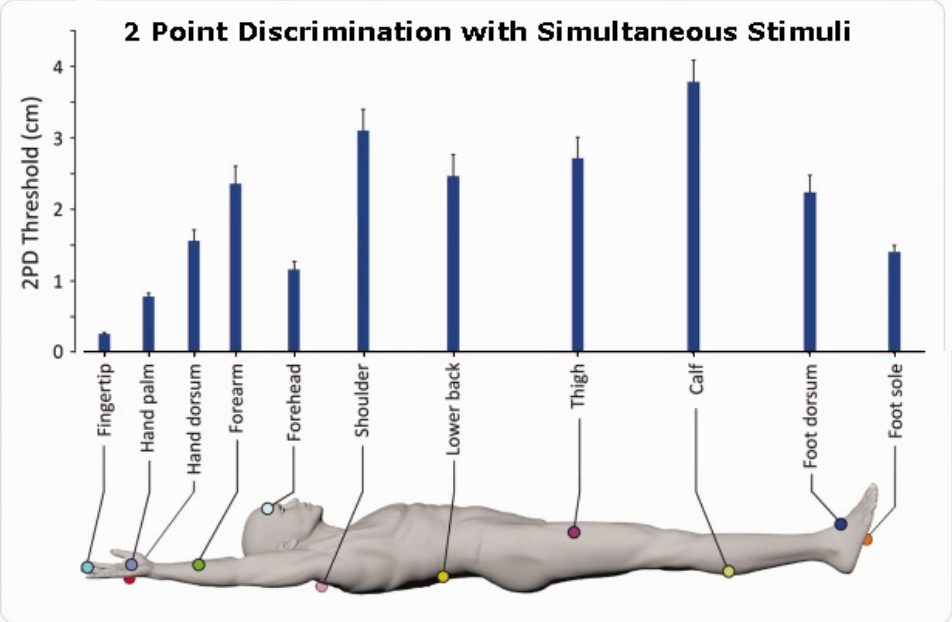

Figure 2.4: Figure showing values for tactile two point discrimination with simultaneous stimuli in different region across the human body. *This diagram was sourced from [18] and modified to only show the information on tactile.*

Spatial acuity is a parameter that denotes the minimum space between two stimuli required for them to be distinctly resolved. This acuity has been studied in humans via techniques like two point discrimination [62] and grating orientation [63]. These studies have both scientific and medical benefits, for example producing expected values for healthy humans that can be used to identify medical conditions that could deteriorate spatial acuity, such as damage to the somatosensory neural pathways [64]. These studies have demonstrated a difference in spatial acuity across the body that fits with the distributions of the somatosensory system demonstrated in the sensory cortical homunculus. Acuity is reported to average 0.51 mm at the lips, 0.58 mm at the tongue, and 0.94 mm at the fingers, these being the most sensitive regions (Grating) [64], and drops to as low as 25 mm for the lower back and 37 mm for the calf (two point discrimination) [18] (Figure 2.4).

The properties of the mechanoreceptors alone do not completely determine their functionality; the location of the receptors and the surrounding tissue morphology also influences sensing. For example the positioning of the SA-I receptors within the tip of the intermediate ridges (protrusions of the epidermis into the dermis within the human fingertip) has been shown, via finite element modelling, to focus the stress of contact and increase the signal over background noise to allow finer edge detection [65]. There is a physical connection between these intermediate ridges and our fingerprints (Papillary ridges) and since it has suggested that fingerprints link to slip detection [66, 67] and texture perception[68] then it can be extended that the location of SA-I receptors are also linked to these functions. Each of the four types of mechanoreceptors function

Table 2.1: Table of glaborous skin mechanorecptors and some associated calssification data. In the 'Type' filed the following abbreviations are used; SA - slow adapting, FA - fast adapting. The material in this table was initially presented in the review paper 'Tactile Sensing-From Humans to Humanoids' by Ravinder S. Dahiya *et al.* [1] with reffrences to [2–7]

Classification Basis	**Merkal Cells**	**Meissner's Corpuscle**	**Ruffini Corpuscle**	**Pacinian Corpuscle**
Type	SA-I	FA-I	SA-II	FA-II
Spatial Acuity (mm)	0.5+	2	7+	10+
Stimuli Frequency (Hz)	0.4-3	3-40	100-500+	40-500+
Effective Stimuli	Spatial deformation; Sustained pressure; Curvature, edge, corners	Temporal changes in skin deformation	Sustained downward pressure; Lateral skin stretch; Skin slip. 0	Temporal changes in skin deformation
Sensory Function	Pattern/form detection; Texture perception; Tactile Flow perception	Low frequency vibrations and Motion detection; Grip control; Tactile flow perception.	Finger position; stable grasp; Tangential force; Motion direction.	High frequency vibration detection; Tool use

due to a different combination of these parameters, Table 2.1 shows these in detail [1, 6].

The versatility and sensitivity of human touch, in addition to what we can do with it, make it the perfect benchmark for artificial tactile sensing. Achieving human level touch artificially, either through biomimetic approach or by other means, is a technically challenging goal but could yield many benefits for robotics as a field.

2.3.2 Artificial Tactile Sensors

Design, fabrication, and technology of tactile sensors is in many ways an open problem, with no one artificial tactile sensor providing an ultimate solution. Here we will discuss a selection of commonly developed and used tactile sensor types.

There are some key design considerations for tactile sensors that are important to consider here: high spatial resolution, high sensitivity, high frequency response, low hysteresis, efficient and numerically low cabling connections, and high surface friction. These were outlined by Kappassov *et al.* within their publication that provides a comprehensive review of artificial tactile sensing [8].

Piezoresistive The piezoresistive effect is where the resistive property of a material changes when mechanically deformed [69]. By measuring this change in resistance, it is possible to measure the deformation of the material. This is useful in tactile sensing as the amount of deformation is a key element of the perception. Technologies for piezoresistive sensors include: pressure sensitive conductive rubber, piezoresistive fabric, force sensing resistors, and piezoresistive foam.

Sensors of this type are relatively easy to manufacture, can be produced to be low profile and flexible [70], and have many commercially available options (e.g. Flexiforce, Tekscan, Weiss Robotics, ATi industrial automation). This technology does however suffer with many traits that are not ideal for tactile sensing. This is due to properties of the conductive rubber used in these sensors, which exhibit non-linear force/resistive characteristics. The elastic properties also introduce a high level of hysteresis, that may even impact sensitivity after prolonged use due to permanent changes in the material's relaxed state. In addition to these issues the sensor technology output is vulnerable to changes in thickness from wear and tear as it influences the resistive output, and variations in temperature and moistness could also modify the sensor output. Although having many negative traits, the sensor's ease of production, access, and integration have made it a popular choice for use on robot hands.

Capacitive As with piezoresistive sensors, capacitive sensors exhibit a change in output when deformed. In this case the 'capacitance' between two conductive plates sandwiching a compressible dielectric material. Additional embedded capacitors allow for shear sensing [71] and overlapping row and column electrodes isolated by the dialectic can be used for form pressure arrays [72]. This technology has been adapted into a variety of high profile systems such as the Allegro hand [73] and the iCub [74]. Although widely used, it is worth noting that the technology also suffers from hysteresis effects in addition to susceptibility to interference from electromagnetic (EM) noise and temperature changes.

Piezoelectric These sensors utilise the generation of electrical charge by a crystalline material whilst it is being deformed. This is known as the piezoelectric effect and is also exhibited in some human-made ceramics and polymers. One such material is polyvinylidene fluoride or PVDF is the preferred piezoelectric for tactile sensing due to its flexibility, workability, and chemical stability [1, 75].

This technology benefits from a high bandwidth of up to 7 kHz [76]. The sensors only respond to dynamic contact which is considered a disadvantage, although this is much like FA mechanoreceptors in the human fingertip which work in conjunction with other mechanoreceptors to provide useful information. This combination of sensor types, dynamic and static, is presented by Goger *et al.* with a PVDF polymer and piezoresistive foam for a fluidic hand [76, 77]. A major concern of the technology is its sensitivity to temperature.

Barometric Methods for measuring air and liquid pressures have been understood for a long time. The pressure based nature of tactile sensing makes using such an established technology a logical solution. Barometric tactile sensors embed standard digital barometric sensors within various mediums, either a fluid or solid medium. The SynTouch Biotac is a multi-model sensor that uses a liquid medium to detect slip by measuring the pressure created by vibrational waves transmitted through the medium [78, 79]. Another barometric tactile sensor is the TakkTile; this

Table 2.2: Showing advantages and disadvantanges of major tactile sensing archetype. This table was initially presented in the review paper 'Tactile sensing in dexterous robot hands - Review' by Z. Kappassov *et al.* [8]

Type	Advantages	Disadvantages
Piezoresistive	Many commercial solutions exist, simpler for manufacturing, can be flexible.	Non-linear response, temperature and moistness dependence, fatigue, permanent deformation, hysteresis.
Capacitive	A number of commercial solutions, can be flexible, may have higher bandwidth than Piezoresistive.	Susceptibility to electromagnetic noise, sensitivity to temperature, non-linear response, poor hysteresis.
Piezoelectric	Very high bandwidth.	Temperature dependence, dynamic sensing only.
Barometric	High bandwidth, high sensitivity, temperature and moistness independence.	Low spatial resolution.
QTC	Linear response, higher dynamic range (w.r.t. Capacitive and Piezoresistive).	More complex for manufacturing (w.r.t. Capacitive and Piezoresistive).
Optical	High spatial resolution, high sensitivity, repeatability, immunity to electromagnetic noise.	More complex for manufacturing (w.r.t. Capacitive and Piezoresistive). Bulky, high-power consumption, high computational costs.

sensor uses a solid moulded silicone medium to transmit pressure from the compression of the rubber to the sensor [80].

The frequency response of the sensors are dependent on the transmission medium, being high for liquids and low for solids. In addition, these sensors suffer from a poor spatial resolution.

Quantum Tunnelling Effect A technological advancement of the principles used for piezoresistive and capacitive sensors, quantum tunnel composite sensors also change their properties under compression. Here, the sensor material transitions between insulator and conductor when deformed. This is due to metallic particles within the sensor reaching the proximity at which quantum tunnelling can occur without coming into contact [1].

This sensor type boasts a linear force profile in x, y, and z as well as good dynamic range (0 N-22 N) [81]. As these sensors undergo wear and tear the sensitivity decreases, with increase effects over time. The complexity of this sensor type makes it both difficult and expensive to produce.

Optical This class of tactile sensors incorporates a wide range of varying technologies and techniques, but all utilise optical principles to extract the tactile data from the contact surface. These principles include light intensity changes between mediums of different refractive indices, frustrated total internal reflection and direct observation with a charged coupled device (CCD) camera.

Traditional optical tactile sensors utilise the principles of frustrated total internal refraction, where light escapes an optical wave guide due to changes in its refractive indices created by increased pressure of a disrupting elastomer interface [69, 82, 83].

Direct observation methods use a camera to observe the internal state of the sensor. The transduction of information from these observations can be achieved through patterns of dots [84], floating or coloured markers [85], and lines [86]. The GelSight optical tactile sensor [87] and GelSlim [88] utilise a novel photometric stereo algorithm to generate 3D height maps of stimuli interacting with the sensor's reflective elastomer. In extension, markers have been added to the sensor surface to allow for the perception of shear and torque.

Optical tactile sensors benefit from a high spatial resolution and sensitivity relative to other tactile sensor types. It is important to note however, the data output from these sensors can be computationally expensive due to this. Another drawback is the bulky and heavy bodies created by the use of optical technology within these sensors.

2.3.3 Interpreting and Using Tactile Data

As with other sensory fields like vision and hearing, having the hardware and raw output is not enough to perform useful tasks or classifications. The literature contains a variety of computer intelligence and machine learning methods for an equally varied number of tactile tasks and sensor designs [89]. Some examples include: Bayes for texture classification [90]; Decision Trees for Object identification [91]; Support Vector Machine (SVM) for grasp stability and object recognition [92]; Deep Neural Network (DNN) for pose, pressure, and hardness estimation [93, 94]; and Random Forests [95] and K-Nearest Neighbours (KNN) [96] for object classification and feature extraction.

Due to the variety of sensors, methods, and tasks, benchmarking methods or identifying a best method is challenging. To this end it appears that the use of methods seems to be situational. Here we briefly expand upon the Bayesian method, as it is has existing use with the chosen sensor, and deep-learning due to its recent rapid gain in popularity.

Probabilistic These classifiers implement a probabilistic model of the sensor outputs and are a popular choice for supervised machine learning on tactile data. An example of this is the Bayesian methods, due to their relative simplicity yet powerful performance with the appropriate prepossessing. The methods are based on Bayes' theorem, where the probability of an event is based on prior knowledge.

Examples in literature include: tactile exploration (active perception) of different objects for classification [97], texture classification [98] implemented on data from the iCub tactile fingertip to classify object and location simultaneously [27, 99], and to perform shape exploration via contour following [100]

Deep-Learning In the last five years Deep-Learning has become both a buzz word and an extremely powerful tool for classification in vision and other data driven fields. In tactile sensing however, the immensely large datasets used in image classification are much harder, if not impossible, to collect. This aside there are still many cases where Deep-Learning with tactile sensing has been presented [94, 101, 102].

For example Baishya *et al.* utilised a convolutional Deep-Learning network to perform 'real world' texture perception. The network was fed on 24,000 spatio temporal signals (collected with a Grip VersaTek resistive sensor) from a selection of textured cylinders and achieved a classification accuracy of 97.3%, higher than both a Gaussian and SVM classifier that it was compared to [101].

2.4 Robotic Hands and Dexterous Manipulation

Manipulation, put simply, is the action of controlling or moving something. The definition of dexterous manipulation is a little more complicated and open to interpretation, but within this thesis the definitions compiled and outlined by *Ma. R et al.* in the publication *'On Dexterity and Dexterous Manipulation'* [103] will be used. Put simply, dexterity refers to the variety of tasks that the system can complete and also how well it can perform those tasks. Additionally, dexterous manipulation is described as the manipulation of an object by a system of multiple cooperative 'manipulators' (arms, fingers, etc) with a stable start and end grasps configuration, within the systems workspace [104–106].

As with human tactile sensing, our hands and the capability to perform complex and controlled dexterous manipulation with them is both inspirational and desirable from a robotics perspective [107]. The human hand has four fingers, each with three phalanges, that can be folded over a palm and an 'opposable' thumb (two phalanges) that can be brought into an opposing position with each of the fingers. With a total 27 degrees of freedom controlled by a system of intrinsic and extrinsic muscles all directed by an exceedingly powerful brain, the hand is capable of an extremely versatile array of motions and interactions. In addition the hand is covered in highly tactile skin that is both compliant and self repairing.

Unfortunately this complex and powerful natural tool set of muscles, sensors, and control is far more advanced than the current available technologies that echo them. This has created a glass ceiling for roboticist who are trying to achieve any substantial portion of our hands' capabilities. Due to this, it is not clear whether taking a highly biomimetic or anthropomorphic approach to robotic hands is currently the best for exploring the dexterous manipulation problem [105].

This section will explore a variety of simple and complex robotic hands and consider how equipping tactile capabilities helps with manipulation and other functions.

2.4.1 Robotic Hands

There is a vast variety of robotic hands present in literature, here we will categorise a small sample of these devices into grippers, non-anthropomorphic, and anthropomorphic. We will briefly discuss a comparison of these categories. Examples from each of these categories can be seen in Figure 2.5, alongside a human hand.

Robotic hands with two digits range from simple parallel grippers, to more complex designs utilising under-actuated principles [19, 108–110]. This style of hand is simplistic but effective, being able to pick up many objects, and thus is widely used. These hands, which will be referred to as 'grippers' from here, are too simple to provide the required actions to perform most dexterous manipulations, rolling and sliding aside [104].

Hands with more than two fingers provide a substantial increase in dexterity. For the sake of discussion we will separate the hands into two categories. Anthropomorphic refers to human shaped hands with two or more fingers, a palmer region, and an opposable thumb. Non-anthropomorphic devices have three or more fingers in any configuration that is not anthropomorphic.

Actuators and Freedoms For devices as complicated as robotic hands, a distinction between the parameters of degrees of freedom (DoF) and the number of actuators should be made. This is valuable for understanding the complexity, controllability, and dexterity of the system. In robotics, DoF is the parameter that describes the modes of independent motion that can occur and the 'number of actuators' describes how many actuators are used to control the system. If the number of DoF is equal to the number of actuators then we can describe the system as fully actuated; this is a common engineered state for robots as it provides control over all the system's movements.

In robotic hands, however, the principle of under-actuation (DoF > number of actuators) is commonly used. Under-actuated hands use morphologically intelligent designs to move multiple joints with a single actuator. This allows digits to conform around objects to maximise the contact surface area, whilst minimising the number of actuators used [19, 109, 111, 112]. Due to the compact nature of hands and the low power-density of conventional actuators, under-actuation is commonly used in anthropomorphic hands that have high DoFs in small space [23, 113–116]. An extreme form of under-actuation occurs with the use of 'continuum actuation', where the systems lack 'discrete' joints and instead use a flexible material that can bend at any point [117]. These systems are described as having an infinite (∞) DoF due to this property.

Conversely, over-actuation (DoF < number of actuators) is rare in robotic hands for the same reasons that under-actuation is preferred. One example of an over-actuated hand was presented by Williams *et al.* [118]. Here, each of 17 joints was directly controlled by small low power

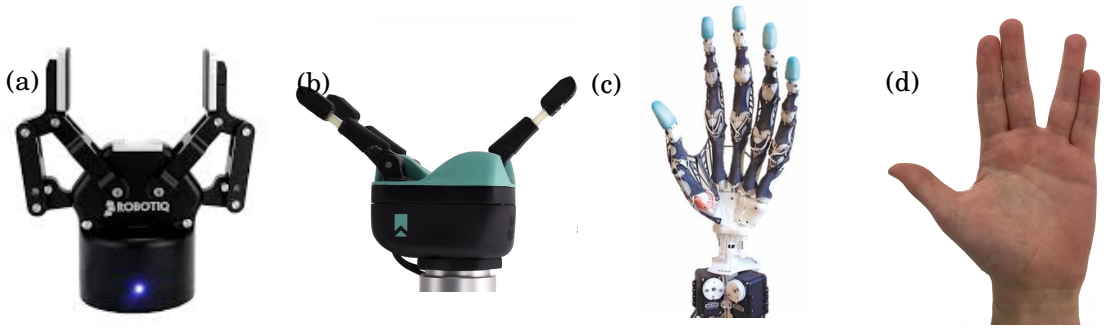

Figure 2.5: (a) Robotiq 2F-85 Gripper [19] *Source:[20]*; (b) RightHand ReFlex Plus Non-Anthropomorphic hand [21] *Source:[22]*; (c) Xu Anthropomorphic Hand [23] *Source:[23]*; (d) Human Hand.

servos embedded within it, with each finger being supplemented by an additional flexing tendon (connected to the distal) that was driven by a liner actuator extrinsic to the hand. This set-up allowed for dexterous control of all of the joints via the motors, and then provided power for grasping from external actuators.

These definitions become more complicated when the actuators are not back drivable, in particular tendon systems can only provide pulling actuation. This means that they can only move a freedom through one of its directions, such as forward, but not backwards. In nature, animals only use muscles and tendons but move through all directions of a freedom by using agonist and antagonist pairs. These pairs can be considered as a single actuator as they are both required to move the freedom completely. One way to address this in tendon driven hands, without adding more actuators, is to use a passive partner to the tendon such as a spring [111].

The human hand is a complicated under-actuated system with 27 DoFs and 34 muscles (these numbers can vary slightly between individuals and sources). Some of these muscles form agonist and antagonist pairs, but many affect multiple joints, and group together with various combinations to provide high degrees of control. A good example of the complexity within the hand is the thumb. It is the most dexterous part of the hand, with five DoFs controlled by eight muscles; three that abduct the thumb, one that flexes the proximal at the metacarpophalangeal (MCP) joint, one that flexes both the proximal at the MCP and distal at the interphalangeal (IP), one that extends the MCP and the thumb at the carpometacarpal (CPC), one that extends everything (IP, MCP, CPC), and lastly one to rotate and flex the metacarpal into opposition.

Anthropomorphic Taking a biomimetic approach from the most dexterous hands in nature, anthropomorphic hands resemble and mimic the look and functionality of human hands, having multiple parallel fingers that close on to a palm, and a thumb that can be brought into opposition with each or some of the fingers. Many of these hands utilise the full four fingers one thumb configuration [23, 113, 114], with varying degrees of actuation and freedoms.

Table 2.3: Robotic hands exist in abundance, rangeing in many forms, degrees of freedom (DoF), comercial avilibilites, and dexterities. This table presents a a small selection of some of these hands. Details such as the number of digits, actuators, and DoFs are documented and additional infomation on grip strength is also presented where available. *(Hands noted (*) are commercial products).* ****The human hand is a natural system subject to variations in all values represented here. Age, gender, fitness, genetic variations, and data source are but a few reasons for any variations in these values.** *Hands with '∞' DoF are constructed using principles of continuum actuation.*

Type	Hand	Digits	Actuators	DoF	Pinch Force (N)	Payload (Kg)	Ref
Gripper	GRAB Lab Model T42	2	2	4	9-14	-	[110]
	Robotis Hand*	2	1	2	170	5	[109]
	Robotiq 2F-85*	2	1	2	20-235	5	[19]
	GR-2	2	2	2	-	-	[108]
Non-Anthropomorphic	GRAB Lab Model T	4	1	8	-	-	[119]
	Shadow Modular Grasper* (3 finger configuration)	3	9	9	10	2	[35, 120]
	Barrett Hand*	3	5	8	15-20	6	[121]
	Robotiq 3-Finger Adaptive Robot Gripper*	3	4	11	30-70	10	[19]
	Kinova KG-3*	3	3	6	40	-	[122]
	RightHand ReFlex Plus*	3	5	8	-	-	[21]
	iHY	3	5	8	-	-	[111, 123]
Anthropomorphic	iCub hand	5	9	19	30	<0.3	[12]
	DLR Hand II	4	13	13	30	-	[124]
	Shadow Dexterous Hand*	5	20	24	-	5	[113, 125]
	Over-Actuated Prosthetic	5	22	17	21	6.7	[118]
	Gifu Hand II	5	13	20	<12	-	[114]
	Schunk SVH*	5	9	20	-	-	[126]
	RBO Hand 2	5	7	∞	-	-	[117]
	Pisa/ITT SoftHand 2	5	2	20	-	-	[116]
	Xu Anthropomorphic Hand	5	10	-	-	-	[23]
Human	Hand**	5	34	27	~79	~47.6	[127–129]

There are many reasons for developing and using these hands, for example to provide machines with the dexterity and versatility we posses is one of these or to use the tools and objects we have designed for our own hands. There are some more human-centric reasons for this form as well, such as tele-operation, where a one to one relationship between the tool and the users will provide intuitive and efficient usability. There are also uses in the field of prosthetics, where the human appearance of the limb is important for both user interface and acceptance.

As mentioned, a major drawback of anthropomorphic hands is their complexity; with too many DoF to efficiently control with current technologies and algorithms they prove, in many cases, to be worse at many tasks that the simpler alternatives [105]. It should be noted that due to the biomimetic embodiment of the features and functions present in the human hand, anthropomorphic designs have the potential to eventually reach the versatility and dexterity of human hands.

Non-Anthropomorphic As an observation, non-anthropomorphic hands are more complex than grippers and tend to be less complex than anthropomorphic hands, although this is not a defining rule. These hands are designed with both fundamental and intuitive engineering techniques to recreate some of the abilities of human hands from a different perspective. This also means that the hands are designed around the limitations in costs and available technologies resulting in tools are very efficient at their targeted tasks.

Current settled designs of these hands (three fingers and under actuated) are commercially available and widely used for grasping [19, 21, 111, 121, 122]. However, for more complex tasks, these designs lack the versatility of human hands and the potential of anthropomorphic hands.

2.4.2 The Dexterity Challenge

Successfully matching the capabilities of human dexterous manipulation with a robotic hand will be a crucial milestone in the evolution of robots, although this has proved to be a real engineering and computing challenge. This section will discuss the state of the art in robotic dexterous manipulation focusing on approaches using sensor and/or robotic hands and briefly discuss other examples of manipulation and dexterous manipulation.

2.4.2.1 Manipulation and Dexterous Manipulation

Manipulation is a core aspect of robotics as moving components into desired positions is necessary for automated assembly, the most common use of conventional robots. Much of this manipulation is open loop and purposed for simple and specific tasks. Although simple, there are tasks like sliding, rolling, and pushing that are important primitives for understanding and potentially performing dexterous manipulation.

This step from manipulation towards dexterous manipulation is one that has been an active area of research for decades [104, 105, 130, 131]. This field has yielded research into a variety of

methods and strategies that demonstrate one or more manipulation primitives within a dexterous system (rolling:[132], sliding:[133], pushing:[134]), and work on extrinsic dexterity, where the system uses either gravity, external contacts or dynamic arm motions to change the grasp [135]. In addition to this there is work on manipulations that can only be achieved with a dexterous system such as finger gaiting: 'a periodic movements of fingers, to form a new grasp consisted of fingers lying within their workspace limits' [136].

2.4.2.2 Closing the Loop on Dexterous Manipulation

Many examples of dexterous manipulation use well defined models of the system and the object to calculate the desired trajectories, which are then performed open-loop. An issue with these strategies is that they are highly dependent on the accuracy of the models, where any discrepancies or un-modelled disturbances will cause failure.

Closing the loop for manipulation by introducing sensory feedback allows for adjustments and corrections during on-line operation to make up for inaccuracy within the models. The sensory modalities that have been used for closing the loop are namely vision [137, 138] and tactile [139, 140]. Vision systems calculate the pose of object and hand to feed into the model, but can be impaired when the manipulating hardware blocks the visual of the object. Tactile sensing uses the contacts between the object and the manipulator to determine pose and state, although the supporting research and algorithms for this modality are less mature than those of vision. Combining these modalities simultaneously is one possible strategy for minimising the disadvantages of both [73].

An example of using tactile sensing for closed loop manipulation was presented by van Hoof *et al.* [140]. Here the authors utilised reinforcement techniques to learn generalised policies for a rolling primitive. The reasoning behind the use of this strategy was to provide a non-model based approach, to address the fact that both tactile sensors and under-actuated hands (authors used a version of the ReFlex hand) are problematic for modelling. After learning, the system performed competitively with hard coded policy with a higher average of performance.

These closed loop tactile strategies also enable other useful abilities such as grasp adaptation [141] and impedance control [142] both of which are supplementary to dexterous manipulation.

2.4.2.3 In-Hand Dexterous Manipulation

The complexities and challenges of dexterous manipulation are compounded when the system is reduced to the size of a hand. Nevertheless, in-hand dexterous manipulation has been addressed multiple times by the research community, with varying successes [73, 111, 125, 137, 140].

Arguably one of the most impressive demonstrations of dexterous manipulation, to date, was recently presented by the Open AI group. The work implemented Deep-Learning techniques to perform a very sophisticated dexterous manipulation of a cube [125]. The hand used for this task

was the 'Shadow Dexterous Hand', and the goal was to continually reorient the object within the hand, through way-points, until dropped. Using a simulation and associated training techniques, the group was able to apply contemporary deep reinforcement learning algorithms to the task. Matching this simulated environment to the real world was achieved through visual sensing via PhaseSpace markers. The results of the study presented a median of 50 successful reorientations before being dropped in simulation and 13 on the real system. Although this highlights the reality gap, the results are still an unprecedented performance level for dexterous manipulation.

Another demonstration of in-hand dexterous manipulation was presented by Kumar *et al.* [137], where a five finger hand was trained to perform a non-prehensile (not grasping) rotation of a bar. The study employed both nearest neighbour and a Deep-Learning in conjunction with expert demonstration by a human. The findings show both methods were capable of generalising, with the nearest neighbour (using vision) performing better than the Deep-Learning (proprioceptive and tactile only).

2.5 Assessment of Review and Closing Remarks

From assessing the literature presented in this review, there are a number of remarks and conclusions that can be made with respect to the aim of this thesis. Firstly, efforts towards the end goal of dexterous manipulation are decades old, with recent demonstrations of unprecedented levels of dexterity showing that community is still moving forwards. Although when compared to the benchmark that our own biology has set, the field is still a long way off its ultimate potential.

We also found that investments into tactile sensing technology have produced a variety of sensors with different attributes, strengths, and weaknesses, with a relatively equal spectrum of computer intelligence and machine learning methods to utilise them. Even with this variety, the field still appears to be within relative infancy compared to other sensing modalities like audition and vision.

Nature's solutions to tactile sensing and manipulation have arguably set a benchmark that is both awe-inspiring and inspirational. This creates a perfect environment for the use of the biomimetic principles to solve the engineering and robotic problems in these areas.

Overall this literature review presents aspects of tactile sensing, manipulation, and biomimetics and shows that the three fields together are relevant and possibly necessary considerations for attempting to achieve dexterous manipulation. With momentum already existing in the use of biomimetics, tactile sensors, and robotic hands, there is both support and drive to continue to develop and explore the combination of these for the goals and questions set out for this thesis.

CHAPTER 3

THE TACTIP SENSOR: A TOOL FOR TACTILE PERCEPTION AND DEXTEROUS MANIPULATION

In 2009 the need for accurate, reliable, and sensitive tactile sensors lead researchers at the Bristol Robotics Lab to develop the TacTip optical tactile sensor. This sensor was demonstrated to address many of the desired attributes of a tactile sensor and has since proved to be a useful tool in tactile research. In this chapter we introduce and discuss the original TacTip and present the development and evolution of the sensor into the completely 3D printed TacTip V2. This new 3D printed sensor is designed to open up new possibilities for rapid-prototyping and complex morphologies.

The result of the developments discussed in this chapter culminate in the author's publication 'A Biomimetic Fingerprint Improves Spatial Tactile Perception' which discusses results of a hardware modification to the TacTip sensor surface in the form of a fingerprint. *Contributions are detailed in full at the beginning of each section that includes published material.*

3.1 Preface

In biology, skin is the largest organ in the human body and contains within it the somatosensory system. This system importantly enables the sense of touch and ultimately the dexterity that we humans have utilised to completely recreate our environment. It is not a large jump in logic to claim that the introduction of the sense of touch to robots will push the boundaries of their capabilities.

3.1.0.1 Original Sensor

The core theme of the work presented in this thesis is tactile sensing. To explore the boundaries of this sensing modality, a sensor dubbed as the TacTip has been used for all of the research presented. The TacTip was first shown by Craig Chorley and Jonathan Rossiter in 2009 as a biologically inspired optical tactile sensor with edge encoding capabilities [143] (Figure 3.1). From analysis of the output, via vector velocity fields and point tracking, the authors demonstrated a sensitivity to a 0.05 N point contact as well as a correlation between the shape of the marker array and the stimuli, in particular, edges.

Work and development of the TacTip has continued from Chorley's seminal publication. For example, a reduced size design was developed by Winstone *et al.* in 2012 for integration with robot hands [144], work that highlighted difficulties in reducing the size of the sensor. In 2014, Assaf *et al.* evaluated the sensor against human performance in an edge mapping task [145]. demonstrating that the sensor is capable of emulating human level performance on the edge based task. Also, the TacTip has been shown to be hyper-acute, showing a resolvable perception in location of 0.1 mm with a taxel spacing of 4 mm [146].

This research and development of the TacTip builds a strong case for continued work with the sensor. The sensor has been shown to be robust and versatile with many demonstrations of uses for the sensor. In addition as the sensor was developed at the Bristol Robotics Lab the author has access to expertise and knowledge of this hardware. Due to this strong foundation the TacTip was chosen as the tool to explore the tactile domain.

This chapter will detail design changes and modifications on the sensor hardware that the author either performed or contributed to. To this end a description and analysis of the original TacTip is presented here to justify the changes made to the sensor hardware.

The original TacTip comprised of the core elements of the sensor that are present in all subsequent versions of the sensor. These elements are: a flexible contact surface (skin), a compliant and optically clear filling (flesh), an opaque hollow chamber, and a camera.

3.1.0.2 Sensor Inspiration and Description

The TacTip is a biomimetic design, where the intermediate ridges of glabrous skin of human hands and feet have inspired the form of the contact surface of the sensor. These ridges are the protrusion of the outer layer of skin (Epidermis) into the inner layer (Dermis), and are home to the Merkal cell complex (MCC), one of the 4 types of mechanoreceptors attributed to touch [1, 143]. In the TacTip the intermediate ridges are implemented as cylindrical protrusions of the skin, perpendicular to tangent of the surface. These cylinders, or pins, are capped with a contrasting colour (the markers) so as to be clear in the camera image. The pins move relative to the camera and each other when a tactile stimulus is introduced to the skin. This movement is an amplified transduction of mechanical information from the surface to the pin marker and is imitative of

Figure 3.1: The TacTip optical tactile sensor discussed and described in 3.1. The sensor tip is made of a flexible skin with raised markers on the interior that are inspired by intermediate rides in human glabouras skin .

the function of the intermediate ridges' transduction of information from the skin surface to the MCC (Figure 3.2).

The sensor is a flexible hemispherical skin, the interior of which is endowed with the pins. The skin is filled with an optically clear gel that provides structure and compliances to the skin, and is kept in place with an acrylic lens. A camera is used to extract the data from the pins and is connected to the posterior of the sensor, looking at the interior of the skin. The camera and tactile tip are connected via a solid hollow body that does not impede the camera view of the pins whilst minimising the presence of external lighting. A ring of LED's are placed inside the sensor body, near the lens, to illuminate the pins for the camera.

3.1.1 Analysis of the sensor

To use and develop the TacTip sensor it is necessary to understand the sensor's design, as well as its strengths and weaknesses as a tactile sensor. The following section describes the materials' property requirments and the materials used to address them. The section will also briefly discuss the design of the sensor.

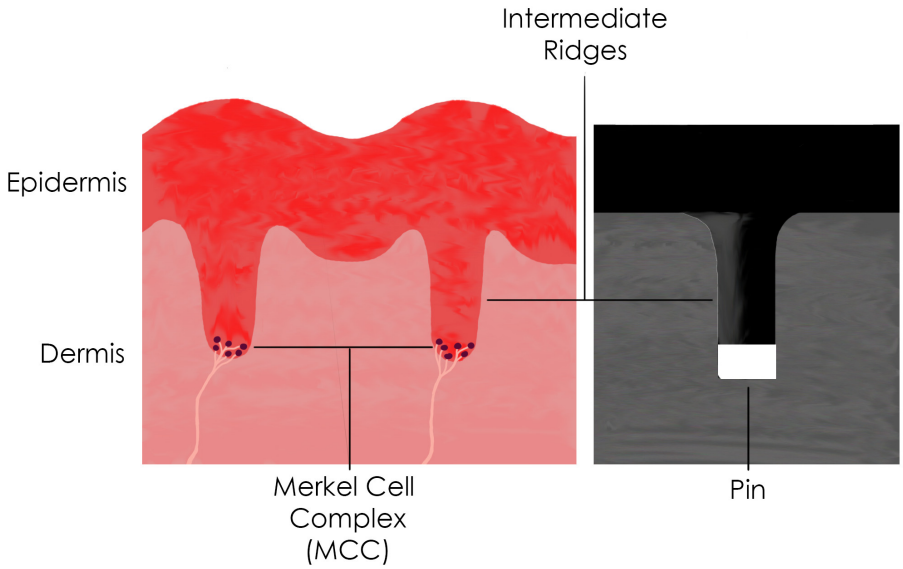

Figure 3.2: Simplified diagram of human glabrous (hairless) skin with intermediate ridges protruding from the epidermis into the dermis. These ridges are home to Merkal cell complex mechanoreceptors, attributed to elements of curvature, edge, and corner perception [1, 24]. In comparison, the TacTip has cylindrical pins with a white marker, these pins perform in such a way as to transduce information like the intermediate ridges in biology.

3.1.1.1 Materials and Design

Some of the materials used in the sensor are structural and others fundamental to the sensor function. The material used to construct the body of the sensor provides the structural element to bind the camera and tip together. The only restraints on the choice of this material are that it has sufficient strength to withstand repeated tactile contacts, and more importantly that it provides suitable optical conditions within the chamber. These are a minimised reflection from internal walls, and the obstruction of external lighting as this can interfere with the camera. The availability of 3D printing provides a suitable construction method for the body, which also defines the choice of material. The available printer uses the process of fused deposition modelling (FDM) and prints ABS thermoplastic.

The material used for the skin and flesh heavily influences the sensing capabilities of the TacTip, thus the skin needs to meet the following criteria:

- Robustness: The tactile surface of the sensor is frequently compressed and sheared during usage. This requires that the material is robust to tearing and splitting under these conditions. In addition, accidental collisions of the sensor can occur and the material should be able to withstand forces that exceed normal operation range.

- Flexibility: Translation of contact forces into movement of the pins is fundamental in the function of the sensor. To this end the skin must flex under contact to allow the pins to move, in addition to supporting the compliance of the sensor.
- High opacity: Due to the optical element of the TacTip, external lighting can interfere with the identification of the pin markers. With the loss of markers comes the reduction in information, a scenario undesirable for any sensor. The skin needs to have a high opacity to remove this impact.
- Low time dependency: Hysteresis an important factor to minimise in any sensor. For a tactile sensor perceiving contact after it has ceased or changing sensory readings for the same stimuli after prolonged use, can lead to failures in grasps and manipulations. Thus the material must minimise this aspect.

As with the skin the flesh material also has criteria it must satisfy for the sensor to work and perform as desired:

- Compliant: The compliance of the tactile element is required to allow the skin to flex and translate the tactile information to the pin markers. The flesh must produce this compliance whilst providing structure to the sensor tip, as that is needed to exert adequate contact forces, particularly in grasping and manipulation.
- Good optics: A challenging requirement placed on the flesh is its optical properties. As the pins are within the flesh the only way to see them with the camera is if the flesh is highly translucent (preferably transparent).
- Low time dependency: As with the skin material, the flesh should be chosen to minimise any adverse time dependent effects on the sensor.

The skin is designed as a hemispherical shell of moulded silicone with a thickness of 0.3 mm and 532 markers raised on 0.2 mm columns of material. The silicone used is VytaFlex 60 with hardness Shore A 60. A black dye is added during the mixing of the silicone resulting in high opacity that satisfies the need to block external light. The material has a high flexibility and is robust to shear forces and tearing with a elongation at break of 480% and a tear resistance of 24.3 Kg/cm [9]. The elasticity of the silicone returns the skin to its original shape, although a delay in returning to the original shape adds a small amount of hysteresis, as the skin cannot return instantaneously. Part of this moulding process is shown in Figure 3.3.

For the flesh a optical silicone sealant, Techsil, RTV27905, is used. This material has a Shore hardness of Shore 00 10, similar to that of the fatty tissues in the human finger tip; this provides the tactile surface of the sensor with compliance and structure [147]. Importantly this material is optically clear, allowing for the camera to view the pins. Mechanical properties of Techsil are poorly defined, due to the fact that is is not meant for use as a filler or moulding. This creates a

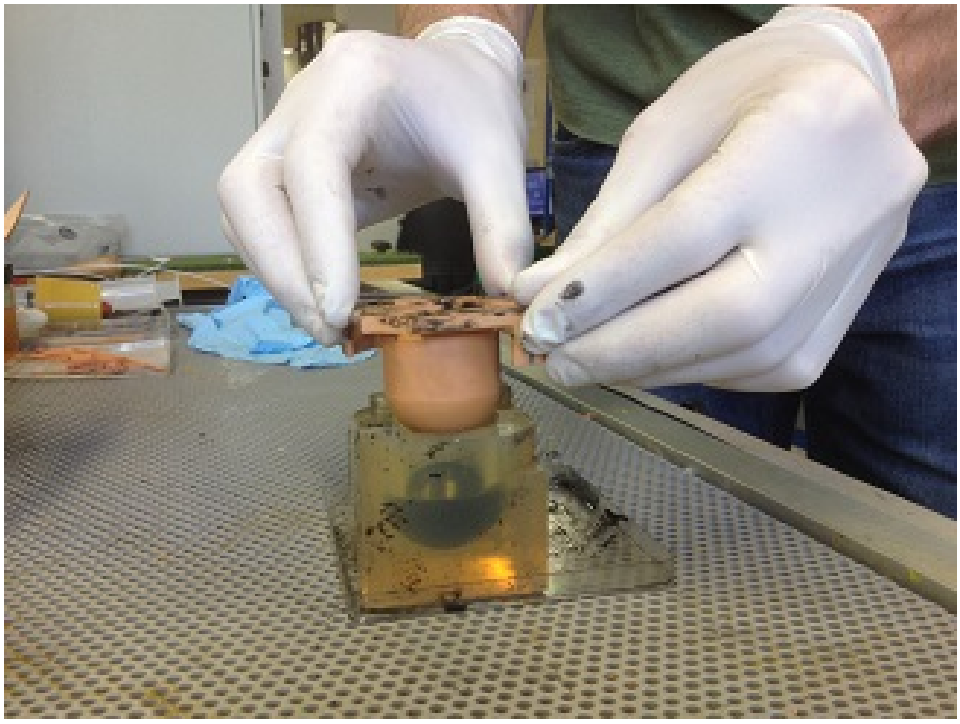

Figure 3.3: Photo of a Vita-flex skin being cast in the silicon negative mould.

challenge for mechanically defining the properties of the tactile tip, although its optical properties have not been found in any other material and thus outweighs the need for definition.

The camera used for the sensor is a Microsoft LifeCam [148]. The camera provides a wide-screen 720p image at 30 fps and is situated 38 mm from the lens of the tactile element. The camera is plug and play and has adjustable settings allowing for easy set-up.

3.1.1.2 Critical Analysis

The original TacTip has been used in many publications, demonstrating key strengths in exploring the tactile domain. Performing a critical analysis of the sensor's strengths and weaknesses with regards to other sensors, and its own design goals, will aid in developing the sensor for future research.

Advantages The contact based nature of tactile sensing requires sensors to be robust to repetitive strains, high forces, and accidental impacts. The TacTip has a few features that provide advantages to robustness when compared to other sensors. Firstly, the sensitive electrical components (camera and LEDs) of optical tactile sensors like of the TacTip are separated from elements of the sensor that experiences the contact. This means that the components are safe from damage from both usage and accidents. In contrast, sensor types such as capacitive, piezoresistive,

force/torque, and barometric have sensitive electrical components that are required to be under contact for the sensor to function, risking them to damage during use [8].

The use of a flexible skin filled with a gel creates a tactile surface that has a high degree of compliance. In grasping and tactile exploration, compliance allows the sensor to adapt to the stimuli, increasing surface area of contact. By doing this the sensor is able to gather more information and improve grip of grasped objects [149].

A challenging aspect of creating a tactile sensor array is cabling [8]. In many tactile sensors each taxel is an independent sensory component with power, ground, and data out, resulting in substantially large numbers of cables for larger sensory surface areas. Utilising a camera as the sensing element in the TacTip reduces the number of cables required to the single USB output of the camera. Although with tactile arrays larger than the field of view of the camera, extra cameras will be needed.

Production cost of the sensor (basic version) is under £200. This is due to the inclusion of an off the shelf web-cam (Microsoft life cam) and a low cost 3D printed body. This is much cheaper than the commercially available tactile sensors such as the BioTac from Syntouch at £7,600 ($10,000) [78].

Disadvantages Tactile sensors of the optical class use a variety of optical equipment such as camera and fibre optics. The optical tactile sensors (OTS) that use cameras as the sensing element all have a common fundamental limitation. This being the space required between the observed tactile surface and the camera due to focal length. This is an issue for using the sensor on platforms where size is important, specifically when integrating the sensors with robotic hands and manipulators. The use of Macro or wide angle lenses in many cases does not aid in reducing the sensor size as the lenses themselves tend to increase the camera size by the difference gained in moving the lens closer to the surface. Donlon *et al.* presented GelSlim, a version of the GelSight OTS, where the use of mirrors was used to move the sensing element and reduce the vertical profile of the sensor [88]. This allows the design to be able to fit in to smaller spaces, like grasping from a box. Another possible solution to this issue could be a custom camera system with wide field of view, short focal length, and small profile. This solution would prove expensive and would remove the low construction cost that the TacTip currently has.

In comparison to other technologies used for tactile sensing, the data that OTS's like the TacTip produces are very large. This is as, rather than producing a value for each taxel at a given time frame, the camera provides a frame of $n \times m$ pixels that in many cases need to be processed via computer vision techniques to extract the taxel values or tactile data. This proves very expensive to process time and can limit the frequency of data.

Moulding the skin is a complex process requiring the mould to be custom built. The negative mould is created with another silicone compound using a 3D printed positive of the skin. This 3D printed positive is produced on an Eenvision-Tec Perfactory digital light projection stereolithography (DLP) machine, providing high quality prints (42 μm in xy) with a material suitable

for moulding [150]. These parts are expensive to produce, although they will be used to mould multiple skins. The major drawback is the cost and flexibility of this method of producing skins, restricting the variety and frequency of changes that can be made to the skins design.

The pins are arranged in a dense geodesic pattern on the skin, providing a large number of taxels with an even distribution. For the methods used in the work discussed in Section 3.1, this was not a disadvantage. This arrangement of pins makes individual identification of pins difficult due to the quantity and the way that the spacing appears on the camera. A geodesic spacing, although providing evenly spaced taxels in 3 dimensions produces taxel bunching towards the edge of the sensor in the 2 dimensional camera image, further complicating the individual identification of pins.

3.1.2 Research Question

The invention of a system with new sensing capabilities can open up doors to new tools, products, and careers. For example visual sensing invention in the form of photography and subsequently film lead to new ways of documenting history and telling stories. These sensors themselves have not stood still since, and they continue to grow and evolve. Bringing us to a point where we have highly detailed images at high frame rates that we now use for computer vision. These developments in hardware have lead to new uses and capabilities of the sensors, the same should apply to tactile sensing. This chapter sets out to explore this by attempting to answer the following research question.

Question Can developments and improvements in the TacTip hardware lead to gains in its tactile sensing capabilities and new directions in which the sensor can be utilised?

3.1.3 Hardware Modifications

3.1.3.1 Modularity and 3D printing

The cost involved in modifying the skin of the original TacTip design has limited the ability to explore different shapes, pin layouts, and their affects on the sensing. Exploring these can be achieved with powerful prototyping techniques such as multi-material 3D printing and printing of rubber-like compounds. Available to the author was the Stratus Objet 3D printer, with which it is possible to print in a black rubber-like material (TangoBlack+) and a solid plastic (VeroWhite), the combination of which can be used to construct the sensor tips for the TacTip.

To fully exploit the rapid prototyping capabilities of these 3D printed tip variants, the TacTip was redesigned to be modular. This is achieved by creating the tips as separate elements of the sensor, consisting of the skin and pins, the flesh, a lens (for securing the gel into the tip), and a supporting body that can be attached to the main body of the sensor. A bayonet style attachment

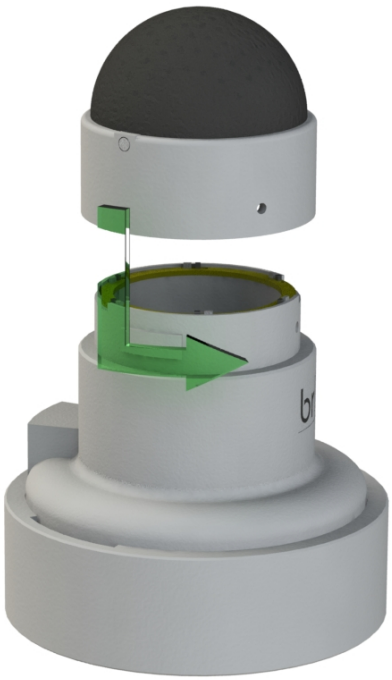

Figure 3.4: One of the modifications applied to the TacTip design was to utilise multi-material 3D printing methods to construct the tactile tips. This increases the speed and versatility of prototyping tip designs. To fully exploit these 3D printed tips, the sensor is designed to be modular. Using a bayonet style attachment allows for quick and easy changing of the sensor tips along with a repeatable attachment.

is used for connecting the tips to the sensor, allowing for quick changing and accurate attachment of new or replacement tips (see Figure 3.4).

3.1.3.2 Pin Layout

The 3D printed tips can be made with varied pin layouts. As mentioned earlier the original sensor's pin layout provided challenges for the current methods of extracting the tactile data. This method is centroid detection via OpenCV and requires the markers to be resolvable through binary image threshold. This is difficult for the software to achieve when the pins are moving, particularly when the pins cross or meet. To limit the occurrence of the pins crossing, the pin density can be reduced from 1 mm to 3 mm.

In addition to modifying the pin density on the skin, the density is modified from the camera's perspective, by generating the pins as a projection (from the camera's perspective) onto the skin. This creates a pin layout that is more evenly spaced in the camera image, reducing the bunching caused as the perceived density increase radially from the centre. The pattern of these pins was chosen to be hexagonal (triangular base) due to the regular nature of this shape when tessellated.

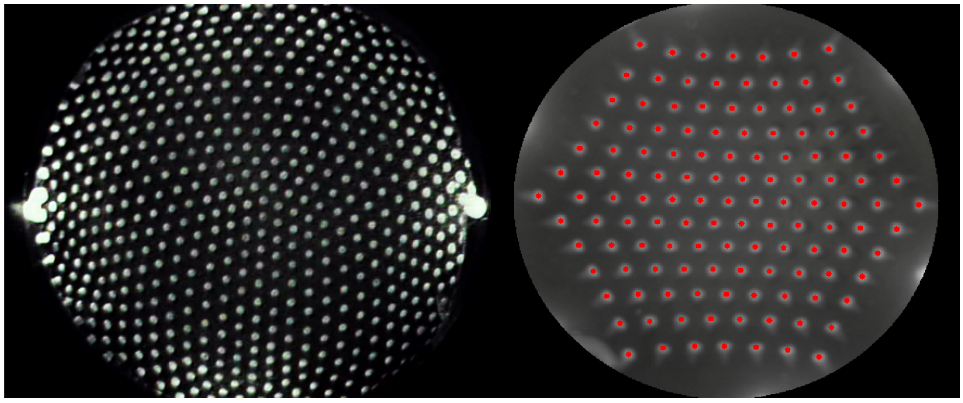

Figure 3.5: Comparison of the 532 pin geodesic layout of the original TacTip and the 127 pin hexagonal projection of TacTip V2. The new layout is designed to be sparser to avoid pin crossing under contact as well as to provide a constant density of pins in the camera frames.

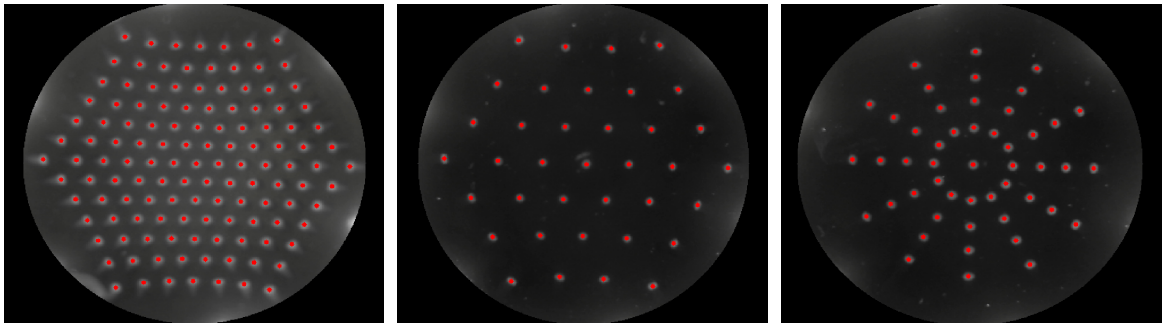

Figure 3.6: Variants of 3D printed tip pin layouts. (From left to right) Standard 127 pin hexagonal projection, sparse 37 pin hexagonal projection, and a 49 pin symmetrical layout for exploring training generalization.

Other layouts of pins have been explored such as a sparse variant and one with a radial symmetry for exploring training generalisation [37] (see Figure 3.6). These tips have been designed to explore different aspects of tactile robotics, but highlight the flexibility of method for 3D printing the tips. Examples of these layouts can be seen in Figure 3.5.

3.1.4 TacTip-V2

The following sections describes the modified TacTip from a hardware perspective. This version of the sensor is the design of the sensor that is either directly used, or provides the design basis, for the work presented in this thesis.

3.1.4.1 Hardware Breakdown

The TacTip is comprised of four core elements the tactile tip, LED board, hollow body, and camera. The function of the sensor is dependent on each of these. To further elaborate on and explain the

Figure 3.7: CAD render of the TacTip (exploded) with components, from left: Tactile tip(cross sectioned), lens, LED ring, Sensor body, modified Microsoft LifeCam, and a cover for the camera compartment.

sensor, each of these elements are described in greater detail below.

The Tactile Tip The tips are the part of the sensor that comes in contact with the world. They translate tactile contact with stimuli into a physical change in pin marker positions readable by a camera. The tips themselves are a collection of different materials and elements. The tactile surface is a flexible skin endowed with an array of biologically inspired pins capped with contrasting markers. The skin is fused to a solid ring of material that provides support to the structure as well as the mechanism for connecting to the rest of the sensor. These parts are produced using a 3D printer capable of multi material printing. A clear acrylic lens is glued to the interior of the tip body to contain the flesh. The flesh is a compliant optically clear silicone compound that is inserted in to the skin/lens cavity. Once cured it provides the tactile tip with structure and compliance. All these components can be seen in the exploded view of the sensor shown in Figure 3.7.

Camera As with the original TacTip the sensor uses a Microsoft LifeCam as the sensing element. The difference here is that the camera is deconstructed so that is just a board and a camera. This reduces the profile of the camera and reduces the overall size of the sensor. The LED's can be powered off the USB power and ground connectors on the camera circuit board reducing the sensor cabling.

Body To connect the sensor into a single unit a 3D printed body is used. This part is printed in ABS plastic by FDM process for efficiency of cost and strength. In addition to structure the body plays an important role in the sensor function by blocking external light from reaching the camera.

LED Ring The white markers on the pins must be visible to the camera for data to be collected. As the combined system is closed the presence of light within is minimal, thus the markers need

Matirial	Vytaflex	Tango Black+
Tensile strength (MPa)	6.1	1.5
Elongation at Break (%)	480	220
Hardness (Shore A)	60	28
Tear Resistance (Kg/cm)	24.3	4

Table 3.1: comparison of material properties used for the skin. Smooth-On Vytaflex 60 used for the original TacTip and Stratasys TangoBlack+ for the new 3D printed version [9, 10](note values for TangoBlack+ are the high values given by the referenced data sheet).

to be eliminated. This is achieved with a ring of white LED's. The ring is placed so that when the tip is attached it is close enough to the lens that the LED light does not glare in the camera field.

3.1.4.2 Comparison to the Original TacTip

The modified TacTip has some notable differences to the original sensor. In advantage, the new version is better suited to the centroid identification methods used throughout the work presented in this thesis. Different versions of sensor tips can be rapidly designed and produced to allow for faster progress in the exploration of tactile robotics. The modular tips also make it faster, easier, and cheaper to replace them when damaged.

The de-constructed web cam and a tighter packing of the hardware has resulted in the new sensor being 30 % smaller than the original. This reduction of size has not reduced the sensor to a size suitable for a robot hand, but has made it easier to mount the robot onto robot arms.

In addition to the advantages of the new design, there are also disadvantages. The TangoBlack+ rubber-like material mechanical properties are inferior to Vytaflex 60 moulded silicone across the board (Table 3.1) [9, 10]. Of particular note is the lower resistance to tearing and splitting, 4 Kg/cm for the printed material compared to 24.3 Kg/cm of the moulded material, results in a substantially reduced robustness of the tactile tips. It is also slightly translucent, allowing enough light through to interfere with the sensor under intense lighting conditions. Due to this the skin is made thicker (1 mm rather than 0.3 mm) also increasing the presence of the hysteresis in the sensor readings.

With these in mind the author believes that the modified sensor provides a platform that, due to versatility of 3D printing, can accelerate the sensor development and in turn the research able to be performed with it. Although with a settled design or a larger budget, the moulded skin of the original TacTip is the superior material option as it is cheaper to produce in bulk and suffers from less hysteresis.

3.2 Publication: A Biomimetic Fingerprint Improves Spatial Tactile Perception

The inclusion of multi material 3D printing into the sensor design enables fast prototyping of tactile tip variants. It also allows the inclusion of complex features in the design previously not possible, for example a biomimetic fingerprint. This section presents the author's publication detailing research into adding a biomimetic fingerprint to the 3D printed tips.

The following section has been published in a paper entitled *"A biomimetic fingerprint improves spatial tactile perception"*. This publication was peer reviewed for the robotics and automation letters (RAL) in 2017. The contributions for this publication are as follows.

- Luke Cramphorn:
  - Conceptualised the idea of exploring the effect of an artificial fingerprint on perception of spatial scales with the second author.
  - Designed the fingerprinted sensor tips.
  - Assembled all sensory tips used in the work.
  - Designed the experimental procedure and stimuli.
  - Performed the data collection and subsequent analysis.
- Benjamin Ward-Cherrier:
  - Conceptualised the idea of exploring the effect of an artificial fingerprint on perception of spatial scales with the lead author.
- Nathan F. Lepora:
  - Provided supervision over the work. Helping the lead author formulate the best implementation of the work.
  - Produced the base architecture used for classification and validation (Section 3.2.3.2).

Abstract - The fingerprint is a morphological aspect of the human fingertip that has interesting implications for our sense of touch. Previous studies focused on how the fingerprint affects the perception of stimuli that excite high temporal frequencies, such as for texture perception. These studies also only add papillary ridges to their sensors. Here we endow a biomimetic sensor with both papillary ridges (fingerprint) and a dermal stiffness contrast (stiffer intermediate ridges), and assess the impact on localisation perception accuracy. The sensor is based on a novel modular version of a 3D printed tactile sensor (TacTip). Tactile data was collected with these tips on nine stimuli with varying curvature. The location perception acuity of three tips (smooth, fingerprint, and fingerprint [cores]) were compared with a probabilistic classification method. Finding that

both fingerprinted tips increase the perceptual acuity of small spatial scales. Interestingly the fingerprint variant had poorer accuracy than the smooth tip for larger spatial scales; however, adding cores to enhance the dermal stiffness counteracted the degradation of accuracy. This supports the theories that the fingerprint aids the classification of edges and smaller spatial scales, and demonstrates that the addition of a fingerprint to an artificial tactile sensors improves its acuity.

3.2.1 Introduction

The human fingertip is an extremely complex and efficient sensing device that provides us with the key information for manipulating objects and tools. It has evolved multiple morphological aspects that aid its perceptive performance. One of these aspects that is particularly interesting is the fingerprint. The fingerprint has multiple aspects that can be linked to the sense of touch, including but not limited to an intricate interaction between the two layers of skin and concentrations of sensory cells located under the ridges that make up the fingerprint. Utilising these features in biomimetic systems may make it possible to enhance the functionality and performance of existing tactile sensors, which will in turn improve the abilities of systems to perform more complex tactile tasks such as in-hand manipulation where shape detection and object reconnection are crucial [139].

In this paper, we explore the effects of a novel combination of a simple papillary ridge structure and an enhanced stiffness contrast on biomimetic intermediate ridges upon the accuracy of location perception on stimuli with varied curvature (Figure 3.8). Thus we aim to identify if a fingerprint is a beneficial feature for a tactile sensor in spatial perception tasks. The use of fingerprints on tactile sensors is not a new idea and research into the effect of fingerprints has shown some interesting tactile enhancements. Multiple studies support the finding that textural perception and classification (temporal features of tactile contact) are improved by the presence of a fingerprint [68, 151, 152]. Artificial papillary ridges have been used to enhance the local shape classification of stimuli [153] to show that the inclusion of these ridges may enhance the detection of curvature. Also FEM studies [65, 154] on the effect of intermediate ridges in the human fingertip have pointed towards a lensing affect that focuses the stress of a contact to allow finer detection and localisation of edges.

There is limited coverage, in literature, on the effect of an artificial fingerprint for localisation perception on small spatial scales. Also, endowing a biomimetic fingertip with both epidermal and dermal enhancements based on the human fingertip is completely unexplored. To examine this, we use multi-material printing methods to produce three tips for a modified TacTip optical tactile sensor [143]. These tips are the same in volume, diameter, and pin layout but differ in their morphology. Firstly, there are papillary ridges made from nodules on the exterior skin that mirror the pin layout on the interior, in the same way that papillary ridges mirror the intermediate ridges in the human fingertip. Secondly, there is an increase in the contrast of stiffness between

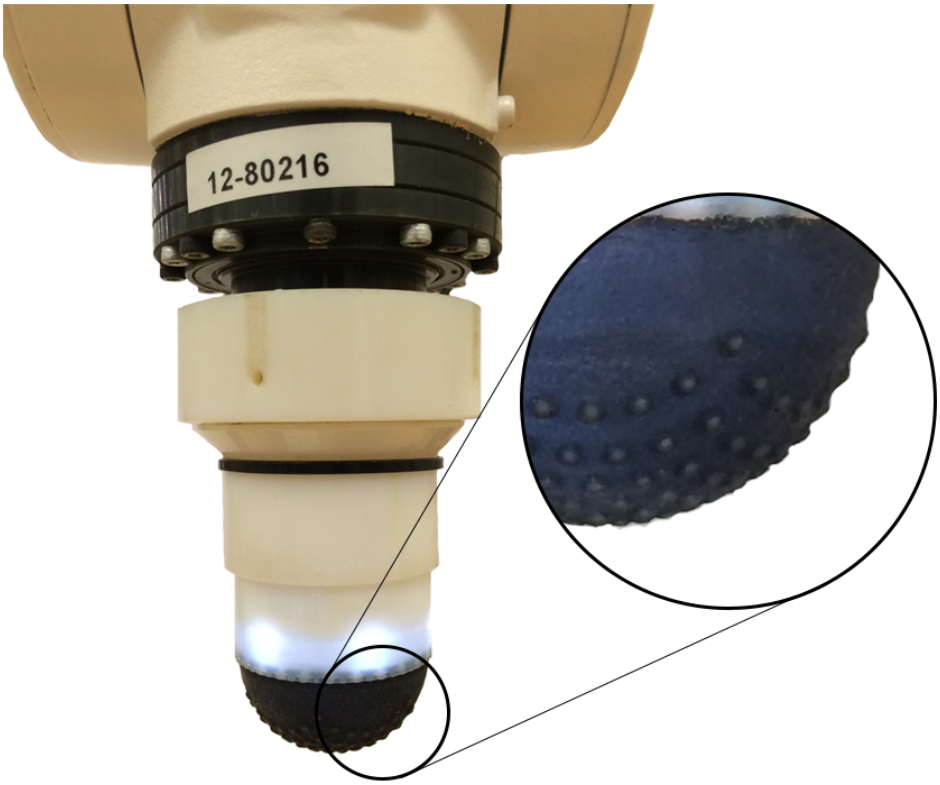

Figure 3.8: Biomimetic fingertip (TacTip) with a tip endowed with an artificial fingerprint. This sensor is used in this experiment, with variations in tip design, to demonstrate the improvements in location perception acuity on smaller spatial scales due to a fingerprint.

the skin (epidermis) and flesh (dermis). The latter is achieved by adding a solid core that runs through the pin body to the pin tip. We expect to see improvements in the localisation accuracy of the tips on smaller spatial scales by including the artificial papillary ridges, as well as a further improvement at these scales due to the inclusion of the enhanced dermal stiffness contrast.

The acuity of location perception of these tips is calculated from an off-line probabilistic classifier and compared for nine stimuli of varying curvature. We show that the addition of papillary ridges improves the sensor sensitivity (lower ambiguity between sensory readings) which in turn improves accuracy of our tactile sensor to localisation tasks on features that are smaller spatially (lower curvature). Interestingly the enhancement of dermal stiffness contrast does not further improve the detection at these ranges as expected. Although the enhanced stiffness does appear to negate negative effects due to the presence of fingerprint on larger spatial scales, possibly due to supporting the structure of the pins creating a more consistent deformation. Hence we demonstrate that the inclusion of the papillary ridges and stiff intermediate ridges of the human fingertip in a biomimetic fingertip improves the sensor's locational perception acuity to smaller spatial scales without impairing sensing on larger scales.

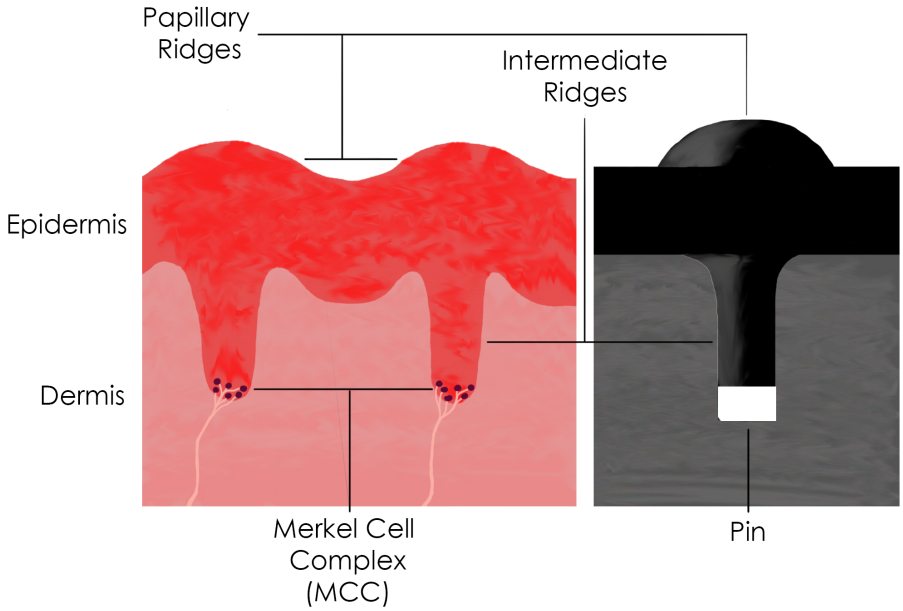

Figure 3.9: Structure of the fingerprint. The top layer of the skin is the epidermis, which has protrusions on the surface called papillary ridges (fingerprint). These ridges overlay epidermal protrusions into the dermis (inner layer of skin) called intermediate ridges. At the tip of these ridges are touch receptor cells (Merkel cells). The right image depicts the biomimetic principles of our sensor, with an epidermis and dermis, as well as papillary ridges and intermediate ridges.

3.2.2 Background and Related Work

The fingerprint is believed to have a purpose in tactile sensing. It is made up of parallel whorls of ridges on the outer layer of skin (epidermis) known as papillary ridges. The epidermis protrudes into the dermis (a deeper layer of skin) creating a junction of interlocking sections of tissue [1, 155]. This interlock creates ridges of epidermal tissue known as intermediate ridges, that mirror the papillary ridges. Limiting ridges follow the grooves between the papillary ridges and act to limit movement between the two layers. The tips of the intermediate ridges have a cluster of 5-10 mechanoreceptors known as Merkel cells, that adapt slowly (SA) throughout contact with stimuli [1, 24]. This is known as the Merkel cell complex (MCC). This structure produces a sophisticated interaction between stimulus and sensor (Figure 3.9).

There have been many theories on the function of the human fingerprint, many of which may not be mutually exclusive; thus, the fingerprint would appear to aid the human sense of touch in many ways. One hypothesis is that the fingerprint assists grasping by acting as a high friction surface between the fingertip and the contacted object [156], or as an aid for slip detection [66]. Another suggestion presented in *The Anatomical Record* in 1954 by Cauna [155] suggests that the fingerprint aids tactile perception by allowing the intermediate ridges to follow the motion of the papillary ridges acting as a small mechanical lever which magnifies the response to tactile

contact. Although recent publications by Gerling and Thomas, 2005 [154] and Gerling, 2010 [65] have shown that the 'mechanical lever explanation' may not be adequate, by producing FEM models of a human fingertip that explore the effect of intermediate ridges on the transference of stresses from a contact to the sensory cells. Their findings have shown that the intermediate ridges focus the stress of contact and increase the signal over background noise to allow finer edge detection. It is important to note that this model focuses on the intermediate ridges and does not include papillary ridges. It was also found that the stress distribution through the tip is not altered by the ridges and thus does not aid classification between the edge and gap probes that they explored.

Many tactile sensors have been developed and each has properties motivated by convenience of fabrication, durability, biomimesis, and intended use [1, 8, 157]. Some applications of tactile sensors include object identification, control, and manipulation (combination of identification and control). A desirable property of tactile sensors is that they are soft and compliant, for example to allow the sensor to conform to the stimulus as well as to exhibit hyper-acuity/superressolution properties. A sensor with superresolution utilises the compliance of the surface to spread the contact over multiple nodes (taxels, pins, or mechanoreceptors) thus enabling a triangulation to contact localisation on a scale smaller than the resolution of the sensor [158].

There is some existing work on integrating fingerprints into tactile sensors. One such integration was shown in *Science* by Scheibert *et al* [68] where an artificial fingerprint improved fine texture perception (spatial scale <200 μm) possibly due to spectral selection and amplification of the features. Similarly, other work has considered improving texture identification [151, 152]. In both cases the fingerprint is used as an amplifier of the temporal frequency features of the textured surfaces, with results demonstrating that use of an artificial fingerprint improves perception of texture. Another study using a fingerprint on a tactile sensor was performed in 2011 by Salehi *et al* [153], in which they used three stimuli (flat, curved, and edged) to show that shape detection is improved with the presence of a pair of papillary ridges. The curved stimulus was chosen to be the same spatial scale as the sensor to avoid confusion between flat and curved surfaces.

This is not the first attempt to endow the TacTip tactile sensor with a fingerprint. In 2013 Winstone *et al* [152] moulded a miniaturised silicone sensor equipped with raised bumps on the exterior of the sensing skin, directly over the sensors pins. In this study, the aim was to demonstrate the perception of texture as an additional feature that the TacTip Technology can perceive. To achieve this the authors, use biomimetic principles to tune the sensor to texture. Firstly, the authors state that as the (fast adapting mechanoreceptor responsible for texture in humans) is stimulated at around 250 Hz, and thus the 60 Hz frame rate of a standard web cam is not sufficient. To this end a high frame rate camera that can capture tactile data a 1 kHz is introduced. Secondly there is the introduction of a fingerprint to investigate the magnification of subsurface strains that it is believed to perform during the exploration of texture. In this work

constraints are placed to perform the texture recognition. These are; the tracking of only a single pin marker that is situated at the centre of the tactile surface and the absence of a flesh (gel) filling to remove damping of vibrations on the pin. The notable findings of this work are in the improvements from a smooth TacTip to a fingerprinted TacTip in the sensitivity to the smoother test stimuli.

Building on the knowledge that the addition of a biomimetic fingerprint to the TacTip aids perception of temporal features, this work aims to explore the lesser explored space of fingerprints and spatial features. Thus, there are some differences between the approach taken here and the work presented in [152]. For example, the exploration of spatial features is more aligned with the slowly adapting MCC mechanoreceptors than the fast adapting Pacinian corpuscles, and thus the high frame rate camera is not required. This also allows the sensor to be used in its standard form with all pins tracked and the flesh filling. In this study we expand on the biomimetic principles of adding a fingerprint to the sensor by including a rigid core to enhance the dermal stiffness contrast, in order to gain the advantages for edge encoding presented by Gerlings FEM model of the human fingertip [65].

In addition, the present study utilises probabilistic methods for biomimetic tactile perception that have been demonstrated to be robust and accurate over many different stimuli and tasks with similarities to biological sensory encoding [159], enabling comparison with other work in tactile perception such as superresolution [146, 158].

3.2.3 Methods

3.2.3.1 Experimental procedure

The Tactile fingertip The TacTip is an optical tactile sensor developed at Bristol Robotics Laboratory [30, 33, 143, 145, 146, 152, 158]. The TacTip sensor was designed to be primarily 3D printed. This makes the sensor relativity cheap and easy to modify. The sensor uses an off-the-shelf CCD (LifeCam Cinema HD) to track an array of pins on the internal side of a silicone skin. It is important to note that previous work on the sensor has utilised incorrect terminology to describe the biomimesis of the sensor. The pins were claimed to be inspired by the dermal papillae, although this feature of the fingertip is the part of the dermis created by the protrusion of the epidermis. Upon closer inspection the pins are more akin to the intermediate ridges that protrude from the stiffer epidermis into the softer dermis tissue.

The TacTip has multiple beneficial aspects. The ready availability, low cost, and plug'n'play properties of modern webcams mean that this sensor benefits from only having a single cable, being easy to install, as well as remaining low cost. The silicone skin (Vytaflex (Shore A 60)) is filled with an optically clear gel that gives the sensor compliance. There is a difference in the hardness of this flesh material and the skin, similarly to the difference in stiffness between the stiffer epidermis and more compliant dermis in the human finger. The skin has a relatively low

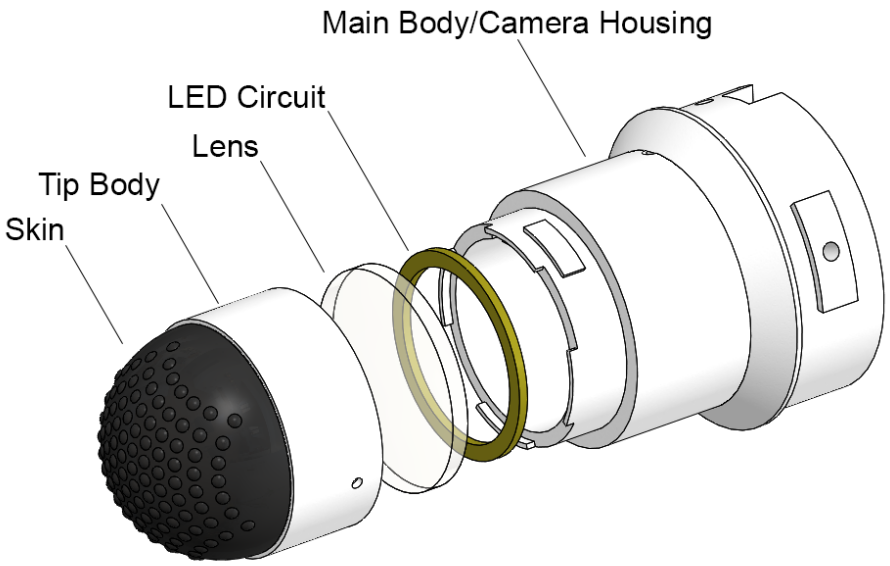

Figure 3.10: Exploded view of the modular TacTip; the tactile skin, modular body (with bayonet fitting), and a clear acrylic lens make up the interchangeable tip module. The main body of the sensor acts a focal length spacer for the camera, houses the LED circuit, and is the part connected to the robotic arm. Finally, the camera mount fits to the top of the main body, and securely fits a modified Microsoft Lifecam.

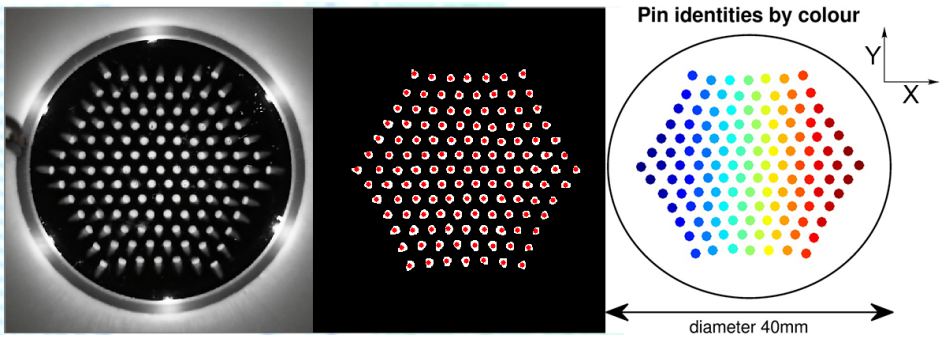

Figure 3.11: The tip modules used in this study use a hexagonal projection for the pin layout, which creates evenly spaced pins on the 2D CCD image (~3.0 mm between pin centres on the CCD image). This new layout helps support robust pin tracking without sacrificing resolution due to the superresolved properties of the system. On the left is raw image and right is processed image

cost and keeps any contact far from any delicate electronics, meaning the sensor is robust and easily replaceable if damaged.

TacTip Modifications In recent work, Ward-Cherrier *et al.* modified a TacTip so that the sensor could be integrated into a thumb on a modified openhand model M2 gripper (TacThumb) [33]. In this case the skin and pins are printed as part of the body of the sensor, rather than molded

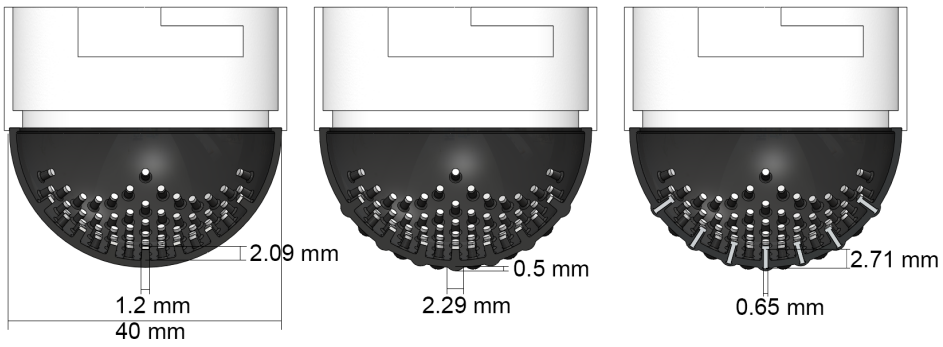

Figure 3.12: Cross sectional comparison of the TacTip tactile sensor tested in this paper. The left tip is the basic TacTip sensor with a smooth surface. In the middle is the tip with artificial papillary ridges. Finally the tip on the right has the fingerprint and the further addition of an enhanced dermal/epidermal stiffness contrast

separately and attached later. High material and time costs for setting up manufacture of the original tips has limited the past optimisation of the TacTip, but as the 3D printed tips can be cheaply and easily produced in different configurations, many different versions can be tested for optimisation.

To test the different tips the TacTip was redesigned to be modular. This allows the tips to be interchangeable, which in turn speeds up the test process and lowers cost (as otherwise an entire sensor would be needed for each new tip). The modules are a tip module that has the Tactile tip (3D printed Tango Black + [Shore A 26-28]), gel (RTV27905, Techsil UK [~Shore 00 10]), lens, and a body (Vero White). The base holds the LED ring, and is the bulk of the 3D printing (Vero White), as well as being the connection to the Robot arm. These modules are connected together by a secure bayonet fitting (Figure 3.10).

The original TacTip was designed with a high density (~1.5 mm between pin centres on the surface) of small pins in a geodesic pattern to produce an evenly spaced pin layout [143]. The geodesic pattern on the hemispherical surface leads to greater pin density towards the edges of the CCD image. Therefore a hexagonal projection is used to create even visual spacing in the CCD image (~3 mm between pin centres on the CCD image). The resulting pin layout is far more suitable for robust pin tracking (Fig. 3.11).

The biomimetic fingerprint design was inspired by the human fingertip by considering the mirroring of the papillary ridges and the intermediate ridges. This was done by adding domes (diameter 2.29 mm, height 0.5 mm)on the exterior of the skin in a concentric alignment to the pins, to mimic the role of the papillary ridges. The second adaptation of the tip is to include an enhanced stiffness contrast achieved with a plastic core (Vero White 3D printed material (Shore A 85)) that starts in the interior of the dome/skin and connects directly to the pin tip (2.71 mm from base of tip to base of dome). These cores are only possible by utilising dual material 3D printing

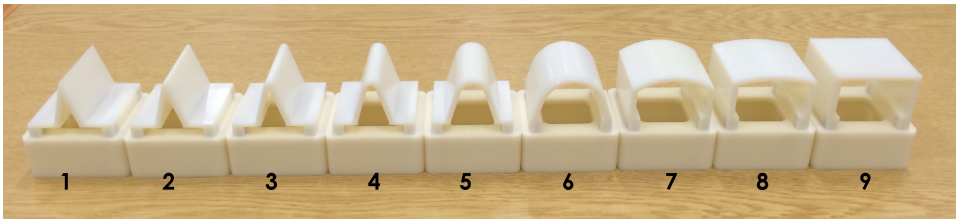

Figure 3.13: The 9 stimuli used in this experiment, ranging in spatial scale from an edge (1) to flat surface (9) with intermediate curvatures ranging from 0.8 (2) to 0.0125 (8). The sensor travels (y) from right to left on each stimulus, covering 30 mm symmetrically about the apex of the stimulus.

(Figure 3.12). The publication by Gerling [65] shows that the location of the mechanoreceptors on the tip of the intermediate ridges is adventitious due to the fact that the epidermis is stiffer than the dermis. Thus the idea is that increasing this stiffness contrast will improve the perception of edges, as suggested by the FEM models.

Experiment To test effects of the enhancements, a set of stimuli were developed for the sensor to examine. These stimuli had varying curvatures, as curvature can be conveniently linked to spatial scale. The curvatures chosen ranged from $0.8000\,\mathrm{mm}^{-1}$ to $0.0125\,\mathrm{mm}^{-1}$; the set is completed with an edge (as close to ∞ curvature as possible) and a flat surface (0 curvature). These can be seen in Figure 3.13.

Table 3.2: Table of the stimuli curvatures

Stimuli (ncs)	Radius (mm)	Curvature (mm^{-1})
1 (Edge)	0	∞
2	1.25	0.8000
3	2.5	0.4000
4	5	0.2000
5	10	0.1000
6	20	0.0500
7	40	0.0250
8	80	0.0125
9 (Surface)	∞	0

Curvature is calculated as $(\text{radius})^{-1}$. It is important to note that stimulus nine should be completely ambiguous to all sensor tips due to its lack of changing features across the range. Stimulus six mirrors the curvature of the sensor itself, and three is approximately the same scale as the spacing between the artificial papillary ridges. Hence we describe spatial scales of

≤ 2.5 mm as small and ≥ 20 mm as large, with the middle range bridging the gap between them. Note that these definitions of spatial scale may change for other fingertips, as the interpretation of spatial scale depends on tip morphology.

Data collection The platform for the system was a six DoF robot arm (IRB 120, ABB Robotics), which precisely positions the attached end-effector with an absolute repeatability of 0.01 mm. The TacTip sensor is used as the end effector on this arm for this study.

The system is trained with supervised learning, by tapping the stimuli and recording the tactile information. This is done for every class (0.1 mm) along the y direction, up to the full range (30 mm) for each of the stimuli. Each of the taps is a 5 mm press from 1 mm above the stimuli apex (maximum tap indentation of 4 mm, corresponding to a maximum force of 0.3 N on the tip) and records approximately 1.5 seconds of data, with ~35 recorded frames per tap. By tapping the stimuli, aspects of the material such as texture, caused by surface roughness, will be minimised and are thus not considered here. The data acquired for the results in this paper were collected in two distinct sets for each stimuli, ensuring that the training and test sets are different, and that the validation of the results is based on sampling from an independent data set to that used to train the classifier.

Data preprocessing The data from the TacTip sensor is extracted from the recorded frames of each tap. Time series are constructed from ~35 frames with a resolution of 640×480 pixels. These frames are subsequently filtered in opencv (http://opencv.org/) using a Gaussian spatial filter with adaptive threshold, which accommodates varying luminosity in the tip, and a mask is applied to the edge of the image to remove glare caused by LEDs.

Each pin is tracked from frame to frame by linking that pin's new location to the nearest location in the prior frame. A limitation of the original TacTip was that it was difficult to track pins due to a non-uniform pattern and high spatial density; this has been improved with the new design by adopting a more regular pattern with slightly larger spacing (but still sufficient for fine spatial perception). By having a reduced density of pins (127 pins) this issue is avoidable and creates a method of pin tracking that is robust.

There are some fail cases in this tracking method that can be avoid by being aware of them. Firstly, rapid deformation of the sensor tip results in large displacements between frames, such that a different pin may be closer to its location in the previous frame, causing a swapped identity. Another issue occurs when the computer vision, employed to separate the pins from the image, fails to extract all the pins. This results in a 'dropped pin,Äô and can cause the tracking of that identity to jump to the nearest resolved point. Both optimising the pin extraction and identifying when a pin has been dropped such to replace it with its previous location, help reduce the occurrence of this fail case.

The training data is collected for a range of distinct locations x_l, $1 \leq l \leq N_{loc}$ where $N_{loc} = 300$

over a 30 mm of stimulus. This is stored as a multi-dimensional time series of taxel values z:

$$z = \{s_k(j) : 1 \leq j \leq N_{samples}, 1 \leq k \leq N_{dims}\} \tag{3.1}$$

where the x and y components of the pin deflections are treated as distinct data dimension $s_k(j)$, and thus the number of dimensions is equal to the number of pins multiplied by the number of spatial dimensions, $N_{dims} = 127 \times 2 = 254$. Each time series is zeroed before analysis, meaning that only deflections are considered, irrespective of the pin's starting position. This effectively resets the sensor before each tap in the data, and acts to reduce long term hysteresis of the sensor tip. The time series are also truncated to 15 frames, $N_{samples} = 15$, for each tap. Thus the overall data dimension is $(300 \times \{254 \times 15\})$.

3.2.3.2 Classification and Validation

The collected training data set is used in a standard 'histogram' likelihood model. The histogram model has been indicated as analogous to spatial and temporal summation in neurons [159], but those aspects will not be central here. This classifier has been used in past work by the group for similar work with posterior estimation [146, 158, 159]. Hence, for constancy with past work we continue its use here. The histogram model is constructed by encoding the training to determine the increment of evidence for each perceptual hypothesis based on the logarithm of a likelihood model of the contact data.

$$\log P(z|y_l) = \sum_{k=1}^{N_{\text{dims}}} \sum_{j=1}^{N_{\text{samples}}} \frac{\log P_k(s_k(j)|(y_l)}{N_{\text{samples}} N_{\text{dims}}} \tag{3.2}$$

Where we assume statistical independence between all data dimensions k and time samples j. A histogram method is then applied to the training data, where sensor values s_k are binned into equal intervals $I_b, 1 \leq b \leq N_{\text{bins}}$ for the entire range of the training data.

$$P_k(s_k|y_l) = P_k(b|y_l) = \frac{n_{kl}(b) + \epsilon}{\sum_{b=1}^{N_{\text{bins}}} n_{kl}(b)} \tag{3.3}$$

The sample count in each bin b for dimension k over all training data in class y_l is $n_{kl}(b)$ ($\epsilon \ll 1$ a small constant that regularizes the logarithm).

A Monte Carlo procedure is used to randomly sample data from the test set. The sampled data is used in the above method to classify locations, returning the training class with the maximum likelihood to the sampled data. This is repeated with 10000 iterations of a Monte Carlo procedure to sample all the data classes in the test set. The difference in perceived and actual class location is the error in the perception.

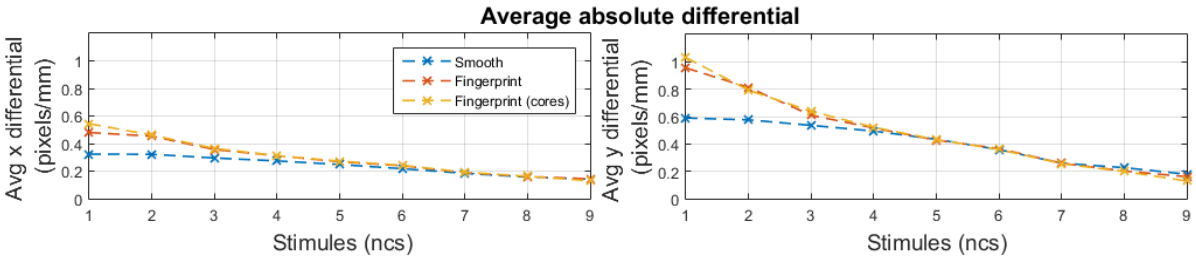

Figure 3.14: Plotting the average absolute differential for each tip on each stimulus shows that the rate of change of pin deflection for the fingerprinted tips is improved over that of the smooth tip, for small spatial scales. This is most notable in the direction of travel (y). This difference in rate of change of pin deflection quickly dissipates as you increase the spatial scale of the stimulus and may help make the data for the fingerprinted tips less ambiguous at lower spatial scales.

3.2.4 Results

3.2.4.1 Inspection of data

The effect of varying sensor location (y) over the stimulating feature changes the extent to which the pins displace, both in magnitude and direction. Each time-series is a distinct set of displacements for that particular surface structure. The data contain a large amount of information about specific locations, therefore permitting location perception. As with any classification, the lower the ambiguity is over the stimulus/data, the greater the accuracy of perception. The data sets are shown in a table of figures (Table 3.3) (for stimuli 1, 4, and 8) to demonstrate the effects of varying the spatial scale.

Data from the tips contacting smaller spatial features show a high rate (deflection/class location) of change in pin deflection (e.g. stimulus one shown in Table 3.3) when compared to that of the high spatial scales (e.g. stimulus eight shown in Table 3.3).

When comparing the data sets for the smaller spatial scales between the tips, there is a visible change in the structure of the data. This is an increase in the rate of pin deflection per unit length (Table 3.3 Stimuli 1-FP and Stimuli 1-FP(C)). This increase in rate of deflection at smaller scales is highlighted by the values of the average absolute differential of the data. These values are obtained by calculating the differentials at every class for each taxel, after noise is reduced via a 5 point moving average. The differentials are taken as absolute and averaged across taxels, between the contact range of 5 mm and 25 mm, then for the set. The average absolute differential shows that, in the direction of travel (y), the value is up from 0.59 pixels mm^{-1} for the smooth to 0.96 pixels mm^{-1} and 1.03 pixels mm^{-1} for the fingerprint and fingerprint with cores respectively, on stimulus one (Figure 3.14). The direction of travel is relevant here as it appears that the fingerprint has the greatest influence in that dimension for this stimulus. This means that the data for the fingerprint tips is inherently less ambiguous (sharper) in the direction of sensor travel (y), and thus more conducive to perception of location and classification.

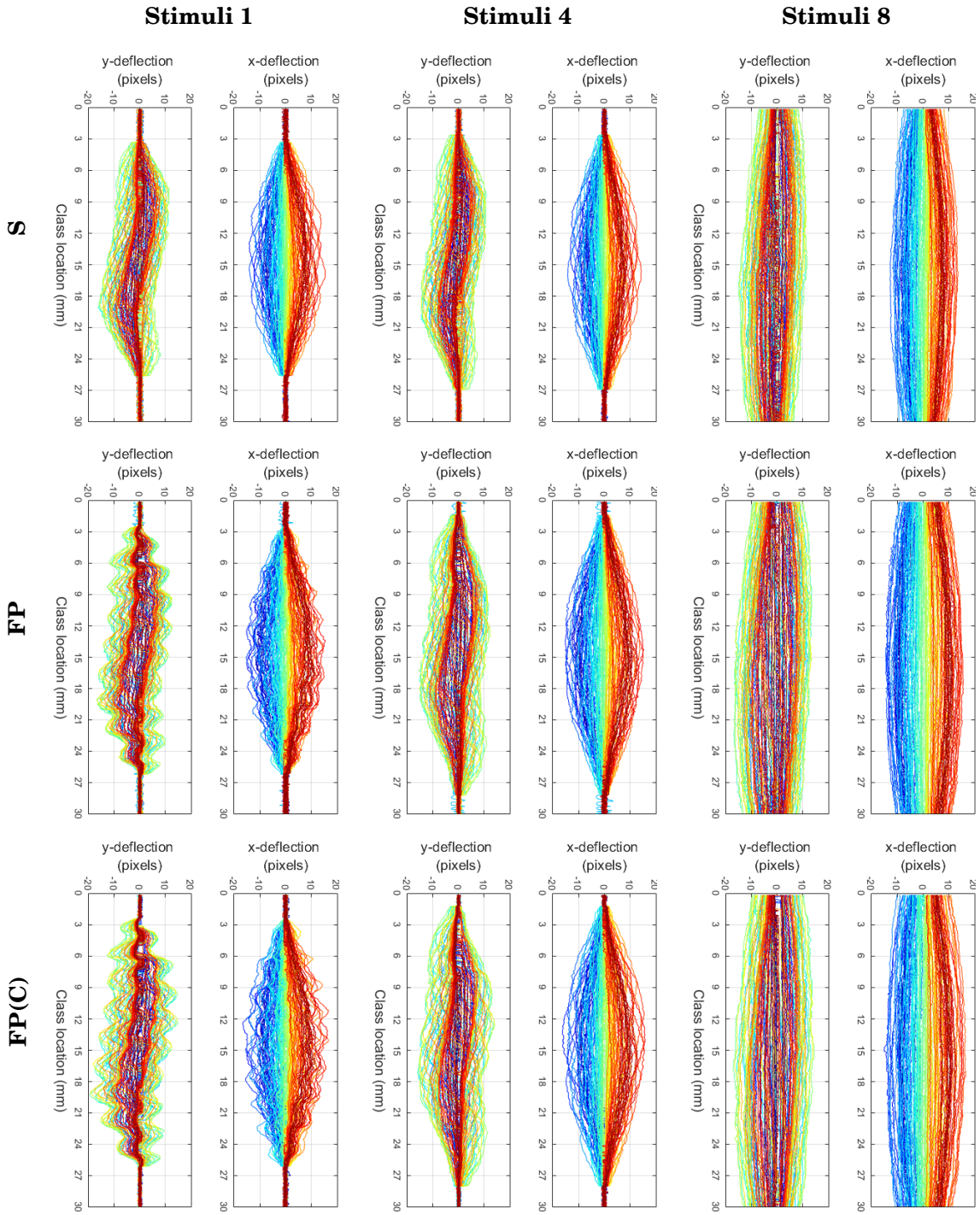

Table 3.3: These graphs present the pin deflections collected by the smooth tip (**S**), fingerprint (**FP**), and fingerprint with cores (**FP(C)**), for stimulus **1**, **4**, and **8** over a 30 mm range. It can be seen that the rate of change of pin deflection over the length of the recording, becomes lower on higher spatial scale stimuli. It is important to note that this rate is improved for the fingerprint tips, over the smooth, on the smaller spatial scales.

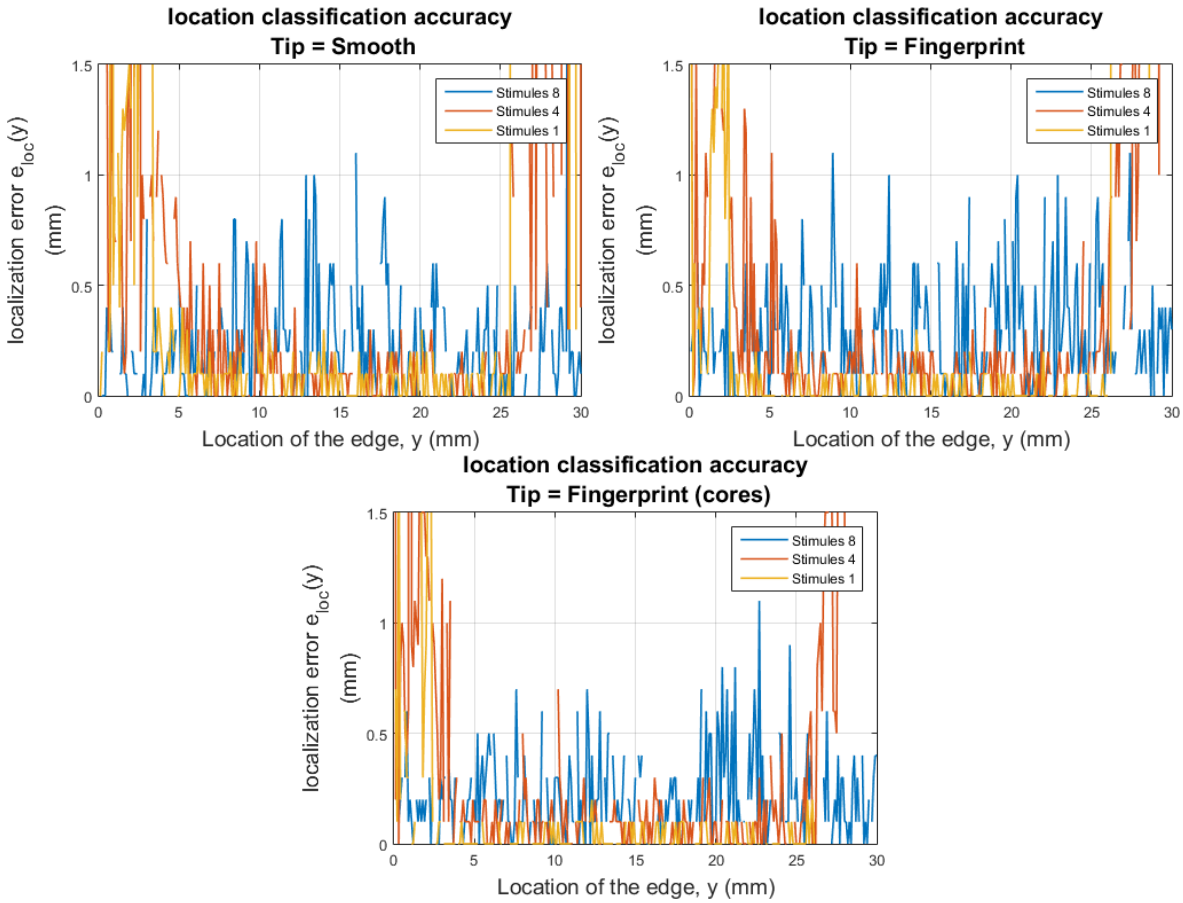

Figure 3.15: For the same three stimuli as show in Figure 3.3 the graphs represent the error in perception over the stimulus. The range of 0-5 mm and 25-30 mm show poor errors for stimuli one and four, this is expected as the sensor is not in contact at these locations. Through the considered range (5-25 mm) it is clear that the errors are lower for stimulus one, and higher for stimulus eight (consistent for all tips). It can be seen from the graphs that the fingerprint (cores) is better over all shown stimuli, whereas the fingerprint appears to be the least accurate for eight, and the smooth has the highest errors for one and four.

3.2.4.2 Error analysis of classification

Using the Monte-Carlo analysis described in Section 3.2.3.2, the data is processed off-line to determine the perceived location class of samples from a test set. The distance from the real location is taken as the error in localisation $e_{loc}(y)$. These errors can be plotted to highlight regions of high and low ambiguity (Figure 3.15). The graphs (using the same stimulus sample as in Figure 3.3) show the regions of no contact for stimuli one and four, these are below 5 mm and above 25 mm. These no contact regions inherently detect no changes in the sensor and thus are totally ambiguous. The contact region of stimulus one is the smallest and it is chosen to be the comparison range for all the stimuli (5 mm-25 mm). In this range it is clear that error increases in size, for all tips, as you move up in stimulus scale. This is consistent with the visual increases

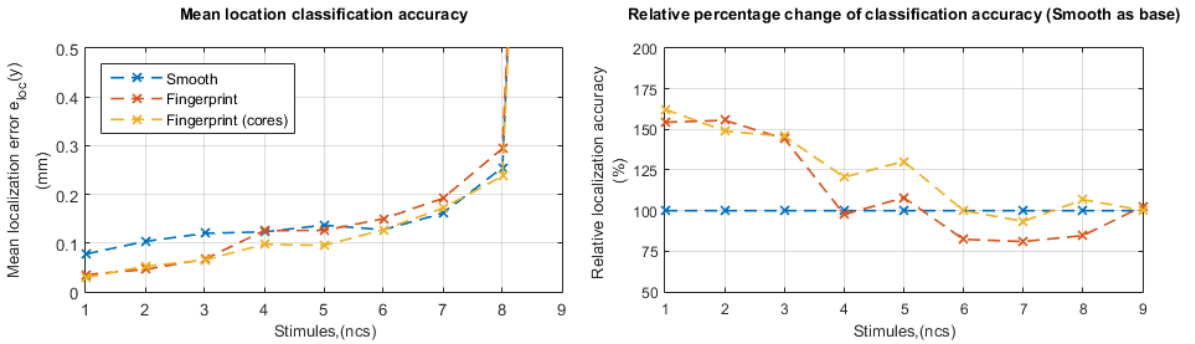

Figure 3.16: By taking the mean error for each tip and stimulus, over the contact range (Top), it can be seen that the errors increase with the size of the spatial scale, as expected from the data sets. Stimulus nine is a flat surface with 0 curvature and thus is totally ambiguous, hence the sharp rise in error. To fully identify the effect of the modifications, the errors are calculated relative to the smooth tip (Bottom). This demonstrates the increase in location perception, due to the fingerprint, on smaller spatial scales. It also highlights the negative impact of the fingerprint on large spatial scales, and that this is negated by the fingerprint (cores) tip.

in ambiguity displayed in Figure 3.3.

To compare the tips themselves the mean error of the contact range (5 mm-25 mm) is taken. The mean localisation error provides a single value for the overall performance of the tip on that stimulus. When plotted together it can clearly be seen that the error increases with the spatial scale (Figure 3.16 Top). The errors become extremely large for stimulus nine; this was expected as a flat surface has no discernible features.

To draw out the changes in sensor accuracy, due to the presence of the added features, the relative errors are calculated using the smooth tip as the base (Figure 3.16 Bottom). The results show that the presence of the papillary ridges, irrespective of the enhanced dermal stiffness contrast, improves the accuracy of the sensor to 140-170% of the accuracy of the smooth tip, for spatial scales of 2.5 mm and less. For stimuli four and five the accuracy of the fingerprint tip is similar to that of the smooth tip, before dropping of to 80% of the accuracy of the smooth tip for the reaming stimuli (spatial scales 20 mm and greater). Interestingly the fingerprint (cores) tip remains more accurate for stimuli four and five and tends towards a similar accuracy to the smooth tip for the larger spatial scales, in contrast to fingerprint tip. This suggests that the enhanced dermal stiffness contrast contracts negative effects of the artificial papillary ridges on larger spatial scale stimuli. By the looking at the average root mean square difference of taps between data sets, where the values are 0.303, 0.316, and 0.286 pixels for smooth, fingerprint, and fingerprint (cores) respectively, it can be said there is an improvement in the repeatability of the sensor.

3.2.5 Discussion

In this study we set out to show that the addition of biomimetic aspects of the human fingerprint to a biomimetic fingertip would improve the localisation perception accuracy of small spatial scales in much the same way as they are believed to in the human fingertip.

We found that the inclusion of papillary ridges on our tactile sensor improves the accuracy of location perception on small spatial scale (≤2.5 mm) to 140-170% of the accuracy of the sensor without this feature. This confirms our prediction that including papillary ridges on a biomimetic tactile sensor enhances the focusing of the stress induced by contact down the pins (intermediate ridges), increasing the rate of change in deflection directionality (from 0.59 pixels mm^{-1} in smooth to 1.03 pixels mm^{-1} in the fingerprint [cores]), thus sharpening the sensory recordings. This result also supports the belief that these ridges are linked to edge encoding in human tactile sensing. As mentioned, the definitions of spatial scale used here may change for other fingertips, as the interpretation of spatial scale depends on tip morphology.

There was an expectation that enhancing the dermal stiffness contrast would aid edge encoding and sensing on the smaller spatial scales. However, the results did not support this expectation: the tip with this enhancement was no better nor worse than the fingerprint tip without it. At first sight this would appearer to contradict the FEM model from Gerling [65], which claims that the stiffness contrast at the tip of the intermediate ridges enhances edge encoding. On close examination however, the TacTip already has a contrast between skin and flesh, thus the enhancement used may not have been a necessary addition for enhancing edge encoding.

There was a clear impact on the perceptual accuracy of the tip with the papillary ridges on the larger spatial scale of 20 mm up. The reason for this impact is unknown but may be due to noise in the deflection of the pins, instigated by the interaction between the ridges and the more gradual surfaces at this scale. Interestingly this same effect seems to be absent in the fingerprint (cores) tip. This suggest that the fingerprint tip could be noisy due to the compression of the ridges into the pins causing inconsistent deflections, as the cores would resist compression and thus reflect the surface of more gradual surfaces as if it was a single plainer surface like the smooth tip. This is supported by the average root mean square differences that show that the fingerprint (cores) tip has better repeatability across sets (0.286) when compared to the fingerprint (0.316) and the smooth tip (0.303).

To date, research has shown that the fingerprint aids high temporal frequencies perception [68, 151, 152] and lightly touched on its influence on local shape detection [153]. The present research provides strong evidence for advantageous influences of the fingerprint on the perception of small spatial scales for both robotics and biology. In addition to this, our findings have shown that having very stiff intermediate ridges may support the papillary ridges and prevent them from impairing tactile sense on large spatial scales.

The inclusion of the fingerprint on the tactile sensor requires minimal extra material, yet

provides a strong increases in the versatility of the sensor. Thus papillary ridges could be used to improve other compliant tactile sensors. We expect that the inclusion of the artificial fingerprint in biomimetic fingertips will improve their ability to perform tactile tasks such as edge perception/exploration following and fine feature classification, with potential implications for object perception and manipulation with robotic hands.

3.2.6 Conclusion

This study demonstrates that the location perception of a biomimetic tactile sensor can be improved on small spatial scales by the inclusion of papillary ridges (by up to 140-170% when compared with the smooth tip). It was also found that an enhanced dermal stiffness contrast negates the negative effects of papillary ridges on larger spatial scales in our tip. Therefore, the inclusion of these biomimetic features on other tactile sensors with biomimetic properties should improve the tactile acuity and versatility of the sensors. Also this study supports the concept that the fingerprint is an amplifier of small spatial scale stimulus, and is thus an extremely versatile adaptation of the human fingertip.

Acknowledgements: The authors of this paper would like to thank N. Pestell, M. Giannaccini, K. Aquilina. Data used in this letter is available at http://doi.org/bzn8

3.3 Postface

3.3.1 Summary, Paper Analysis, and Closing Remarks

The publication detailed above demonstrates improvements in location perception by the TacTip when a biomimetic fingerprint is added. In addition, the work supports theories that the fingerprint aids the classification of edges and smaller spatial scales.

In Section 3.2.3.1 the spatial scales of stimuli are described as being large, small, or in-between, based on the curvature relative to the sensor curvature or fingerprint spacing. It also proceeds to mention that these definitions will change for other fingertips, due to the relationship between spatial scale and tip morphology. Although the work demonstrates a clear improvement of location perception of the spatial scales described as small, the study would be improved by exploring different densities of fingerprints under the same criteria to confirm that the findings hold.

Figure 3.15 shows the error in perception of location across three stimuli for all three tips. The figures show the greater error in the tip absent of the fingerprint, highlighting the improvement provided by the addition of the fingerprint over the centre of the stimuli.

In this chapter it was posed to answer the research question of; ‘Can developments and improvements in the TacTip hardware lead to gains in its tactile sensing capabilities and new directions that the sensor can be utilised?’

To answer this a number of modifications were made to the design of sensor. Firstly multi-material printing methods were introduced with modular sensor tips. This allowed for more rapid design changes. The new printing method presented the opportunity to explore more complicated tactile tip structures. In particular the addition of a biomimetic fingerprint was explored, demonstrating improvements in localisation perception on stimuli with small spatial scales.

The solid cores of the 3D printed fingerprint inspired the idea of extending these cores into passive whiskers. These whiskers deflect the pins within the sensor, which are in turn perceived as tactile information in the same way pins provide information in the standard TacTip. The exploration of these whiskered TacTips is documented in further scientific contributions [39, 40].

To conclude: Developments and improvements of the TacTip hardware has lead to gains in tactile sensing capabilities, notably due to the addition of a biomimetic fingerprint. These modifications have also provided new directions in which the sensor can be utilised as the 3D printing process allows for more versatility in the form of the sensor, due to the simplified manufacturing process.

CHAPTER 4

BASIC MANIPULATION: ROLLING TOWARDS THE ULTIMATE GOAL

With the goal of dexterous tactile manipulation in mind, and a sensor with the potential accuracy and versatility to be up to the task, this next chapter discusses the first baby steps into manipulation. Prior work with the TacTip has developed and examined the sensor's perception capabilities, where here we demonstrate the utilisation of developments in active perception to perform basic tactile manipulation of a cylindrical stimulus. This research is to take steps towards the ultimate goal of dexterous tactile manipulation in robotic systems.

In this chapter we will initially discuss manipulation and why its development in robotic systems is important. The author's publication 'Tactile Manipulation with Biomimetic Active Touch' is the core of this chapter and will discuss an initial exploration into tactile manipulation. Finally the chapter will discuss the continuation of the research onto more practical platforms. *Contributions are detailed in full at the beginning of each section that includes published material.*

4.1 Preface

The term *robot* in English comes from the Czech word, *robota*, meaning "forced labour" and was first introduced in the 1920 play R.U.R. (Rossumovi Univerzální Roboti - Rossum's Universal Robots). In the play artificially created beings are made to work for humans (who ultimately rebel and kill humanity, but that is not relevant here). This idea of a machine doing our labour for us is now a core of what is perceived of a robot. When we consider these laborious task it is easy to see that manipulation skills are required. Using a mechanical interpretation of manipulation, it is the process of providing a physical action on the state of an object. For example picking up, pushing, rolling, assembling, modifying, or using a tool. Manipulation is already a fundamental aspect of robotics as it plays a major role in automation of labour intensive industries like the car industry.

The most common example of manipulation in robotics is in the industrial setting. These machines perform repetitive tasks on parts and components with little to no versatility. These tasks, such as moving parts into place, use hard-coded moves with a known start and end location for the part. Although this form of robotic manipulation has served to redefine how large scale industrial fabrication is done, its lack of versatility is not conducive to human environments where objects and parts do not constantly exist in these 'known' locations. This, in addition to the danger presented by these machines, has created a segregation between robotic and human labour.

The introduction of tactile manipulation into robotics presents the possibility to remove the constrictions of a highly controlled environment. This is due to the fact that tactile sensing enables perception and reaction to errors in objects and the environment, and thus the information to react to them. Reacting to errors is crucial for robotic systems to be able to function in human environments; as compared to their traditional environments, human environments have large errors, unknowns, and unpredictable humans.

4.1.1 Relevant Background

The paper presented in Section 4.2 was preceded by work produced prior to the author's PhD, by the paper's co-authors Nathan F. Lepora and Benjamin Ward-Cherrier. In this preceding work the authors outline methods for active Bayesian perception and use it to demonstrate super-resolution of location perception [27, 146]. An import aspect of this work is the 'active' approach to perception, where the sensor is moved to a more 'perceptually desirable' location on the stimulus based on current and prior beliefs. Active perception shows greatly improved performance of localisation when compared to passive perception.

Dahiya *et al.* distinguish between "action for perception" during active perception and "perception for action" in manipulation [1]. The prior work demonstrates the former, and thus can provide a platform to achieve the latter. To this end the paper uses the active perception methods to produce active manipulation methods.

4.1.2 Research Question

The human species has many biological traits that have contributed to our success. Without doubt the ability to create and use tools is one of the most important of these. Tool use and construction uses manipulation capabilities unparalleled in the animal kingdom, and has literally been used to change the planet. These manipulation skills are achieved through both a highly evolved tactile sensory systems and powerful interpretation of tactile signals [160]. This is supported by research that shows severe impairment of manipulation skills when fingertips are anaesthetised [59]. This connection between tactile sensing and manipulation capabilities in humans provides strong evidence that the inclusion of touch in robotics will greatly enhance the manipulation potential of

those incorporated systems. This has resulted in growing interest in tactile robotics with many different sensors and integrations being developed academically and commercially [1, 8].

Question Can tactile sensing be used to provide the necessary information and feedback for performing basic manipulation of an object based solely on the state of contact?

4.2 Publication: Tactile Manipulation with Biomimetic Active Touch

The existing platform for active tactile perception with the TacTip provides the ideal starting point to begin the author's initial exploration into tactile manipulation. This section presents the publication documenting the research conducted by the author on the subject of tactile manipulation.

The following section has been published in a paper entitled *"Tactile Manipulation with Biomimetic Active Touch"*. This publication was peer reviewed for and presented at the International Conference on Robotics and Automation (ICRA) in 2016. The contributions for this publication are as follows.

- Luke Cramphorn:
  - Designed the experimental procedure presented to explore basic tactile manipulation.
  - Designed and constructed the roller rig used to constrain the manipulation of the roller.
  - Set-up and implemented the system for collecting continues rolling tactile data required for training.
  - Set-up the system for online verification of the method.
  - Performed the analysis of results and collected data with assistance and input from both other authors.
- Benjamin Ward-Cherrier:
  - Provided input and assistance for implementation of methods for data analysis, and for the interpretation of the experimental results.
- Nathan F. Lepora:
  - Provided supervision over the work.
  - Produced the base architecture used for classification and validation.
  - Provided input into the construction of experiments, data collection, and data analysis.

Abstract - Tactile manipulation is the ability to control objects in real-time using the sense of touch. Here we examine tactile manipulation from the perspective of active touch with a biomimetic tactile sensor, which combines tactile perception with control of sensor location. Experiments are performed with the tactile fingertip mounted as end-effector to a robot arm, to manipulate (roll) a cylinder in contact with the fingertip. Performance is validated with offline (cross-validation) and online (real-time operation) assessments. Location perception is finer than the sensor resolution, leading to super-resolved tactile manipulation along a complex trajectory. However, the original methods were non-robust to large unknown disturbances of object location, necessitating modification of the perceptual process to diminish prior beliefs relative to past posterior beliefs. In consequence robust and accurate tactile manipulation was attained. In general, it appears there is a trade-off between the responsiveness to unknown change and manipulation accuracy, which must be set appropriately for each task.

4.2.1 Introduction

Tactile manipulation — the ability to control objects in real-time using the sense of touch — is both a key contributor to the success of humans as a species and a capability whose instantiation in artificial devices could revolutionize industrial and service robotics. Applications range from sorting, positioning and assembling parts in manufacturing to assisting, lifting and interacting with humans in healthcare.

Here we study tactile manipulation with a biomimetic fingertip using active touch. A principal aspect of tactile perception, and arguably all natural perception, is that touch is active: we do not just touch, we feel [161, 162]. That understanding of touch has motivated recent work on methods integrating tactile sensor control and perception [163, 164] with a variety of approaches such as dynamical systems, neural networks and statistical inference [27, 90, 151, 165]. Our aim here is to apply recent progress on biomimetic active perception, where action aids perception, to active manipulation, where perception aids action.

Our approach for tactile manipulation is based on methods for active touch that implement optimal decision making while controlling sensor location [27, 166], which were shown recently to attain superresolved spatial acuity [146, 158]. Past work on active perception has controlled the tactile sensor to move to a good location for perception, by using tactile data to infer intermediate estimates of location. Here we use the same approach for perception, but redefine the control policy to move the tactile sensor along a target trajectory. In consequence, the tactile sensor can control an object that it is in contact with using only the sense of touch.

The effectiveness of tactile manipulation is here assessed using a robot comprised of a biomimetic fingertip mounted as end effector to a robot arm. This robot has previously been applied to active perception of fixed objects, such as localization of a hemicylinder [146]. Here we use a novel experiment comprised of a cylinder that rolls within a fixed housing under lateral movements of the tactile sensor (Figure. 4.1). We validate performance with offline (cross-

Figure 4.1: Experimental setup. A tactile fingertip (the TacTip) is mounted as end-effector on an ABB robot arm. This is used to manipulate (roll) a cylinder mounted on a fixed housing.

validation) and online (real-time operation) assessments of controlling the cylinder location. Subtleties were indicated under large unexpected disturbances of the cylinder, which required modification of how prior beliefs are defined for perceptual decision making. Superresolved manipulation at sub-millimeter accuracy was then robustly attained both offline and online. Although the manipulation was validated with a simple task, we expect the approach generalizes to more complex scenarios.

4.2.2 Background and Related Work

Many different kinds of tactile sensors have been developed for manipulation purposes [8]. Tactile sensors have been used for object recognition [167], improving grasp stability with force control [168] and object exploration/manipulation through edge or surface following [169]. Tactile servoing [87] has been applied to a form of object manipulation on an industrial robot arm [170], and particle filter methods for controlling how to push objects using tactile feedback [171]. Here we examine tactile manipulation from the perspective of biomimetic active perception.

Active perception combines a method for controlling a sensor with interpretation of that data [161] (see also [163, 164]). Recent work on active touch with biomimetic fingertips has focussed on algorithms for sensor control and perception [151, 165]. Contemporary statistical approaches to active touch treat percepts as hypotheses. One example, termed Bayesian exploration, selects tactile data that disambiguates a leading percept from its alternatives [90]. Another approach, termed active Bayesian perception, sets a control policy to guide sensor location ('where') during optimal decision making of object identity ('what') [27, 166], typically fixating the sensor over the object. This latter method can result in superresolved spatial perception [146, 158] and closely relates to the approach used here, by having the control policy guide active manipulation

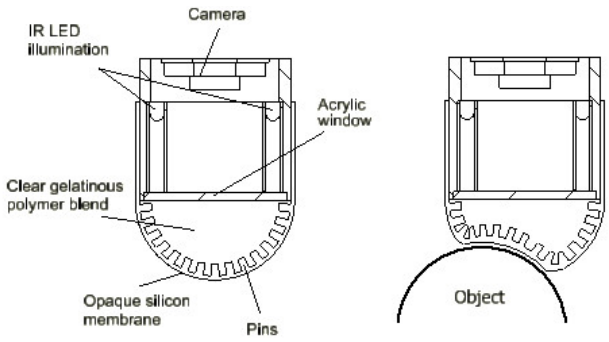

Figure 4.2: Diagram of the TacTip (left) with pins shown on the inside surface of a silicon membrane, which are LED illuminated and imaged by an internal camera. The right diagram is a representation of the deformation of the membrane as it impinges on a test object (a 40 mm dia. cylinder).

rather than active perception.

Active touch has been demonstrated on several biomimetic fingertips having discrete tactile elements (taxels), including capacitive sensors (*e.g.* iCub fingertip) [27, 158, 166], MEMS sensors [151] and barometric sensors (*e.g.* biotac) [90, 165]. Here we use an optical tactile sensor called the TacTip (Tactile fingerTip) developed at Bristol Robotics Laboratory [143, 145, 146, 152, 172]. The TacTip's principal novelty as an optical tactile sensor is that it has an array of pins molded inside the skin that indicate deformations of the surface, with displacements analogous to sensor readings from taxel-based devices.

4.2.3 Methods

4.2.3.1 Details of the tactile sensor and data collection

The Tactile fingertip The TacTip is an optical tactile sensor developed at Bristol Robotics Laboratory [143, 145, 146, 152, 172] that has several highly useful properties (Figure 4.2): (i) the casing is 3D-printed and hence readily customizable and inexpensive; (ii) it uses a standard CCD web-camera (LifeCam Cinema HD, Microsoft) to collect data, which is also inexpensive and connects to a PC via a USB interface; (iii) it has a molded silicon outer membrane that is robust to wear and easily replaced if damaged; and (iv) between the outer membrane and the electronics is a clear compliant gel (RTV27906, Techsil UK) that both enables tactile sensing through compression and protects the delicate parts of the sensor.

The particular design of TacTip used here has a 40 mm diameter hemispherical sensor pad with 18 pins arranged in a regular array on its underside. Six LEDs are mounted on a ring around the base of the pad to illuminate the pins, whose tips have been coated with white paint to give good contrast with the black silicon outer membrane.

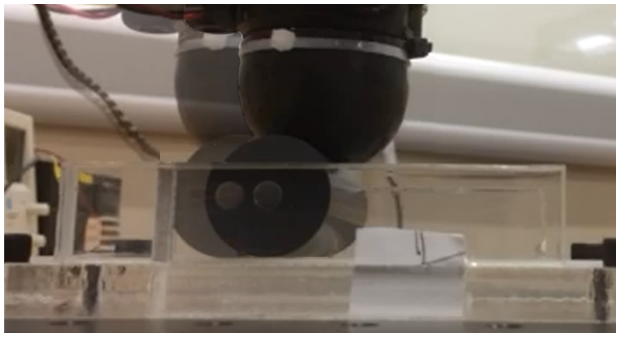

Figure 4.3: Freeze-frame image of cylinder being rolled within housing. The two frames (first shown with transparency) show the beginning and end locations of the cylinder under a lateral movement of the TacTip.

Data collection The TacTip is mounted as an end-effector on a six DoF robot arm (IRB 120, ABB Robotics). The arm can precisely and repeatedly position the sensor (absolute repeatability 0.01 mm).

The present study focusses on the localization of a cylinder rolled by lateral movements of the tactile sensor used as a manipulator (Figure 4.3). As the cylinder rolls its position on the sensor surface changes, permitting localization through touch. A custom roller was built to constrain movements of the roller to one dimension: this consisted of a flat perspex bottom plate that the cylinder rolls over, with two perspex walls separated by 100 mm, the same length as the cylinder (100 mm long, 40 mm dia., cut from plastic). The bottom plate was covered with rubber to ensure the cylinder rolls rather than slips as the fingertip moves laterally. Magnets were mounted at the ends of the cylinder and one end of the roller to give a home position for the cylinder.

Data were collected while the tactile sensor moved 800 mm laterally over the test cylinder, comprising 800 increments $\Delta x = 0.1$ mm. Over about 50 mm and 150 mm at the start and end of the range the TacTip does not contact the cylinder; in the central ~600 mm portion the TacTip is in continuous contact and each lateral movement rolls the cylinder, changing its contact position on the sensor surface. Each incremental move Δx lasted 1 sec and resulted in a time series of sensor readings ($N_{samples} = 15$ per increment). The data used later in this paper were collected twice to give distinct training and test sets. This approach for validation ensured that the results are based on sampling from an independent data set to that used to train the classifier.

Data preprocessing The TacTip collects tactile data as images (resolution 640×480 pixels, sampled at 15 fps), which are filtered to detect and track displacements of pins moulded to the underside of the outer membrane. Images were captured and filtered using opencv (http://opencv.org/). The data preprocessing differed from previous studies with this tactile sensor to ensure good pin tracking performance when the sensor is in continuous contact with a surface. Past work has used punctual contacts and a Lucas-Kanade algorithm to track pins from frame to frame [146]; however, that algorithm suffers from drift over extended periods of tracking,

compromising its effectiveness for the present experiments.

Thus, to track the x- and y- coordinates of the pin centres, the images were first captured, filtered and thresholded in opencv (http://opencv.org/). The centre of the pins were then detected for each frame using contour detection and their x- and y-coordinates recorded. Each pin is identified based on its proximity to a default set of pin positions recorded when the TacTip is not in contact with the surface; if no pin is detected within a radius of 4 mm from its default, then the position from the previous frame is used instead. The two dimensional s_x and s_y pin displacements $s_k(j)$ are treated as distinct data dimensions, with $1 \leq k \leq N_{dims} = 20$ and $1 \leq j \leq N_{samples} = 15$.

One issue with using this method is that arises from the difficulty of maintaining the identity pins from frame to frame. As each pin is searched for within a radius of its initial location, there are possible case where tracking will fail. For example, if the sensor is sheared greater than the search radius pins will either be reset to initial position or be detected by a neighbour's search. Similarly, under large compressions, the pins may move outside of this search radius. In these scenarios, the tracking employed clearly distorts the sensory information. To this end, in this study we avoid placing the sensor in the position where these fail cases will occur.

The TacTip was also modified to aid the effectiveness of the pin tracking, by having only 18 pins spaced ~8 mm apart (compared with ~500 pins in the original design). Using less pins with greater separation provides the space for a larger search radius, preventing the wrong pin from being identified when the sensor surface deforms greatly; it also resulted in lower information transfer rates.

4.2.3.2 Algorithms for location perception and manipulation

We use a recursive Bayesian approach for tactile perception that has been previously applied to passive [173] and active touch [27, 146, 158, 166]. Past work has focussed on making a perceptual decision, when the belief passes a threshold. This passing of the threshold is also the stop rule for the perception. However, the present approach differs by applying the active perception methods to continual tactile manipulation of an object with no threshold for a stop rule (Figure 4.4).

Formally, the algorithms apply to sequences of contact data $z_{1:t} = \{z_1, \cdots, z_t\}$ that are multi-dimensional time series of sensor values,

$$z_t = \{s_k(j) \,:\, 1 \leq j \leq N_{samples},\ 1 \leq k \leq N_{dims}\}, \tag{4.1}$$

with indices j,k labeling the time sample and data dimension respectively. This contact data gives evidence for the present location x_l, $1 \leq l \leq N_{loc}$ with a range of distinct locations. (Here $N_{loc} = 800$ locations spanning 80 mm are used.)

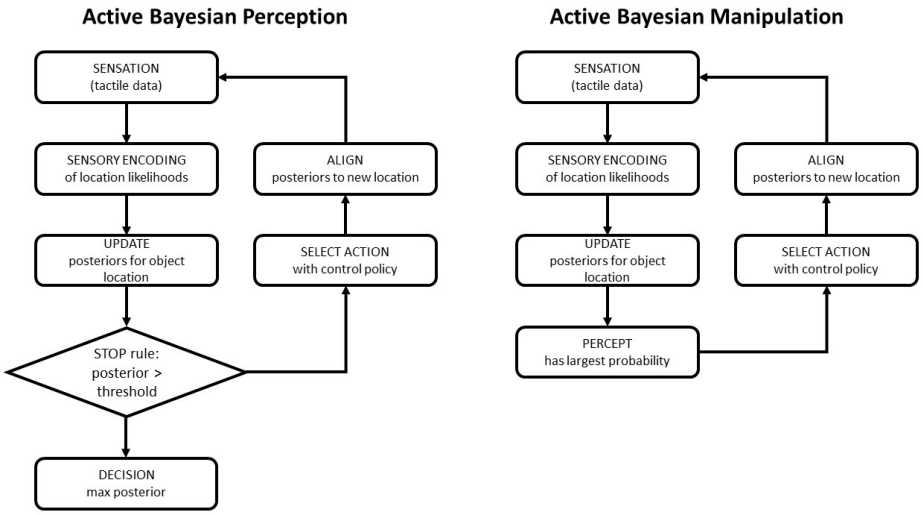

Figure 4.4: The algorithm for tactile active Bayesian manipulation is derived from methods for active Bayesian Perception. The difference between the methods for perception and manipulation are in the end goals. For perception, once the probability of the posterior reaches a threshold, system stops and reveals a decision. Whereas in manipulation the loop is kept closed with no stop rule. In the active manipulation methods used here the tactile data is used to determine likelihoods for object location, which update location posteriors; the estimated location from the maximal posterior feeds into the control policy, and the probabilities are then realigned with the resulting move.

Measurement model and likelihood estimation The location likelihoods $P(z_t|x_l)$ use a measurement model of the training data for each location x_l

$$\log P(z_t|x_l) = \sum_{k=1}^{N_{dims}} \sum_{j=1}^{N_{samples}} \frac{\log P_k(s_k(j)|x_l)}{N_{samples} N_{dims}} \tag{4.2}$$

constructed by assuming all data dimensions k and samples $s_k(j)$ within each contact are independent (so individual log likelihoods sum). Here this sum is normalized by the total number of data points $N_{samples}N_{dims}$ to ensure that the likelihoods do not scale with the sample number of a contact.

Following other work on robot tactile perception [174], the probabilities $P_k(s_k(j)|x_l)$ are found with a histogram method applied to training data for each location x_l. The sensor values s_k for data dimension k are binned into equal intervals I_b, $1 \le b \le N_{bins}$ over their range (here with $N_{bins} = 100$). The sampling distribution is given by the normalized histogram counts $n_{kl}(b)$ for training class x_l:

$$P_k(s_k|x_l) = P_k(b|x_l) = \frac{n_{kl}(b) + \epsilon}{\sum_{b=1}^{N_{bins}} n_{kl}(b)}, \tag{4.3}$$

where $n_{kl}(b)$ is the sample count in bin b for dimension k over all training data in class x_l. Technically, the likelihood is ill-defined if any histogram bin is empty, which is fixed by regularizing

the bin counts with a small constant ($\epsilon \ll 1$).

Bayesian belief update Bayes' rule is used after each successive test contact z_t to recursively update the posterior location beliefs $P(x_l|z_{1:t})$ for the perceptual classes with the location likelihoods $P(z_t|x_l)$ of that contact data

$$P(x_l|z_{1:t}) = \frac{P(z_t|x_l)P(x_l;t)}{P(z_t)}, \tag{4.4}$$

from background information given by the prior location beliefs $P(x_l;t)$ at time t. The marginal probabilities are

$$P(z_t) = \sum_{l=1}^{N_{loc}} P(z_t|x_l)P(x_l;t). \tag{4.5}$$

A sequence of contacts $z_1,\cdots,z_t$ results in a sequence of posterior beliefs $P(x_l|z_1),\cdots,P(x_l|z_{1:t})$ initialized from uniform priors $P(x_l|z_0) = 1/N_{loc}$.

Here we differ in an important way from past work in specifying a relation between the prior location beliefs $P(x_l;t)$ and previous posterior beliefs, rather than assuming the two are identical. We assume a *prior belief model* that the two are related by a (normalized) power law

$$P(x_l;t) = \frac{[P(x_l|z_{1:t-1})]^\alpha}{\sum_{l=1}^{N_{loc}}[P(x_l|z_{1:t-1})]^\alpha}. \tag{4.6}$$

The parameter α represents the influence of past posteriors on the prior: for $\alpha = 1$ the priors equal the previous posteriors $P(x_l;t) = P(x_l|z_{1:t-1})$ and the method becomes standard recursive Bayesian inference; for $\alpha = 0$ the priors are flat $P(x_l;t) = 1/N_{loc}$ so the posteriors equal the location likelihoods $P(x_l;t) = P(z_t|x_l)$; and for $0 < \alpha < 1$, the prior belief model interpolates between these two cases.

Location perception Here we infer the location of the object relative to the fingertip from the maximal posterior belief $P(x_l|z_{1:t})$, with estimated location x_{est} at time t of

$$x_{est}(t) = \arg\max_{x_l} P(x_l|z_{1:t}). \tag{4.7}$$

In the special case $\alpha = 0$ of flat prior beliefs, the location perception reduces to maximum likelihood estimation

$$x_{est}(t) = \arg\max_{x_l} P(z_t|x_l), \qquad \alpha = 0, \tag{4.8}$$

with the perception made only from the present contact data z_t, disregarding the contact history.

Active manipulation Here we use a control policy $x \leftarrow x + \pi$ to move the sensor and hence object based on the present beliefs of relative object-fingertip location. We consider a control policy that seeks to move the object along a target trajectory $x_{traj}(t)$ relative to the fingertip

$$x \leftarrow x + \pi(t), \;\; \pi(t) = x_{traj}(t) - x_{est}(t), \tag{4.9}$$

which for simplicity depends on the posteriors only through the estimated location $x_{est}(t)$ (Equation 4.7). In practise, the change in position $\pi(t)$ is translated into a discrete number of location classes $\Delta l = \pi(t)/\Delta x$, by a linear scaling because move increments Δx are assumed uniform. We also restrict moves to at most 10 mm to prevent large jumps in position.

After a move of Δl location classes, the location beliefs $P(x_l|z_{1:t})$ should be kept aligned with the sensor by shifting the class probabilities by the number of classes moved

$$\begin{aligned} P(x_l|z_{1:t}) \leftarrow P(x_{l-\Delta l}|z_{1:t}) \;\; if \;\; 1 \leq x_{l-\Delta l} \leq N_{loc}, \\ else \; P(x_l|z_{1:t}) \leftarrow P(x_1|z_{1:t}) \;\; or \;\; P(x_{N_{loc}}|z_{1:t}). \end{aligned} \tag{4.10}$$

For simplicity, the (undetermined) probabilites shifted from outside the location range are assumed uniform and given by the existing probability at that extremity of the range (probabilities can then be renormalized to have unit sum).

Offline and online validation Offline validation provides an analysis of localization accuracy and algorithm performance using cross-validation performed after data collection. Two sets of data, termed training and testing, are gathered for cross-validation. A Monte-Carlo method is then used to randomly select data from the testing set for analysis of localization accuracy based on likelihoods determined from the training set. Localization accuracy is quantified with the mean absolute error $e_{loc}(x) = \langle |x - x_{est}| \rangle$ over all classified x_{est} location values with true location class x.

Online validation adds a physical confirmation of the method's performance during real-time robot operation. For online testing, the test data and robot are controlled in real-time using a closed loop between data capture and control, with localization based on likelihoods determined from the same training set used for offline testing. Online validation is applied to demonstrating tactile manipulation performance.

4.2.4 Results

4.2.4.1 Inspection of data

Data for the TacTip (Figure 4.5) were collected while the sensor gradually rolled the test object (cylinder, 40 mm diameter) with a small (0.1 mm) lateral displacement to span a 80 mm location range over 800 incremental displacements. Contact features from the stimulus are encoded in the time-series response of each pin (coloured on Figure 4.5).

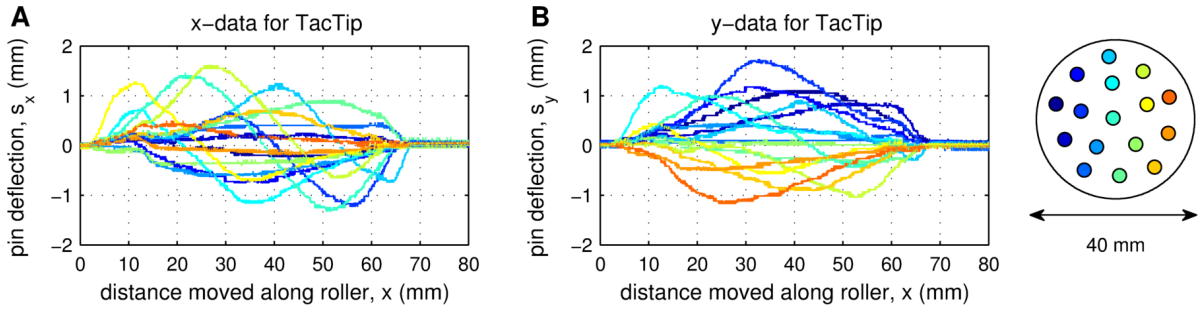

Figure 4.5: Tactile data for TacTip rolling the test cylinder (40 mm dia.). Discrete lateral movements of 0.1 mm spanned an 80 mm location range over 800 increments. Data is shown for the pin s_x-displacements (panel A) and s_y-displacements (panel B). Pins are colored according to location on the fingertip.

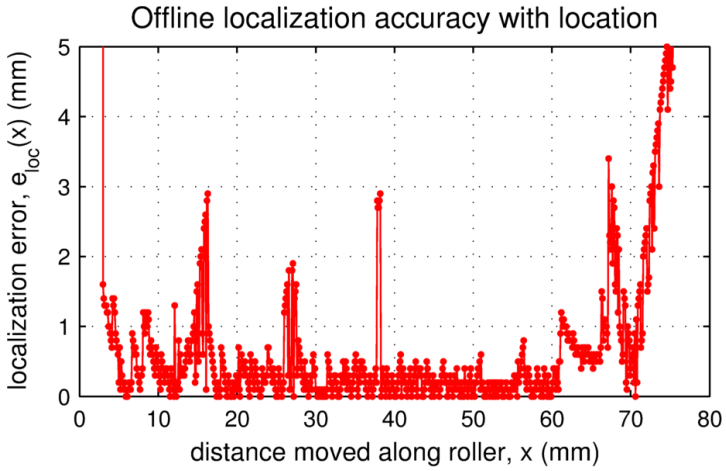

Figure 4.6: Dependence of location error $e_{loc}(x)$ on location x. Location classification uses maximum likelihood estimation. The dependence has an underlying (noisy) U-shaped function with good perception across the central range. (Results over 10000 Monte Carlo iterations.)

The most obvious effect of laterally displacing the sensor to roll the object was a change in the activation of tactile elements, permitting classification of where the cylinder is located relative to the TacTip. For example, in the pattern of s_x and s_y displacements (Figs 4.5A,B), the left-most locations activate the taxels plotted in blue on the left of the TacTip (*c.f.* Fig. 4.5), changing as the TacTip moves rightwards to the taxels plotted in red on the right.

4.2.4.2 Offline localization accuracy

The localization accuracy of the TacTip is first assessed with an offline validation applied to single increments of data at locations x_l across the 80 mm range. Results are generated with an offline Monte Carlo procedure, repeatedly drawing from the test data (Sec. 4.2.3.2) and determining location based on maximum likelihood estimation (Equation 4.8).

The location error $e_{loc}(x)$ varies strongly with test location (Figure 4.6). The largest errors

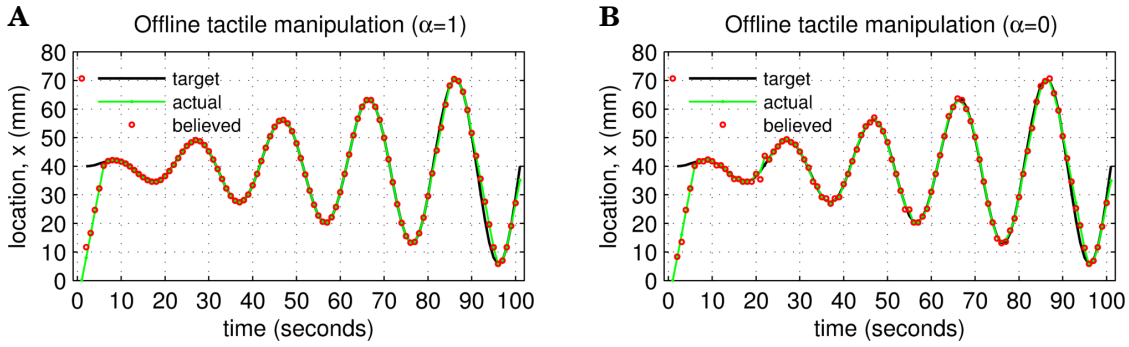

Figure 4.7: Tactile manipulation in a simulated environment drawn from validation data. Performance for (A) recursive ($\alpha = 1$) Bayesian inference; and (B) maximum likelihood estimation ($\alpha = 0$). Target trajectories (black) are well tracked by the actual movements (green) and believed locations (red), with slightly better performance for the Bayesian method.

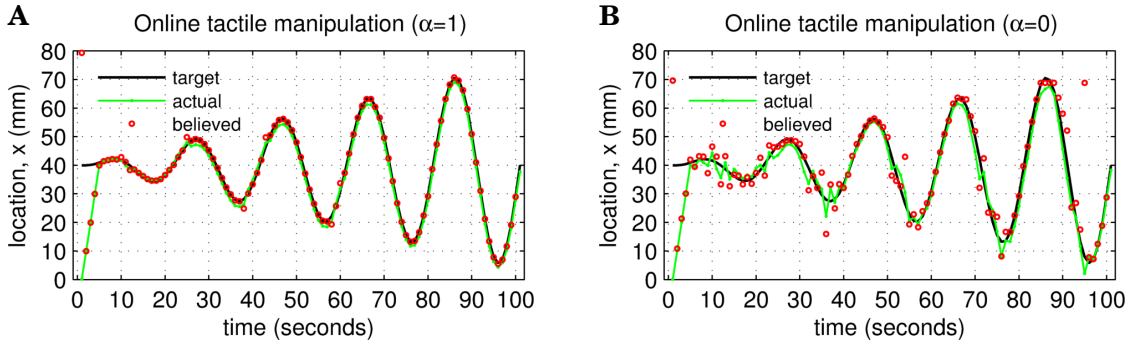

Figure 4.8: Tactile manipulation in real-time on the robot. Panels are as in Figure 4.7. With Bayesian inference, the target trajectories (black) are well tracked (green) according to the believed locations (red), with poorer but still approximate success for the maximum likelihood method.

are $e_{loc}(x) \gtrsim 5$ mm for glancing or no contacts near the extremities ($x < 5$ mm and $x > 65$ mm) of the range. The smallest location errors $e_{loc}(x) \lesssim 0.5$ mm are in the central region (roughly 5 mm$\leq x \leq$ 65 mm) when the sensor is fully in contact with the test cylinder. These results show that the roller can be accurately localized (to sub-millimeter acuity) while the fingertip makes good contact with the object.

4.2.4.3 Validation of tactile manipulation

Validation of tactile manipulation capability was implemented by moving the cylinder along a target trajectory using only tactile data to control sensory location. For all experiments, we used a sinusoidal trajectory with linear increasing amplitude $x_{traj}(t) = 0.4t\sin(2\pi t/20)$ with period 20 sec and amplitude 40 mm after 100 sec.

An initial offline testing of tactile manipulation capability was implemented using the training and test data sets to perform simulated manipulation of the cylinder. Data was sampled from the test set during the manipulation task according to the simulated location of the sensor. For both

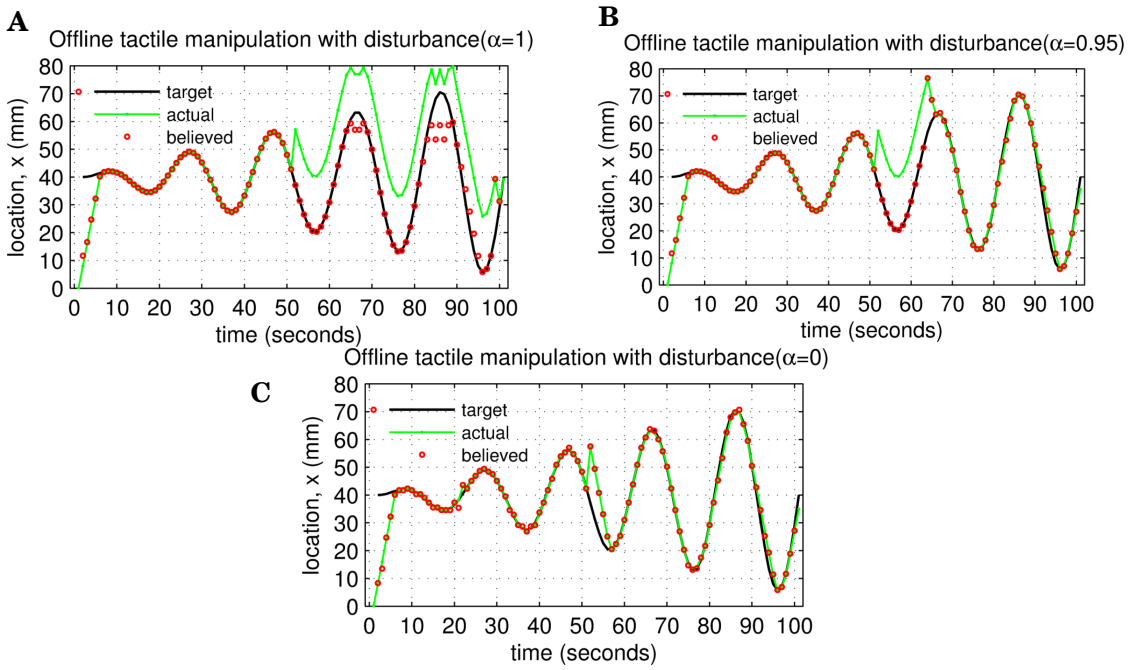

Figure 4.9: Tactile manipulation in an offline environment with disturbance. Performance for (A) recursive ($\alpha = 1$) Bayesian inference; (B) recursive ($\alpha = 0.95$) inference with diminished priors; and (C) maximum likelihood estimation ($\alpha = 0$). Only the methods with diminished priors and maximum likelihood can correct the disturbance, at the expense of reduced accuracy.

recursive Bayesian ($\alpha = 1$) and maximum likelihood ($\alpha = 0$) estimates of location, the simulated trajectory was successfully followed (Figure 4.7). The Bayesian case (Figure 4.7A) had near perfect accuracy, whereas the maximum likelihood case (Figure 4.7B) had sub-millimeter deviations from the target trajectory, consistent with the offline estimate of localization error (Figure 4.5). The superiority of the Bayesian approach is expected because evidence for location is integrated over the entire data history $z_{1:t}$, rather than just one increment z_t.

For online testing, the tactile manipulation was successfully performed in real-time, following the target trajectory similarly to offline validation but with less accuracy (Figure. 4.8). The recursive Bayesian method ($\alpha = 1$) had near perfect accuracy with a couple of small deviations $\lesssim 2$ mm near the beginning of the experiment (Figure 4.8A); the maximum likelihood method ($\alpha = 0$) was more inaccurate with deviations ~ 5 mm over the entire trajectory (Figure 4.8B).

The differences between offline and online testing are due to sources of noise in real-time on the robot not present in the pre-gathered test data. For example, move increments during gathering data are always $\Delta x = 0.1$ mm, whereas increments during online testing can be up to ± 10 mm; and there may be other unknown differences between real-time operation and offline validation. This illustrates the importance of online validation for testing actual robot performance. The overall conclusion is that the recursive Bayesian method ($\alpha = 1$) is superior to the maximum likelihood method ($\alpha = 0$).

4.2.4.4 Tactile manipulation with a disturbance

To test the robustness of the tactile manipulation, the validation was repeated introducing an unknown disturbance into the system. Midway through the trial (50 sec), the cylinder location was moved laterally by 20 mm. The effectiveness of the tactile manipulation to correct for this unknown movement by repositioning the cylinder back onto its target trajectory was then examined.

For offline testing, the tactile manipulation responded in different ways to the disturbance (Figure 4.9) depending on the parameter α from 1 down to 0 that represents a diminishing influence of past posteriors on current priors. The overall behaviour was that the tactile manipulation responds more quickly to the disturbance as the value of α is decreased. At $\alpha = 1$, the tactile manipulation completely ignores new sensory data that the location of the cylinder has moved, and consequently the trajectory after the disturbance is offset from the target trajectory (Figure 4.9A). At $\alpha = 0$, the tactile manipulation responds immediately to the change in location of the cylinder and corrects onto the target trajectory (Figure 4.9C). For an intermediate value $\alpha < 0.95$, the tactile manipulation took ~10 sec to realize the location had shifted, then corrects onto the target trajectory (Figure 4.9B).

For online testing, the tactile manipulation responded to the disturbance similarly to the offline test (Figure 4.10): for $\alpha = 1$, the trajectory after the disturbance was not corrected (Figure 4.10A), for $\alpha = 0.95$, the trajectory after the disturbance was corrected after a delay of ~10 sec

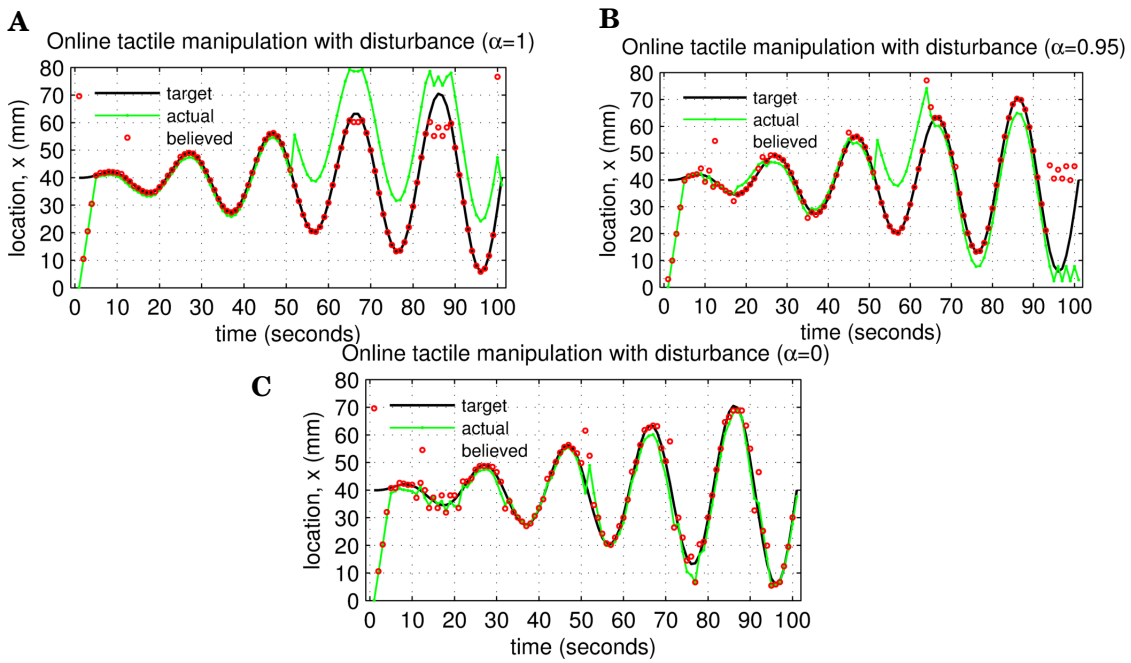

Figure 4.10: Tactile manipulation in real-time on the robot with disturbance. Panels are as in Figure 4.9. Only the methods with diminished priors and maximum likelihood can correct the disturbance, at the expense of accuracy deteriorating with lower α before the disturbance.

(Figure 4.10B), and for $\alpha = 0$ the trajectory was corrected immediately (Figure 4.10C). These improvements in ability to respond to change as α decreases from 1 to 0, representing a diminishing effect of posteriors on priors, were accompanied by a deterioration of the accuracy of the tactile manipulation in following the trajectory, as observed in the previous section. There thus appears to be a trade-off between the responsiveness to unknown change and the manipulation accuracy when using tactile information to control object location.

4.2.5 Discussion

Biomimetic tactile manipulation based on active touch gives accurate control of rolling a cylinder with an artificial fingertip. Experiments were performed with a tactile fingertip (the TacTip) mounted as end-effector on an ABB robot arm, with which lateral movements could manipulate (roll) the cylinder from side-to-side. Location perception was achieved with decision making methods, giving sub-millimeter localization finer than the sensor resolution. In consequence, the tactile manipulation was performed at superresolved accuracy along a complex trajectory.

Subtleties were indicated under large (20 mm) disturbances of cylinder location during testing: the system has no ability to anticipate the disturbance, but can react to the sudden change in perceived object location. The capability of the tactile system to react to a change in object location was found to depend on the Bayesian update rule for the location belief during perceptual decision making. If the prior beliefs for estimating location are set equal to the posterior beliefs for the previous estimate, the system was not able to perceive sudden changes of location. This was because the prior beliefs had become sufficiently peaked late in the trial that new sensory evidence for location was ignored.

These problems with estimating object location could be addressed with a maximum likelihood procedure applied to just the present contact data (equivalently, the prior beliefs are considered flat). However, this solution came at the cost of reducing the accuracy of tactile manipulation. Therefore, we proposed an intermediate solution in which the prior beliefs are diminished by a power law relative to the posterior beliefs, giving moderately accurate performance that can respond to sudden changes in location. In general, there is a trade-off between responsiveness to unknown change and manipulation accuracy, to be set appropriately for the task.

We expect the trade-off between responsiveness to change and accuracy is a general aspect of tactile manipulation. The situation bears analogy with utilizing a Kalman filter to combine information for accurate control, which is linked with recent tactile manipulation methods based on classical control theory [169] and particle filters [171]. Our expectation is that understanding the relation between these approaches and the biomimetic approach proposed here will help in solving the overall problem of attaining robust and general tactile manipulation in complex and uncertain environments

4.3 Postface

4.3.1 In-Hand Rolling

The work discussed through Section 4.3.1 was published in the paper entitled *'Tactile Manipulation With a TacThumb Integrated on the Open-Hand M2 Gripper'* [33]. With the contributions as follows.

- Benjamin Ward-Cherrier:
  - Developed the hardware integration of the TacTip with the M2 gripper.
  - Designed the experimental procedure to explore basic in-hand tactile manipulation.
  - Performed the analysis of data and results.
- Luke Cramphorn:
  - Provided input on the experimental procedure based on the work presented in Section 4.2.
  - Helped with the development of the hardware integration of the M2 gripper.
  - Provided input and assistance for implementation of methods for data analysis, and for the interpretation of the experimental results.
- Nathan F. Lepora:
  - Provided supervision over the work.
  - Produced the base architecture used for classification and validation.
  - Provided input into the construction of experiments, data collection, and data analysis.

4.3.1.1 Taking Tactile Rolling Further

The research conducted in the publication presented in Section 4.2 demonstrated the basic manipulation of rolling, whilst using only tactile feedback. This tactile rolling task demonstrated the function of active tactile manipulation from active tactile perception. Logical continuation of this work was to implement the manipulation on a more practical system. In this case, the performing of manipulation with a hand rather than the constrained system used prior. In-hand manipulation is the main end goal of work like this at it opens up the potential use of robotic systems greatly.

Figure 4.11: Image of the GRAB Lab OpenHand Model M2 with integrated TacThumb. The TacThumb is elongated tactile sensor implemented with the TacTip technology.

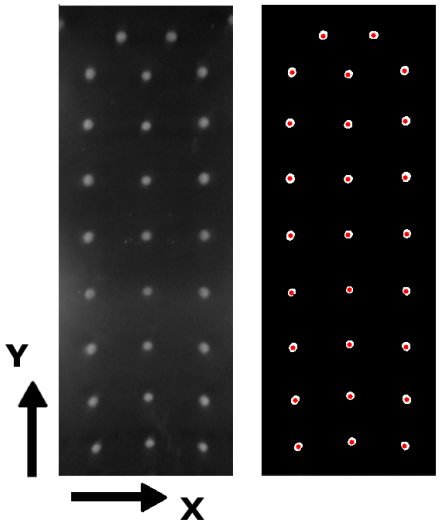

Figure 4.12: The TacThumb sensor uses an array of pin on the interior of a compliant skin (left). These pins are identified using OpenCV and their coordinates are use as data for the tactile perception algorithms

4.3.1.2 Integration of a 3D Printed Sensor and a 3D Printed Hand

Yale university's GRAB Lab conducts a wide spectrum of research, including into robotic manipulation [111]. The group has made a selection of their hand/manipulator designs open source through the Yale OpenHand project [112]. For an initial exploration into tactile in-hand manipulation the OpenHand Model M2 (multi-modality) hand provides a good platform for integrating the TacTip, due to its 3D printed design, low cost, and modular thumb. The hand has two Dynamixal MX-28 servo motors each controlling one of an antagonist pair of tendons, this allows the finger to be controlled in underactuated or a fully-actuated behaviour. Although the hand system only provides a limit range for rolling tasks (~ 20 mm for the consider objects) due to the nature of the mobile finger design.

The integration of TacTip technology and the Model M2 utilises the multi-material 3D printing methods discussed in Chapter 3, as these methods are fast, versatile, and able to accommodate the more complex shape needed. The sensor is designed to match the proportions of the thumb module of the M2 in length and width, whilst providing the tactile capabilities of the TacTip (Figure 4.11). This 'TacThumb' has 26 pins in a square arrangement viewed by a modified Microsoft Lifecam as in the standard design (see Figure 4.12). The skin and flesh of the sensor are TangoBlack+ and Techsil respectively, with a custom LED ring illuminating the interior.

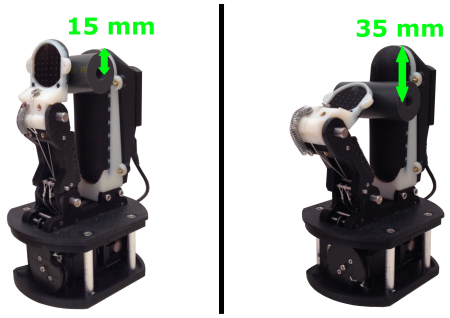

Figure 4.13: The range of data collection and manipulation of the Model M2 gripper. With starting position left and final position right.

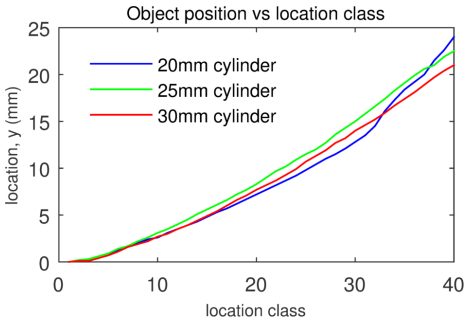

Figure 4.14: The position of the roller along the thumb is tracked using optical software to validate its position. The graph shows these real positions against the recorded data class for the three stimulus used in the experiments.

4.3.1.3 Data Collection

The M2 provides a finger that can be controlled to perform the motion necessary to roll a cylinder up and down the TacThumb. To explore this manipulation tactile data from the TacThumb is collected as a stimulus is gripped and then rolled towards the palm (Figure 4.13). The hand is calibrated to move the roller linearly in 0.5 mm increments over a 20 mm range (40 steps) and validated by optical tracking the position of the roller on the thumb. Data is collected for three cylindrical stimuli of 20 mm, 25 mm, and 30 mm as training data (Figure 4.14).

Testing and is conducted in two forms, off-line and on-line. Off-line testing uses two collected data sets to perform a cross-validation, providing an analysis of localisation accuracy and algorithm performance. On-line testing uses real-time collection of tactile data against training sets to perform the active manipulation of the stimuli.

4.3.1.4 Data Processing and Results

Processing the collected data utilises the methods presented in the Section 4.2 under Methods of the same title, and additionally in the publications by Nathan F. Lepora *et al.* referenced here [27, 146]. Please refer to Section 4.2 for greater detail.

Passive validation A distinct set of data is sampled for testing randomly via a Monte-Carlo procedure (1,000 iteration per location class). At each location a decision error is given by the mean absolute error $e_{loc}(x) = \langle |x - x_{est}| \rangle$ over all classified x_{est}.

Performance at 5-20 mm of the movement range is (20-35 mm from the TacThumb tip) is higher, with errors averaging $e_{loc} \approx 0.1$ mm. In the 0-5 mm movement range (15-20 mm from tip), accuracy drops to $e_{loc} = 0.6$ mm. This is most likely due to a lower number of pins being displaced by the stimulus at this location of the sensor.

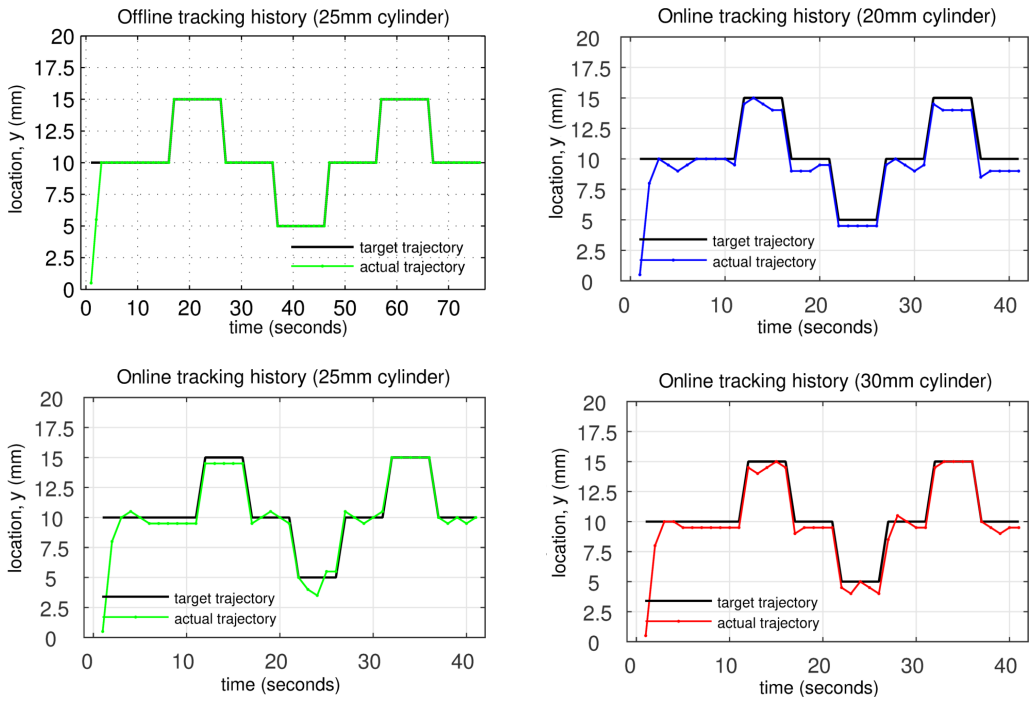

Figure 4.15: Trajectory following results (clockwise from top left): Simulated active tactile manipulation with a 25 mm cylinder. Online active tactile manipulation with a 20 mm diameter cylinder. Online active tactile manipulation with a 25 mm diameter cylinder. Online active tactile manipulation with a 30 mm diameter cylinder

Active Manipulation For the active (on-line) manipulation of the roller, a control policy is used to move the fingertip so that the stimuli follow a goal trajectory. The trajectory used gives the hand the goal to move the cylinder to the centre of the location range (10 mm), then to subsequently displace it 5 mm in one direction and back then 5 mm in the opposite direction and back. This oscillation is repeated 1.5 times for the manipulation.

This is initially tested in simulation using a training and test set to virtually manipulate the stimulus. Simulated results of active manipulation show perfect trajectory following as can be seen in Figure 4.15 (Top Left).

This oscillation is repeated in a real-time active manipulation on the robot for the three different diameter stimuli (20 mm, 25 mm, and 30 mm). The results of these tests can be seen in Figure 4.15 (top right(20 mm), bottom left (25 mm), and bottom right (30 mm)). The error in location perception is typically below 1 mm highlighting the importance of not only testing in simulation.

This work demonstrates versatility of the presented methods by reducing the number of physical restraints on the manipulated stimuli in addition to using a variety of diameter stimuli. It also set the research on the trajectory for further exploration of in-hand manipulation and potentiality more complex dexterous hands.

4.3.2 Summary, Paper Analysis, and Closing Remarks

The work in this chapter has shown an early venture into tactile manipulation. The TacTip tactile sensor was used as an end-effector on a 6 DoF robot arm with algorithms for active perception, modified with a control policy to adjust position, and create an action on a stimuli. This action creates a basic manipulation in the form of rolling, where only tactile feedback is used to perform a trajectory task.

The work on rolling style manipulation was expanded onto a simple hand platform. This platform, GRAB Lab model M2, was modified to have integrated TacTip Technology in the form of a tactile modular thumb or TacThumb. The work showed a versatility of the methods by performing the manipulation with lower physical constraints and a variety of stimuli.

The work presented in the publication demonstrates that introducing tactile sensing provides information and feedback that allows for the control of objects based on the state of contact. In addition the work demonstrates reaction to errors, outlined as an aim of the research, as it moves the work closer to unstructured environments. Although, this reaction to error was found to be a trade-off with accuracy. The work uses a rail and magnet system to limit the motion of the stimulus to a single dimension of rolling. This was done for validation purposes, in that the only disturbances in the system were the ones induced on purpose. This structured experimental set-up is in contrast to the goal of performing in unstructured environments, and thus opens the research to continue into that domain, for example the M2 gripper work.

In continuation of this theme, co-author of the presented publication and lead author on the tactile M2 publication, Benjamin Ward-Cherrier, expanded this research into a more dynamic gripper. In this work another 3D printed hand, the Gr2, with two integrated sensors and two actuated digits, demonstrates precise manipulation of cylinders between the two digits [175].

Further work on tactile manipulation will need to explore more complicated systems with a greater variety of manipulations. Such systems will need multiple sensors, digits, and degrees of control thus moving closer towards the goal of dexterous tactile manipulation.

In answer to the research question posed for this chapter, it can be said that the basic manipulation of rolling a cylinder can be achieved using, solely, the tactile perception of the state of contact. Although, greater work will be needed to determine whether this is the case for other modalities of basic manipulation such as sliding or pushing.

CHAPTER 5

TACTILE FEATURES: INFERRING THE INFORMATION FOR GREATER VERSATILITY

Previous chapters presented a Bayesian classifier to perform basic active manipulation of a roller and classification of curvature. The method requires a large amount of training data, which for complicated manipulations will be challenging to acquire. In addition, generality and versatility in unknown environments will be hard to achieve as the method is reliant on this training data.

In this chapter we propose a method that directly infers features from the sensor output, instead of using black box classifiers and regressors. This is achieved by applying Voronoi geometric tessellation to generate a third dimension that helps the inferences of some key tactile features. The author's publication 'Voronoi Features for Tactile Sensing: Direct Inference of Pressure, Shear, and Contact Locations' is the core of this chapter and will discuss development of this novel method detail. *Contributions are detailed in full at the beginning of each section that includes published material.*

5.1 Preface

The concept of 'features' is used frequently in science and technology but is not always used in the same context or with the same meaning. In pattern recognition, computer vision, and machine learning the term is used to describe elements of information needed for solving a computational task. These can be descriptive like an edge, or more general like a collection of pixels. Whereas, in computer aided design the term describes regions of parts with interesting properties. More colloquially we use features in our daily lives as descriptive primitives, such as hard, soft, sharp, smooth, and rough. These phrases embody features as qualitative information that is easy to

transfer verbally.

Here we use 'features' as a term that categorises primitive elements of tactile sensing that have both real world and computational value. These can be either descriptive elements of the interaction, like pressure, shear, and contact location (used in the publication), or they can describe the object, like hardness, shape, or temperature.

5.1.1 Research Question

As with many areas in robotics, new machine learning techniques, like deep neural networks, offers a very promising potential solution to manipulation [94, 101, 102]. In the undefined environments that future robots will need to be able to operate in, tactile perception may be crucial. Although, as tactile data is challenging to simulate this large amount of data would need to be collected in by a physical system. This will be time consuming and challenging. To this end, rather than solving the manipulation via black box methods either solely or at all, the use of preprocessing methods to directly infer key features of tactile sensing, without large training sets, could provide an alternative platform of sensor data to inform dexterous manipulation.

Question What key features can be identified from tactile data without training black-box methods like classifiers or regressors and will this enable greater versatility and generality of tactile sensing?

5.2 (Publication) Voronoi Features for Tactile Sensing: Direct Inference of Pressure, Shear, and Contact Locations

The work presented so far in this thesis has used methods that require large training sets and accurate odometry. As we move away from defined environments and stimuli collecting this data will be more difficult. This has raised the questions on the practicality of using black-box methods with large training sets for aspects of tactile manipulation. This section presents the publication that describes a novel method for inferring key tactile features directly from sensor data, and thus removing the need for large training sets to make perceptions.

The following section has been published in a paper entitled *"Voronoi Features for Tactile Sensing: Direct Inference of Pressure, Shear, and Contact Locations"*. This publication was peer reviewed for and presented at the International Conference on Robotics and Automation (ICRA) in 2018. The contributions for this publication are as follows.

- Luke Cramphorn:
  - Developed the concept of extracting area information from TacTip data for use in the inference of tactile features.
  - Designed and implemented the developed concept within Matlab.

  - Designed the experimental procedure for validating the developed method.
  - Performed the analysis experimental results.

- John Lloyd:
  - Provided assistance and input in to the implementation of the software.

- Nathan F. Lepora:
  - Provided supervision over the work.
  - Provided input into the data analysis.

Some text within this paper has been removed as the information has already been provided earlier in this thesis.

Abstract - There are a wide range of features that tactile contact provides, each with different aspects of information that can be used for object grasping, manipulation, and perception. In this paper inference of some key tactile features, tip displacement, contact location, shear direction and magnitude, is demonstrated by introducing a novel method of transducing a third dimension to the sensor data via Voronoi tessellation. The inferred features are displayed throughout the work in a new visualisation mode derived from the Voronoi tessellation; these visualisations create easier interpretation of data from an optical tactile sensor that measures local shear from displacement of internal pins (the TacTip). The output values of tip displacement and shear magnitude are calibrated to appropriate mechanical units and validate the direction of shear inferred from the sensor. We show that these methods can infer the direction of shear to ~2.3° without the need for training a classifier or regressor. The approach demonstrated here will increase the versatility and generality of the sensors and thus allow the sensor to be used in more unstructured and unknown environments, as well as improve the use of these tactile sensors in more complex systems such as robot hands.

5.2.1 Introduction

Tactile perception is an important ability for any manipulator, whether that be a human or robotic hand. The ability to interpret key tactile features is crucial for making decisions on the perception and manipulation of objects and environments. Increasingly popular tools for these sensory task in robotics are optical tactile sensors. The reason for this being that such sensors like the TacTip, GelSight [176] and MIS sensor from KCL [177] are low cost and customizable, as well as robust with high acuity.

In optical tactile sensors, a common method to transduce deformation of the sensing surface is to fix markers and track them. However, the tracked position of these markers are not directly linked with the physical dimensions of touch. This necessitates the use of black box classification

Figure 5.1: The work presented here infers tactile features from TacTip sensory data by transducing a 3^{rd} dimension of the data via Voronoi tessellation. This data can be used to produce a 3D reconstruction of the sensor tip. Shown here is sensory snapshot, reconstructed and shown with the sensor.

or regression techniques, such as neural networks or Bayesian methods, when utilising the system with robots. While able to perform complex and highly accurate open and closed loop tasks, these methods suffer from being non-transparent in how they work, time consuming to train, and limit the ability of the system to generalise for other tasks.

This paper introduces a novel method for transducing deformation of the sensing surface by computing a third dimension for the data that is directly linked to the physical dimensions of touch, by utilising the natural region properties of Voronoi tessellation. This provides the ability to link the data to physical quantities such as displacement and contact location. We also demonstrate the inference of direction and magnitude of shear forces directly from the centroid locations from the sensor output. With these features it should be possible to utilise optical tactile sensors in classifier-free interpretation of contact that is both general and accurate. A recreation of the sensor surface using the voronoi method is shown in Figure 5.1.

Voronoi tessellation is the mathematical principle of partitioning a plane into regions based on the distance between points and was defined and studied in a general n-dimensional case in 1908 by Georgy Voronoi. The Voronoi tessellation is widely used in science and technology; moreover, due to its versatility, the use of this method has been seen in art, science, geography,

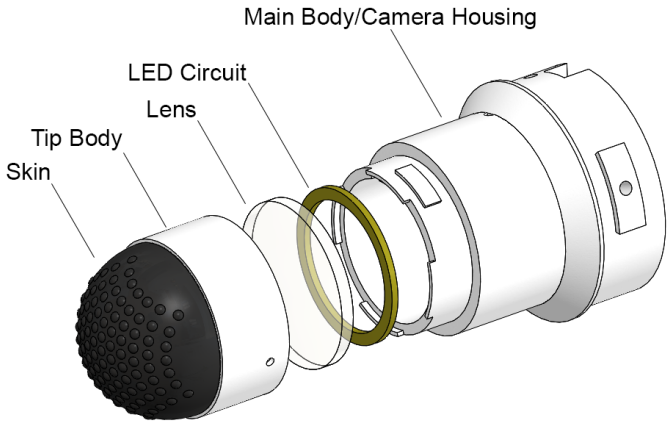

Figure 5.2: Exploded view of a TacTip optical tactile sensor. The contact surface is referred to as the skin, this is a compliant 3D printed rubber that the interior of which is endowed with pins that are tracked by the camera

and many other fields. These diagrams are very effective for extracting extra information from point-based data sets and they also provide a visual adaptation to the data that enhances human visual interpretation of the information [178].

5.2.2 Background and Related Work

There are many sensors that are capable of detecting one or a combination of tactile modalities such as pressure, shear force, torque, slip, vibration, or temperature. Each tactile feature provides information about contact stimuli that can be used for control, perception, or exploration and with each sensor modality available the richness of data greatly aids in expanding the sensor functionality [8, 139].

Surface displacement, pressure, and normal force are commonly used modalities in tactile sensors. With these, the necessary information is available for grasping an object with a sufficiently high force to maintain stability whilst restraining from applying forces that will either damage the stimulus, sensor, or manipulator. Sensors that can detect these features can use capacitive or resistive cells such as Harvards' TakkTile sensor [80], CITECs' flexible fabric-based sensor [179], or force-torque sensors like the OptoForce.

Detection of shear forces is another tactile feature that many sensors exploit. The ability to detect shear forces are, along with normal forces, very useful for optimising the forces and quality of a grasp. Shear can also be used to identify friction coefficients and has been directly linked to slip detection (another important tactile feature) [180]. Tactile systems can be built around force torque sensors such as the OptoForce OMD can directly measure these features.

Contact location is useful from a control perspective, for example knowing the location of contact will enable tactile servoing to move to a different location or even to provide action on a stimulus for stabilising grasp or manipulation. Studies highlighting this important feature

to extract from tactile sensors include work on the BioTac [79] and an anthropomorphic tactile sensor [181].

An important aspect of the present work is the visualisation of tactile data. Other methods for visualising tactile data include snapshots of a tactile contact between the sensor and the stimulus which help to interpret the data [76, 182]. Work by Cannata *et al* has demonstrated a 2D somatosensory map to represent and visualise the contact on a tactile skin [183].

From the initial development of the TacTip optical tactile sensor there have been a variety of methods implemented for interpretation the collected images. Initially, Chorley *et al*, analysed the images using a velocity vector field and centroid tracking [143]. Most work with TacTip sensors has utilised pin tracking methods to record the pin positions from frame to frame. These pin positions are outputted as centroids of the white pin heads in the form of x and y pixel coordinates. This data has been interpreted via Bayesian classification to achieve super-resolved acuity [146], basic manipulation [28], and contour following [36]. Recent work on a cylindrical TacTip designed for detection of submucosal tumours during endoscopy utilised a vector representation of relative pin movement to colour a visualisation of the data; in addition a 3D reconstruction of the test environment was created from this method [184]. This visualisation of the optical tactile sensor data helps the user to interpret the tactile data. For reference, the TacTip sensor is shown in an exploded view in Figure 5.2.

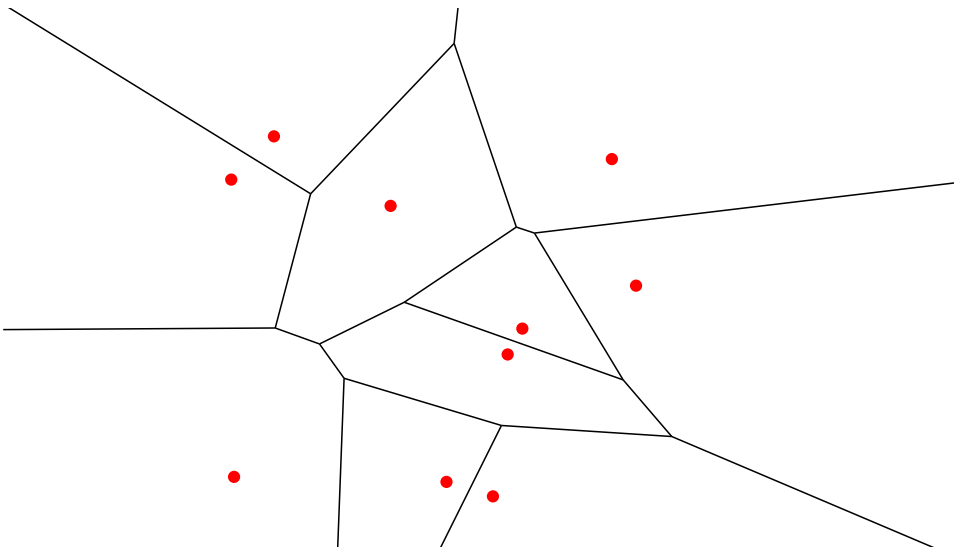

Figure 5.3: Voronoi tessellation of 10 random points. Each point along an edge is equidistant from exactly two points, and each vertex is equidistant from at least three points. The Voronoi tessellation creates unbounded cells on the edge of the data, as lines extend to infinity with no other line to intercept.

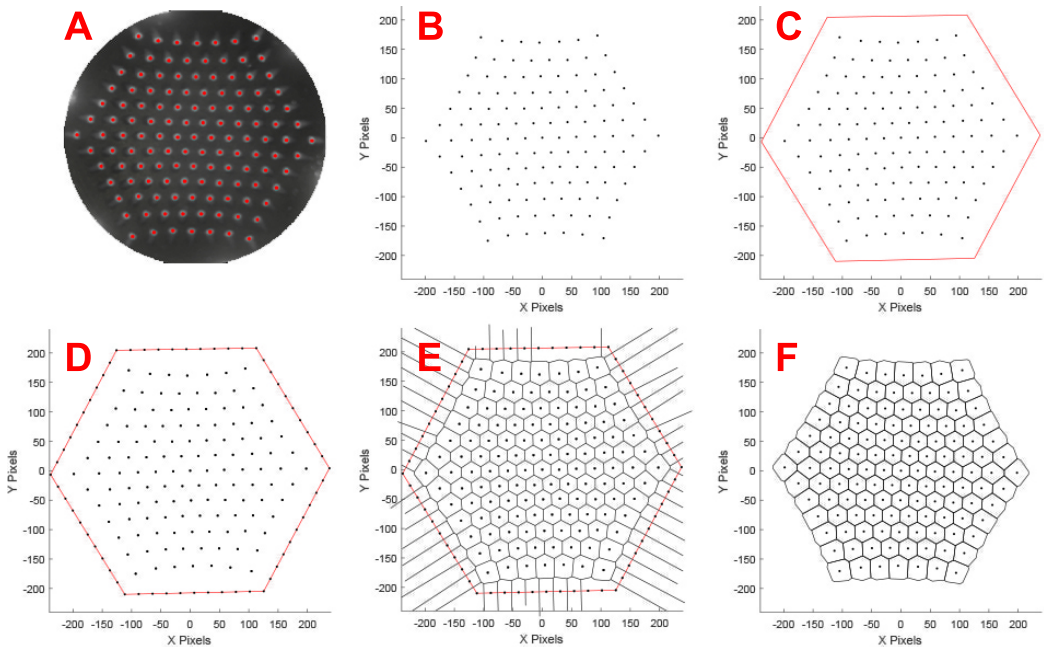

Figure 5.4: To best use the Voronoi tessellation, a bound region is desired for each centroid collected from the sensor (A,B). As the outer centroids generate cells that are unbound a boundary is genarated to enclose all the centroids (C). Along this boundary artificial points are generated (D) allowing for bound cells on the real outer centroid (E). Finally all edges, longer than a threshold, and the artificial points are deleted from the data, resulting in the visual (F).

5.2.3 Methods

5.2.3.1 Voronoi Tessellation

Voronoi tessellation is the mathematical principle of partitioning a plane into regions based on the distance between points on that plane. The regions created by this tessellation are directly associated with the point each is closest to. Rules in Voronoi tessellation are that each point along an edge is equidistant from exactly two points, and each vertex is equidistant from at least three points. Edge lines will tend to infinity if there is no other edge to intercept and create a vertex with. These infinite edges tend to occur at the edge of the point data and will result in unbounded regions. A simple example of this is shown in Figure 5.3, where a random selection of point are shown with the result of voronoi tessellation applied to them.

Construction of Voronoi Cell Data As mentioned, Voronoi tessellation is a powerful tool for extracting information from a plane defined by a series of points. Due to its usefulness there are predefined computational tools for creating this tessellation on a set of input points.

To make the best use of the Voronoi tessellation, it is desirable to have bound cells for every centroid recorded by the sensor (Figure 5.4A,B). The outer centroids generate cells that are unbound, to solve this a boundary (Figure 5.4C) fitted with artificial centroid points (Figure 5.4D enclosing the real data. By doing this the unbound Voronoi cells are around artificial points

rather than real centroid data (Figure 5.4E). The point along the boundary have a density higher than that of the inner points allowing for a more stable outer cell shape when the Voronoi is applied. Removing edges longer than those in the centre and deleting artificial points from the data leaves Voronoi cell structure for all recorded centroids (Figure 5.4F).

The area of the bound cells produced by the Voronoi tessellation provide new information that is valuable for tactile perception. Specifically the change in each regions areas relates to sensor compression when they increase and swelling (due to stable internal volume) when they decrease.

Inference of key Tactile Features Each of the tactile features - pressure, shear, and contact location - provides useful information about contacted stimuli. The combination of these sensory modalities can be used to provide a rich information base for perception and manipulation of objects.

a) Surface Displacement, Pressure, and Normal Force: The normal force exerted on the tip will be proportional to the extent of deformation the sensor undergoes. Thus being able to infer the level of deformation is important. The area values for each Voronoi cell can be used as a z-dimension in a surface fit via cubic interpolation. This 3-dimensional surface produced a proportional approximation of surface deformation and indention. The integral of this surface is the volume of deformation, a value that can be easily calibrated to mechanical units of force or displacement and combined with the area of contact for pressure.

b) Contact Location and Multi-Contact Detection: The 3D surface data created to infer deformation can also be utilised to determine an approximation of the contact locations. Contact location provides information that can be used to asses many aspects of how the sensing surface is interacting with an object. Inferring contact locations can be done by finding the maxima on the surface where the contact location is assumed to be the regions of greatest deformation.

This extends to multiple contacts when the local maxima are taken into account. To find local maxima on the surface, the data is treated as an image ($n \times m$ matrix of values). The regional maxima of this matrix are connected components of pixels (array values) with a constant intensity value with external boundary pixels all with values less than these. The result is a binary $n \times m$ array where 1 identifies the regional maxima and all other array values are 0 (implemented by the *imregionalmax* function in MATLAB). This returns the coordinates of local maxima in the data, of which all maxima below a contact threshold are removed.

c) Local and Global Shear: Inferring shear from the TacTip is achievable by looking at the velocity vectors of each centroid from frame 1 (calibration frame) to the current frame, as noted in the original TacTip paper [143]. Each centroid has an associated vector that measures local shear. These local shears can be grouped to average regions of shears or they can be combined globally to compute the overall global shear on the tip. Naturally this vector can be broken down into an estimation of shear direction and shear magnitude.

5.2.3.2 Experimental Procedure

Validating the tactile modalities inferred here requires a system that can control the sensor position with high precession. Following prior work using the TacTip, the sensor is mounted on a 6 dof robot arm (IRB 120, ABB Robotics) with absolute position repeatability 0.01 mm [29, 33, 146].

The raw values produced through the shear magnitude and surface displacement modalities, mentioned in the above methods, are in the units of the methods used to infer them (e.g. mm). Calibrating the values to mechanical units allows for better understanding of the system and allows comparison with other sensors. Calibration data is collected on a flat level surface using the robot arm. For indentation depth, recordings of 10 sample frames per step, at depths of 0 mm to 5 mm in steps of 0.1 mm. For the physical arm set-up, used here, it is best to calibrate against the displacement of the tip; which will be non-linearly related to the pressure ($\mathrm{N\,m^{-2}}$). Calibrating shear magnitude is done with 10 sample frames per step, collected for shear distances of 0 mm to 2 mm in steps of 0.1 mm. The resulting data (recordings against telemetry) of values is fitted via linear interpolation.

The validation of shear direction is performed by pressing the sensor into a flat level object approximately 3 mm and then creating a lateral move of another 2 mm. This shears the tip without generating slip movements, that would distort the readings for this validation. This is repeated 36 times in 10° increments from 0° to 350°. The sensor output and known shear directions are then compared.

5.2.4 Results

5.2.4.1 Surface Displacement, Pressure, and Normal Force

It can be clearly seen that when contact is made with the sensor surface that the Voronoi cells increase in area (Figure 5.5; showing centroids and camera image with visualisation). For visualisation purposes this is enhanced by assigning a colour shading to the cells based on the percentage change of the area. Shades of red are associated with sensor compression (increase in Voronoi cell area) and shades of blue for sensor expansion (decrease in Voronoi cell area).

Plotting the surface fit, (Section 5.2.3.1) for inferring the contact location, and estimating a proportional surface displacement, produces the 3D figure shown in Fig. 5.6. The maximum value on this fit is marked with a blue star (shown on Figure 5.5 for comparison). Hence the contact location can be inferred in the format of (x, y, z), where z is a value proportional to the maximum surface indentation. The volume of this surface is calculated by integration, and is proportional to an estimate of surface displacement, which in turn can be associated with the applied force on the surface and thus with the pressure exerted. The height of indentation is an amplification of real deformation, and could be calibrated to produce mechanical values for displacement, force, or pressure. Figure 5.5 also shows a ring of slightly concave surface around the peak, which represents an outer region of slight compression around the contact.

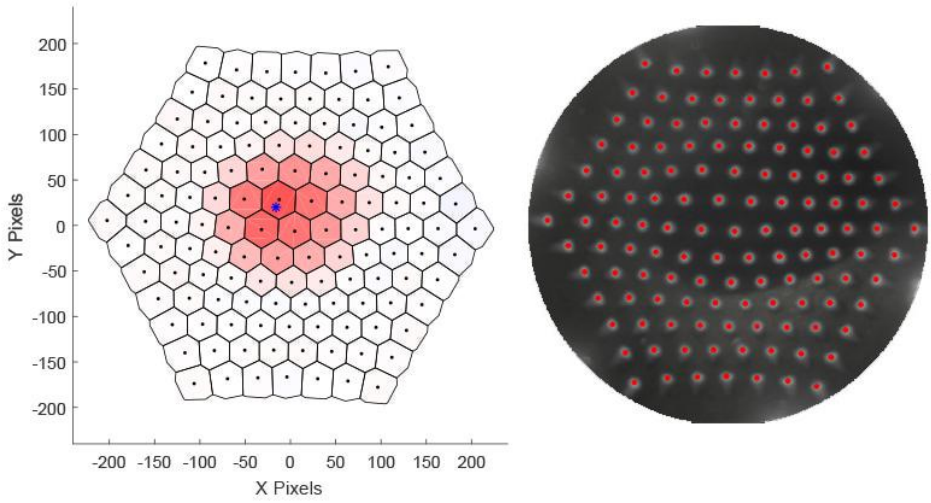

Figure 5.5: Visualisation (left) where Voronoi cells are coloured red proportional to the increase in cell area. This helps to visually interpret TacTip data. The blue asterix is the estimated centre of contact at the maximum of a smooth surface fit (Figure 5.6). The frame prior to visualising (right), emphasises the benefits of the Voronoi cell areas for visually interpreting the data.

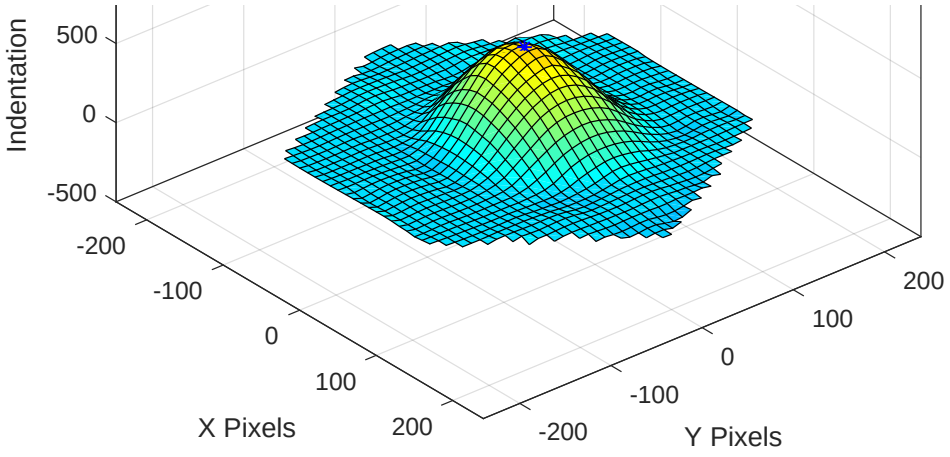

Figure 5.6: Using centroid x and y values along with the Voronoi cell areas as the z values, a 3D surface fit can be applied to the data via cubic interpolation. This fit allows for a proportional reconstruction of sensors' deformation in both compression and expansion. The maximum z value along this reconstruction is the local point of greatest deformation, and in simple contacts, such as a finger press or probe, is the centre of contact.

5.2.4.2 Contact Location and Multi-Contact Detection

Being able detect multiple regions of contact can be used to perceive multiple stimuli or a stimulus with an interesting shape. The maxima approach previously discussed and demonstrated in the pressure section of the results is easily extendible to multiple contacts. This is shown in Figure 5.7 where two distinct points of contact are inferred and then marked (as blue stars) on the visualisation.

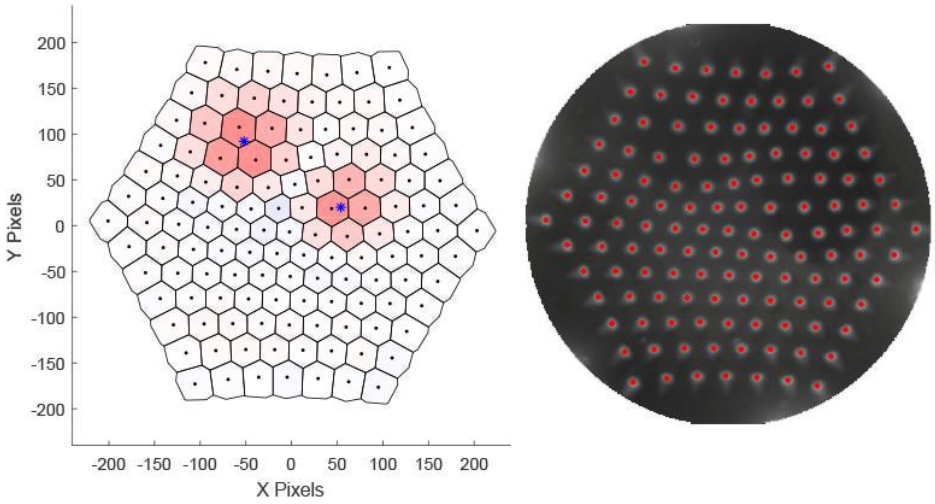

Figure 5.7: Further interpretation of the fit function can be done to detect local maxima. This means that the multiple, distinct, contact points can be identified on the sensor. Here the visual (left) shows the two contact sites with blue star marking the estimated centre of contacts. The centroids and camera image for this frame are also shown (right).

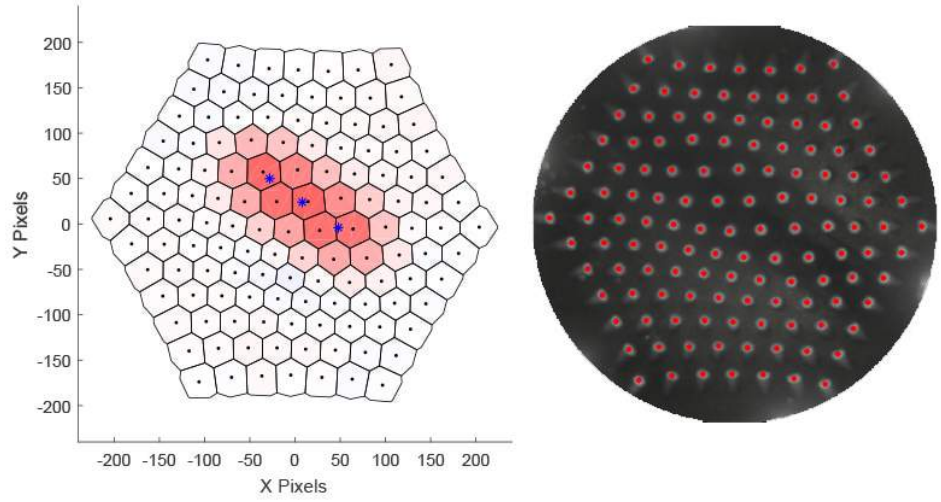

Figure 5.8: An example of an elongated contact on the sensor. The identified contact point number is greater than the number of stimuli, although this may be useful for inferring stimulus orientation.

The number of distinct contact locations that can be identified is limited by the nature of the contact. For example point contacts from simple probes that are sufficiently spaced (~4 mm) can easily be identified as separate objects. Although more complex probes, such as flat or long stimuli, create a elongated region of indentation where multi maxima are found, even though there is only a single contacting stimulus. In addition to this, flat objects create a ring of contact point around the centre of contact, due to the surface fit being a flat plane rather than a hemisphere

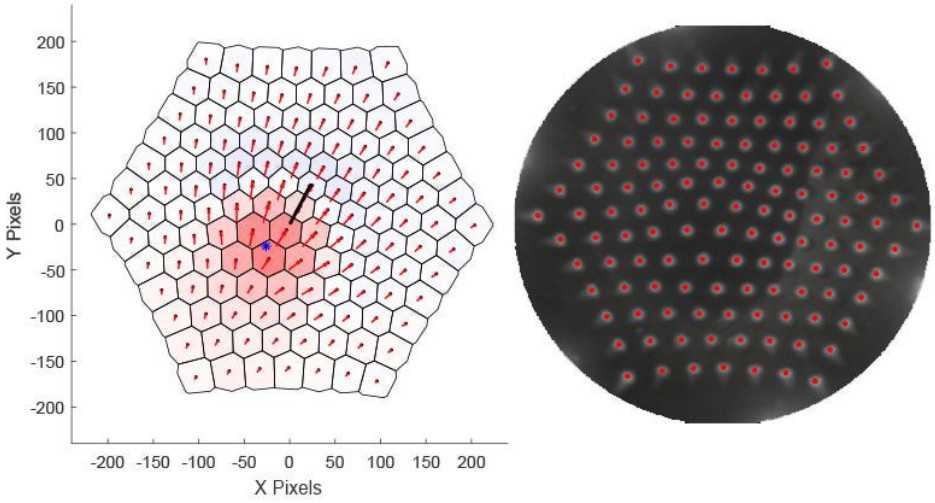

Figure 5.9: The direction and magnitude of the centroid motion vectors are associated with the shear strain on the sensor. Assuming that the velocity vectors for each of the centroids is a local shear (marked as red vectors on the visual (left)), then the average magnitude and direction of all centroid vectors will produce an average global shear vector (black arrow). Again the frame from the camera and the centroids are shown for reference (right).

like the sensor. Interestingly the long thin object generate contact locations that follow the length of the contact, which may be used for the identification of object/edge orientation by taking the direction of a line that connects these points (Figure 5.8).

5.2.4.3 Local and Global Shear

Under shear forces the centroids of the pin move relative to the shear direction, whereas under normal forces the centroids move radially from the point of contact. The global value of shear is the mean of all local shears (individual centroid motion), which will result in a non zero magnitude and direction when the contact applies shear forces. These local and global shear vectors are plotted on the visualisation in Figure 5.9. Here it can be seen that the normal component of contact is still detectable, allowing for both normal and shear forces to be detected simultaneously. The Voronoi method is not used to calculate the shear, due to the fact that it is directly inferred from the centroid data; however, there is a clear increase in sensor expansion (blue shaded cells) in a crescent around the contact site and in the direction of shear.

During the validation for inferring shear direction, the shear magnitude and tip displacement are also inferred. This shows that the modalities can be simultaneously extracted from the sensor data. Applying the calibration, described in Section 5.2.3.2, to the sensor output values produces a calibration curve for both shear magnitude and tip displacement. These represent the relationship between the sensor output and mechanical units of the arm telemetry (Figure 5.10).

The calibration curve for tip displacement (Figure 5.10, top) shows a non-linear relationship between displacement and sensor output. This suggests that the sensor is less sensitive to low

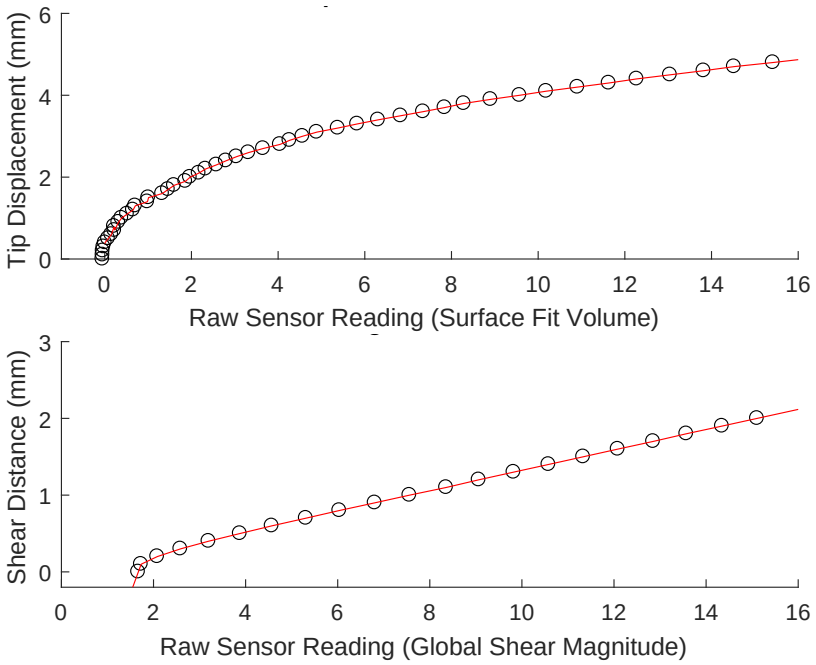

Figure 5.10: Calibration of the sensor is achieved by producing a fit (red line) between the output values (markers) of the inferencer and the telemetry values of a robot arm (see Sec. 5.2.3.2 for detail). The resulting calibration fits can be seen above for displacement (top) and for the shear magnitude (bottom)

tip displacement than it is to higher displacements.

In contrast, the fit for shear magnitude is linear (Figure 5.10, bottom), as the centroid positions when calibrated form a vector linearly related to the shear distance. The exception to this linearity is the first recording in the calibration set which has a higher inferred value than the other data would suggest. As this value has zero shear magnitude, it could be assumed that the sensor recording for no movement was in fact under a preloaded shear, possibly caused by divergence in angle between the normal of the calibration surface and the approach of the robot arm.

Validating shear direction is done by comparing inferred angles with telemetry from the arm used for controlling the sensor position (Figure 5.11). Shears are tested at 36 different direction in 10° increments around a central location. The error in inference of direction is shown in Figure 5.11 showing that the system can infer shear direction to an average of ~ 2.3°. This validation is shown in a video associated with this paper, in which the Voronoi visualisation and contact location are seen along with tip displacement, shear magnitude, and the real and inferred shear directions.

5.2.5 Discussion

This paper demonstrates a novel method for inferring tactile features from optical tactile sensor data, for generalising the use of these sensors, by producing useful information without the need

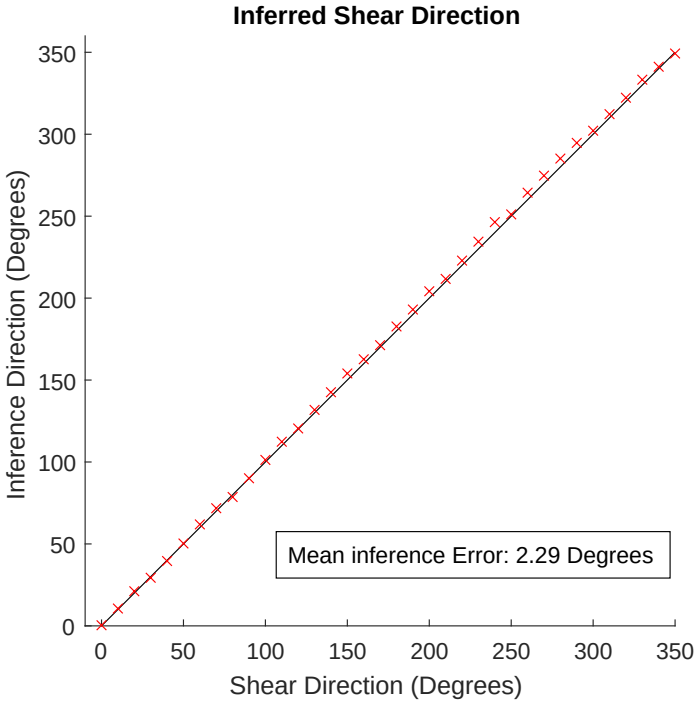

Figure 5.11: Experimental validation of inferred shear direction is done by recording robot arm telemetry. The test is carried out for shears in 10° increments for a full circle. The resulting inferred values (plotted here) shows that the inferred direction is accurate to within an average of ~ 2.3°. Thus, without training, the direction of shear can be accurately inferred.

for black-box classification or regression.

We have found that the natural features produced by performing Voronoi tessellation on the sensor data creates a tool for generating a third dimension that can be used to transduce the deformation of the surface. This transduced deformation can be utilised to produce a data visualisations that provides information useful for the inference of important tactile features. For example, deformation and contact location can be directly inferred, which would be useful for control tasks like tactile servoing [183]. We also show that it is possible to infer shear direction and magnitude directly from the centroid data due to the inherent translational information encoded in the changes of centroid positions.

The inference of shear direction is validated against arm telemetry and showed predications to an average of ~ 2.3°. Although it is likely that the error in shear direction would be lower for classifier methods previously used, it is clear that as there is no training required and the shear can be interpreted under different pressures, the generality of the method will be of benefit for future work.

The methods proposed here are the initial attempts to infer tactile features from the TacTip tactile data. There is the potential to expand the number of features inferable from the data to include inference of torque, slip, and the shape and orientation of contact stimuli. Having data

from all of these modalities will further enhance the usability and versatility of the sensor. One example for this would be to use the inference of these features to control a robot hand, a task that is challenging to do with classifiers due to the lower accuracy of hands in comparison to robot arms [76].

The visualisation of the tactile data, via the Voronoi tessellation, also proved to be a valuable output of this work, as the new visualisations make it much easier to interpret the tactile data by eye. The quote from a leading survey on Voronoi diagrams highlights this as an underlying property of the tessellation that is clearly demonstrated in these visual representations: *'Human intuition is often guided by visual perception. If one sees an underlying structure, the whole situation may be understood at a higher level.'* [178].

5.3 Postface

5.3.1 Summary, Paper Analysis, and Closing Remarks

The chapter presents a method to infer tactile features directly from TacTip data. This is achieved by applying a Voronoi tessellation to the sensor data to extrapolate a third dimension. The 3D data can be used to generate a proxy for surface deformation, that in turn allows for the inference of contact locations. In addition to this the work demonstrates the sensor's innate ability to directly infer shear direction and magnitude.

We asked the question 'What key features can be identified from tactile data without training black-box methods like classifiers or regressors and will this enable greater versatility and generality of tactile sensing?': To which the presented material demonstrated that inference of shear direction, shear magnitude, contact location, and tip displacement can be achieved without black-box methods. The feature of shear direction, in particular, was found to be inferable irrespective of contact depth and required no training. Additionally the shear magnitude and tip displacement of the sensor could be inferred with basic calibrations. With regards to improving versatility and generality of the sensing, the ability to extract a useful feature, irrespective of the contact state, adds valuable generality to the sensor when compared to the methods discussed earlier in this thesis. The extent to which these methods enable greater versatility and generality is still an open question.

These methods provide the possibility of enabling tactile servoing and potentially manipulation without collecting large datasets. This will be of particular benefit to robotic systems like hands where control accuracy is low and thus training data less reliable. Future work on this method should endeavour to demonstrate these by utilising the method on a hand based system to perform manipulation as well as further validating and identifying features that can be inferred.

CHAPTER 6

TACTILE HANDS: ADVANCING DEXTERITY OF TACTILE PLATFORMS

The work presented throughout this thesis so far has demonstrated incremental increases in understanding, performance, and versatility of the TacTip sensing technology. Taking all of these gains and combining them will result in further steps towards the goal of this thesis and hopefully the ultimate goal of dexterous manipulation. By integrating multiple sensors into hand system we open the doors to exploring this fundamental research area. This chapter documents these integrations and their findings.

In this chapter, work performed on extending the family of tactile hands is presented. Initially we will discuss the integration of the sensors with the Shadow Modular Grasper, a fully actuated three fingered robot hand. The tactile sensing of which is used to control the angle between the sensor and the object, maximising contact area. This leads into the author's publication 'The Tac-Manipulator: A tactile robotic hand with the tools for manipulation at its fingertips'(*not yet published*) where the developments of a new design of 3D printed tactile hand are presented and benchmarked. *Contributions are detailed in full at the beginning of each section that includes published material.*

6.1 Preface

6.1.1 Relevant Background

Earlier in this thesis (Section: 4.3.1) an initial venture into TacTip integration was discussed. This work resulted in the TacThumb for the GRAB Lab Model M2, and a demonstration of a rolling manipulation between finger and tactile thumb [175]. In addition to this, the TacTip

sensor has been integrated with another hand, the Gr2, to perform object reorientation via tactile feedback.

6.1.2 Research Question

Being one of the most dexterous tools known to science, the human hand is equipped with a dense and varied array of tactile sensing. To explore how this sensing benefits robotic hands it is logical to integrate tactile sensors and robotics hands. Using the work presented so far in this thesis, this chapter sets out to demonstrate the integration of the TacTip with hands systems.

Question Can the integration of tactile sensing into a multi fingered system provide data to improve dexterous capabilities?

6.1.3 Integration with a Commercial Hand

-

The work discussed through Section 6.1.3 was published in the paper entitled *'A Sense of Touch for the Shadow Modular Grasper'* [41]. The contributions were as follows:

- Nicholas Pestell:
  - Developed the hardware integration of the TacTip with the Shadow Modular Grasper.
  - Integrated the TacTip software with that of the grasper.
  - Set up and implemented the calibration of the centre of pressure.
  - Designed the experimental procedure to validate the grasp adjustment.
  - Performed the analysis of experimental results
- Luke Cramphorn:
  - Aided in the modifications and redesign of the TacTip sensor for integration
  - Designed the methods for inferring sensor data (Section ,Ä¶).
  - Implemented the Voronoi method within Python.
  - Developed the ROS wrappings for the sensor used for the software integration.
- Fotios Papadopoulos:
  - Provided expertise for the Shadow Modular Grasper.
  - Aided in the intergeneration of sensor and hand.
- Nathan F. Lepora:

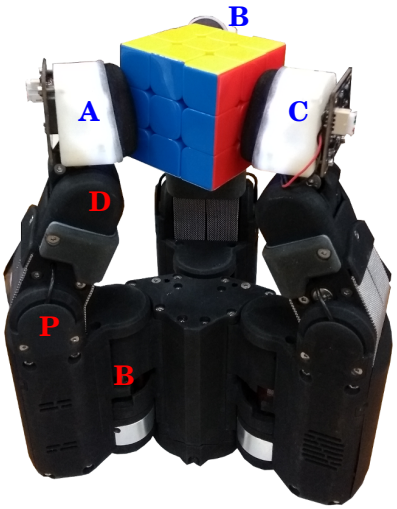

Figure 6.1: Image of the developed tactile sensors integrated with the Shadow Modular Grasper. Base, proximal and distal joints are labelled in red, **B**, **P** and **D** respectively. Tactile fingertips **A**, **B** and **C** are labelled in blue.

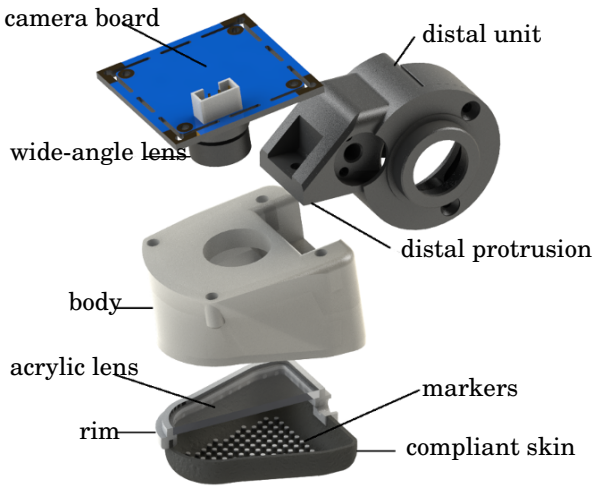

Figure 6.2: Exploded view from the CAD model of the TacTip distal integration.

- Provided supervision over the work.
- Provided input into the data analysis.

Orientation of the fingertip relative to the contact surface may be of importance when grasping an object. This is due to greater frictional forces that occur from maximising contact surface area.

6.1.3.1 Shadow Modular Grasper

At the time of writing the Modular Grasper is the latest device to be produced by the Shadow Robotics Company and has been released to address a lower price point than their other products, whilst providing comprehensive grasping capabilities. The grasper has 9 DoF (three per finger) that are fully actuated. The software of the system is constructed around a ROS framework with user control of both specific joints and whole-hand grasps. The grasping system is constructed of a number (3 in this case) of identical modular digits. Each digit has a base, proximal, and distal joint that is actuated with a DC motor for each. The setup of the Modular Grasper used here has a total mass of 2.7 kg and a payload of 2 kg with each digit capable of applying 10 N of normal force. Each joint has a dedicated torque sensor for closed loop control and also features a back-drivable gearbox enabling inherent compliance. Only two connections are used for the system, these are power and comms (EtherCAT) [120].

6.1.3.2 TacTip Integration

Producing modified TacTip to integrate into the system uses techniques presented in Chapter 3. In short, the sensor skin and supporting body are 3D printed as a flexible rubber like material, Tango Black+ and a rigid white plastic, Vero white (Figure 6.2). This version of the sensor has 97 pins that are patterned by triangular tessellation with 3 mm length and a 2 mm diameter pin head. As with other TacTip designs, an acrylic lens (2 mm thick) is adhered to the Vero white supporting body of the tip, allowing for the sensor to be filled with the gel.

The sensor tip connects to camera house via press fitting into an opening at its base. The camera used for this system is a 2.0 mega-pixel, HD (1920x1080), CMOS array USB web-cam (ELP cameras) that is mounted on the back of body via four M2 screws. This camera views all 97 pins with a wide-angle lens (2.1 mm focal length, 150° view angle) whilst the interior of the body is illuminated by the four LEDs. The fully integrated hand is shown in Figure 6.1.

6.1.4 Voronoi Feature Extraction

This work presents the first practical utilisation of the Voronoi based feature extraction presented in Chapter 5. For this system the methods have been redeployed in a Python 2.7 framework rather than the MATLAB framework previously presented. In Python, the SciPy package is used to calculate the Voronoi cell areas and produce the surface fit. The surface can be plotted and visualised using PyQt-Graph and Open-Gl. The Python version of the methods allows for superior integration with ROS as well as improved inference and visualisation rates.

The feature used for this presented demonstration is centre-of-pressure, a tactile analogue of centre-of-mass. This feature is computed from the average of marker positions weighted by their corresponding cell area.

6.1.4.1 Data Collection

Off-line Calibrating each sensor to roll, ϕ, and pitch, θ, is achieved by collecting sensor data whilst re-orienting (with a UR5 robot arm) in contact with a flat plate. Time series of the centre of contact (~ 60 frames) are collected at random locations within a 2D grid of 255. This grid, $\phi \times \theta$, is defined by the ranges $-16° \leq \phi \leq 16°$ in 2° increments and $-11° \leq \theta \leq 3°$ in 1° increments (Figure 6.3).

Three test sets are collected within the same range as the training with an additional variation in height (-0.5 mm $\leq z_l \leq$ 0.5 mm) between the sets. Training is also extended to generic 3D-printed shapes to explore method generality (Figure 6.4).

Prior to training, data is averaged across frames and centre-of-pressure-xy position is mapped to ϕ and θ via three separate multivariate, linear models: A simple linear model (1^{st}-order polynomial), 2^{nd}- and 3^{rd}-order polynomials. The data for the 2^{nd}-order polynomial can be seen plotted in Figure 6.5.

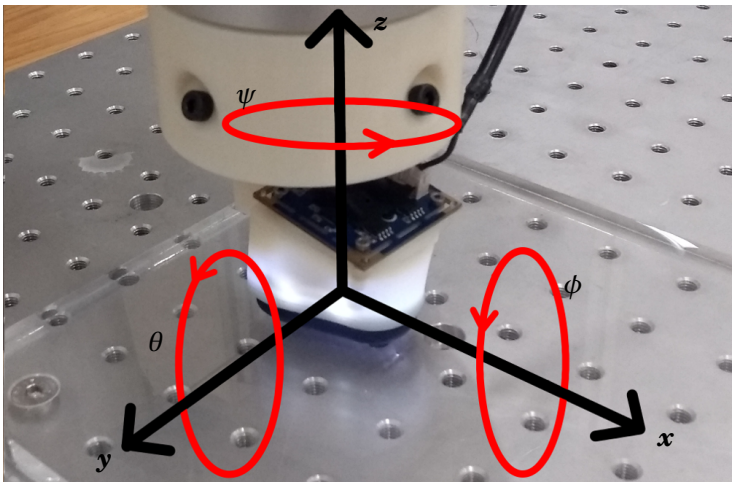

Figure 6.3: Data collection set-up with tactile fingertip mounted as an end-effector on a UR5 robot arm. Showing roll, ϕ, pitch, θ and yaw, ψ orientations relative to the sensor.

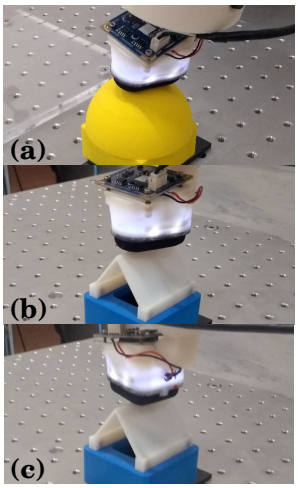

Figure 6.4: **(a)**: Data being collected on the dome stimulus. **(b)** and **(c)**: Data being collected on the edge stimulus at ψ = 0 and 90° respectively.

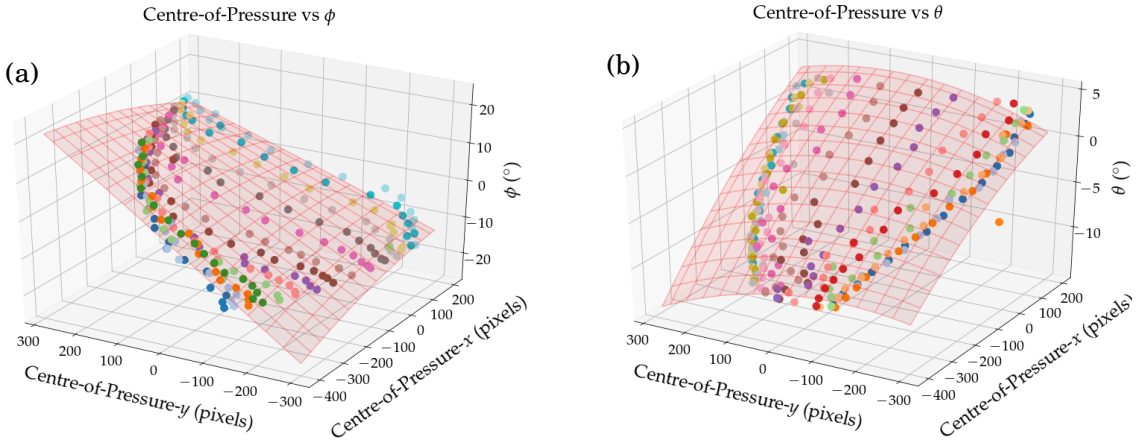

Figure 6.5: **(a)**: Scatter plot of xy-centre-of-pressure vs ϕ. **(b)**: Scatter plot of xy-centre-of-pressure vs θ angle. In both plots, the surface shows a 2$^{\text{nd}}$ degree polynomial fit and each colour represents a constant θ and ϕ in **(a)** and **(b)** respectively.

Online Grasp Adjustment The goal of the presented work is to predicted ϕ and θ to adjust a held grasp. To close the loop each sensor connects to the hand controller via a ROS-network. The controller closes each digit via position control whilst listening for a contact. Once detected the digit is stopped. When contact is detected on all sensors, whilst maintaining an applied torque from the digit, the controller begins adjusting the pitch of the distal phalanx and rolling the base joint such that the centre-of-contact is 0.

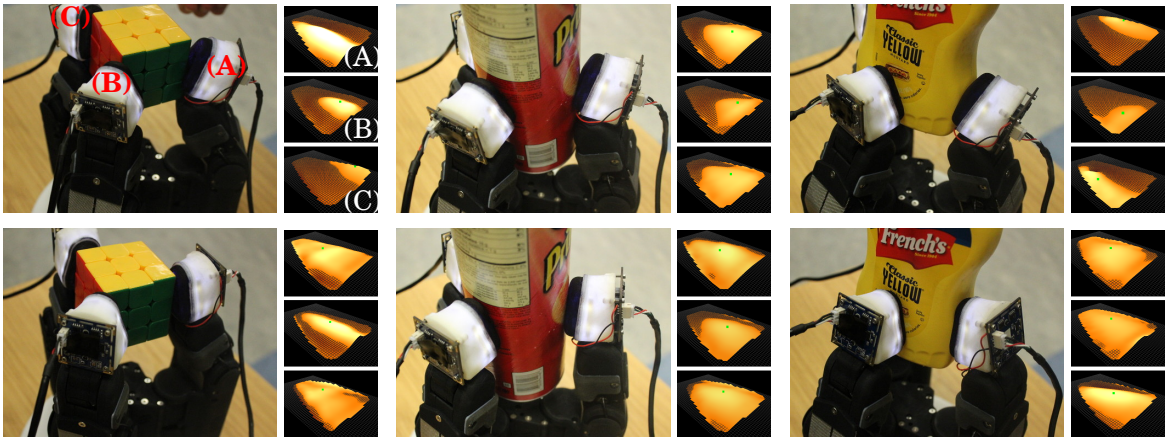

Figure 6.6: Images of the grasps on the Rubik's cube, Pringle's can and mustard bottle, before and after tactile adjustment; top and bottom rows respectively. Tactile visualisations for the three fingertips are displayed to the right of each grasp image. Fingertips are labelled on the top left image and visualisations of tactile input for reference.

6.1.4.2 Results

Offline Testing Three competing model types (1st, 2nd-, and 3rd-order linear models) are compared for predicting ϕ and θ, seeking a balance between accuracy and generality. The fitted regressions are assessed by an R^2 score for all three tips and each test condition.

The 3rd-order polynomial model performed best on the flat plate at known depths but poorly generalised to the two unknown depths. Both other models performed more constantly at the unknown depths on the flat plate.

All models generalised to the dome stimuli, but as with the generalisation to depth, the worst performer was the 3rd-order model.

In all the models on the edge stimulus only ϕ or θ could be generalised to. When the edge is perpendicular to the axis of rotation the centre of pressure moves up the edge and can be generalised to. In contrast, if the axis of rotation is parallel to the edge then the system pivots on the edge and no change in centre of pressure is detected.

From this data, the 2nd-order model appears to be the most suitable for predicting ϕ and θ with the application to robot hands.

Table 6.1: R^2 scores for 1st-, 2nd- and 3rd-order polynomial linear regression for tips A, B and C, as labelled in Figure 6.1, calculated for test sets on the flat acrylic plate at depths of -0.5, 0 and 0.5 mm, the dome and the edge at ψ = 0 and 90°.

	1st Order						**2nd Order**						**3rd Order**					
Stimules	**Flat Plate**			**Dome**	**Edge**		**Flat Plate**			**Dome**	**Edge**		**Flat Plate**			**Dome**	**Edge**	
Depth (mm)	**-0.5**	**0**	**0.5**	**0**	**0**		**-0.5**	**0**	**0.5**	**0**	**0**		**-0.5**	**0**	**0.5**	**0**	**0**	
ϕ(°)	**0**	**0**	**0**	**0**	**0**	**90**	**0**	**0**	**0**	**0**	**0**	**90**	**0**	**0**	**0**	**0**	**0**	**90**
tip-A	0.91	0.90	0.91	0.92	0.42	-0.01	0.92	0.91	0.92	0.90	0.46	-0.07	0.84	0.95	0.67	0.82	0.28	-0.03
tip-B	0.87	0.89	0.72	0.87	0.42	0.25	0.89	0.92	0.71	0.87	0.46	0.29	0.85	0.94	0.28	0.83	0.32	0.29
tip-C	0.88	0.88	0.81	0.84	0.36	0.17	0.90	0.90	0.82	0.80	0.36	0.21	0.76	0.93	0.40	0.61	0.21	0.25

Online Grasp Adjustment For online testing the 2nd-order polynomial regression model is implemented on the TacTip integrated Shadow Modular Grasper. The perceived ϕ and θ are used in a grasp adjustment procedure on three objects from the YCB object set (A Rubik's cube, Pringle's can and mustard bottle) [11]. The objects are passed to the grasper by a human participant who releases the object when all digits are in contact. Figure 6.6 shows both the grasper and sensor visualisation before and after the grasp adjustment for these objects.

For both the Pringle's can and the mustard bottle the system was able to adjust θ and ϕ towards zero and maximise the surface area of contact, whilst maintaining hold of the object. With the Rubik's cube in particular there are many edges which the sensors may contact and, as discussed, edges are an issue for the methods to reduce if aligned with the axis of rotation. In these conditions the system still minimises ϕ if the edge is off-centre, resulting in a move to a flat face. This does not happen if the edge lies close to the central axis, although still results in a stable grasp, despite not maximising contact area.

Figure 6.7 shows base and distal joint angles and centre-of-pressure-x and -y positions vs. time when successfully grasping the Rubik's cube, for digits A, B, and C. It can be seen that after contact is made the joint steadily adjusts the centre-of-pressure coordinates towards 0.

In some cases, grasps were unsuccessful throughout the adjustment phase, as objects spill out, possibly due to over-adjustment. Over-adjustment occurs when the adjustments to ϕ cause the balance of forces from all digits to be non-zero, exceeding the friction of the system.

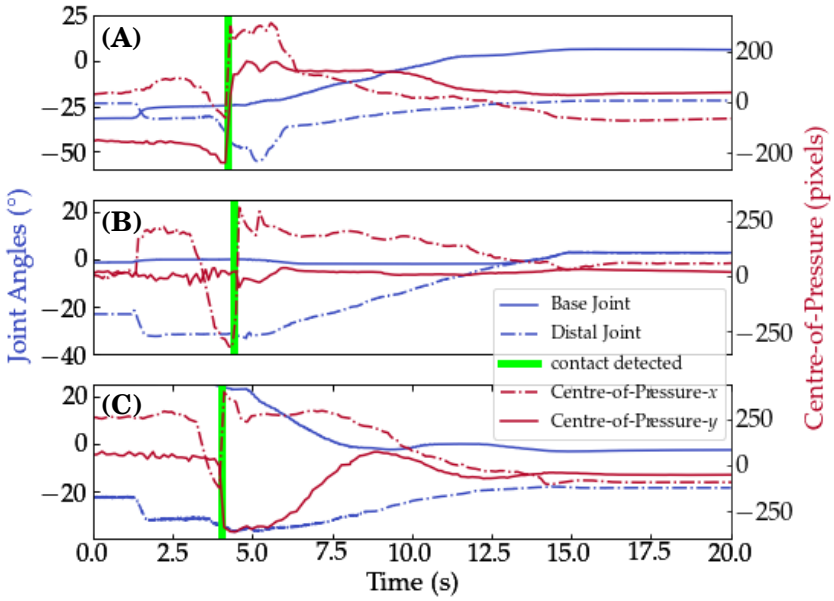

Figure 6.7: Plots of base and distal joint angles (blue) and xy centre-of-pressure (red) versus time, for fingers A, B and C, whilst grasping the Rubik's cube. Vertical green lines show when each finger detected contact.

6.1.4.3 Findings

The methods for maximising the contact area between object and tactile sensor that we discuss here demonstrate the ability to both perceive and correct the centre-of-pressure tactile feature for this purpose. This ability is shown to generalise well to different objects and could prove a useful component in improving grasp stability within a higher level controller.

6.2 Publication: The Tac-Manipulator: A tactile robotic hand with the tools for manipulation at its fingertips

Combining the developments in tactile hardware and software presented earlier in this thesis with the powerful advantages of 3D printing, provides the opportunity to design a 3D printed tactile hand. This design aims to open up exploration of tactile dexterous manipulation by being highly tactile, intermediary complex and dexterous, and relatively inexpensive to produce. This section presents the author's publication on this hand design.

The following section has been submitted for publication in a paper entitled *"The Tac-Manipulator: A tactile robotic hand with the tools for manipulation at its fingertips"*. The contributions for this work are as follows.

- Luke Cramphorn:
  - Designed the Tac-Manipulator hand and the TacTip tactile sensors that are integrated with the system.
  - Constructed the Tac-Manipulator and associated sensors.
  - Programmed the library for tactile inference from Tac-Tip data.
  - Programmed the ROS architecture used for integrating sensors and hand in a closed loop.
  - Designed and programmed the grasp controller for adaptively grasping objects.
  - Conducted the benchmarking validation of the grasping.
  - Performed the analysis of the results and design.
- Jasper James:
  - Provided assistance and input into the design of the TacTip sensors for the hand integration.
  - Prorammed the raspberry pi,Äôs to output pin position data from the camera interface.
- Nicholas Pestell:

  - Provided assistance and input for the design and programming of the tactile inference library.
  - Provided assistance and input into the design and programming of the ROS network used for controlling the hand with tactile feedback.

- Alex Church:
  - Assisted in the conducting the benchmarking validation of the grasping.

- Nathan F. Lepora:
  - Provided supervision over the work.
  - Provided input throughout development of the work.

Abstract - In this publication we present a robot hand design that aims to fill a gap in available hands and related research. This gap is in highly tactile hands with medium complexity and dexterity, with a relatively inexpensive production cost, for the exploration of tactile dexterous manipulation. The 3D printed hand has been integrated with 3D tactile sensing technology known as the TacTip. 3D printing keeps the one-off production costs of the hand and sensors low and the sensors provide versatile tactile sensing. With three fingers, each fully controllable, the hand is simpler than complex anthropomorphic hands and more dexterous than under-actuated designs.

Using the sensing to feedback into a simple grasp controller we validate the design's grasping through the YCB benchmarking protocols, demonstrating the strengths and weaknesses of the design. The overall scores achieved on the basic GAB where 206.5 out of an available 404 and 178 out of an available 208 on an extended set. These are sufficiently high to continue development and exploration of the designs capabilities.

The paper also presents the tactile sensing capabilities of the design, showing the depth of data that is available with the design to begin to explore tactile dexterous manipulation.

Overall the design provides the elements required to fill the desired gap in research. The work will continue in the future to utilise this design in exploring tactile dexterous manipulation.

6.3 Introduction

Dexterous in-hand manipulation is a characteristic skill of humans that has allowed us unparalleled ability to interact with and change our environment. Emulating this ability in robotic systems is arguably a key milestone in future robotic development [105]. It could help improve robot versatility in areas such as industry, care, emergency services, and human robot-interaction, propelling robotics from constrained environments into our human world and beyond.

The goal of dexterous manipulation is an ambitious one, with fields such computer vision, force control, motion planning, grasping, sensor fusion, digital signal processing, human-robot

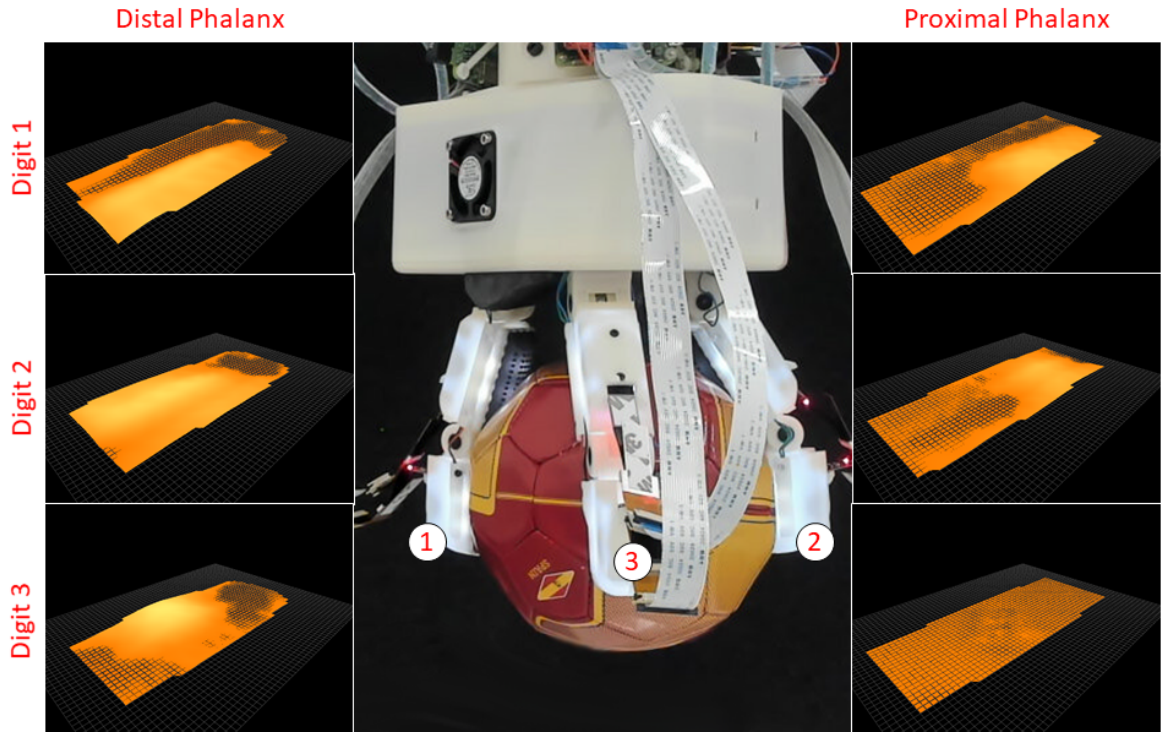

Figure 6.8: In this paper we present a 3D printed hand with 7 actuated degrees of freedom and 6 TacTip tactile sensors. In this image we show the design dubbed Tac-Manipulator grasping a Mini Football from the YCB object set. Surrounding the hand are visualisations of tactile sensing of the grasped ball.

interaction, learning and tactile sensing all having a potential role in achieving it [8]. This has not stopped the scientific community from actively pursuing this goal for decades [104, 105, 130, 131]. For example there are methods and strategies that demonstrate one or more manipulation primitives within a dexterous system (rolling:[132], sliding:[133], pushing:[134]). There have also been some notable recent demonstrations of dexterous in-hand manipulation with Kumar *et al.* (2016[137]) performing non-prehensile (not grasping) rotation of a bar and Open AI (2018 [125]) presenting Deep-Learning techniques to perform a very sophisticated dexterous manipulation of a cube.

Many examples of manipulation use open-loop or visual feedback to perform manipulation [137, 185]. In humans, our sense of touch is largely responsible for our perception and understanding of held objects, which allows us to perform tasks with an unparalleled level of dexterity [67]. Additionally dexterous robotic hands are either complicated and/or expensive ([23, 125]) or cannot perform in-hand dexterous manipulation due to limited DoF or actuation [122, 123]. Here we aim to address the space between these hand designs, providing a tool to explore the role of tactile in these tasks.

In this paper we introduce a design of 3D printed hand with integrated 3D printed tactile sensors (Figure 6.8). This design is a prototype which aims to be highly tactile with medium

complexity and dexterity whilst being relatively inexpensive to produce, filling a gap in research and hardware capabilities. Through the paper we discuss the hardware and software we have developed and present the results of its performance in the basic grasp assessment benchmark outlined for the Yale-CMU-Berkeley (YCB) object set [11]. Additionally, we will discuss the tactile capabilities of the design by presenting an analysis of the sensory outputs.

6.4 Background and related work

In this section the authors present a sample of existing research that we use to highlight a gap in robotics hands. This gap, we propose, is in research and availability of a highly tactile, mid complexity, dexterous, and relatively inexpensive robotic hand. A hand that fits these criteria should enable research on tactile grasping and simple dexterous in-hand manipulation for a wider part of the community than the expensive commercially available options.

Firstly we will discuss the various robotic hands present in literature. These hands cover a range of DoF, digit forms, physical structures, and tactile capabilities, but the three more common forms are simple grippers with only two digits [108, 110], three (sometimes more) digit hands with different grasping modes [111], and the complex anthropomorphic hands based on the human hand [23, 114].

6.4.1 Robotic Hands

6.4.1.1 Two Digit Grippers

Robotic hands with two digits provide the basic grasping requirements of robots, being simple to build and control. These hands can range from simple parallel grippers, to more complex designs utilising under-actuated principles [108, 110]. This style of hand is simplistic but effective, being able to pick up many objects, and thus they are widely used. It is important to mention that these hands do not possess the DoF required to perform most dexterous manipulation actions, aside from rolling and sliding [104].

6.4.1.2 Multi Digit Hands

These Robotic hands have greater DoFs than the simple two digit gripper and lower DoFs than the more complex anthropomorphic hands (as standard). To this end these hands tend to sit between grippers and anthropomorphic hands in terms of their complexity to control and cost to build or buy. These hands are numerous in design variety, although we will only discuss hands with three digits, due to their dominance in this category. Additionally three is the bare minimum of fingers required to perform in-hand manipulation, which therefore means that it is the simplest and cheapest solution for exploration of dexterous in-hand manipulation [105].

In addition to three fingers, the other design choice that is commonly adopted for these hands is under-actuation, the principle of fewer actuators than DoFs. Under-actuated hands use morphologically intelligent designs to move multiple DoFs with a single actuator. This allows digits to conform to the grasped object, maximising contact surface area, whilst minimising the number of actuators needed. Some examples of these under-actuated hands are the iHY hand [111], Righthand ReFlex hand (commercial derivative of iHY), Robotiq 3-Finger Adaptive Robot Gripper, and the Kinova KG-3.

Fully actuated designs are also prevalent, although they are much more expensive to build due to the increase in the power density within the hand, with smaller and more powerful motors in a very similar footprint. These hands do have one physical advantage and that is with the greater control of DoF the tool has greater dexterity. Some examples of fully actuated hands are the Barrett Hand, Schunk 3-Finger Gripping hand, and the Shadow Modular Grasper.

The iHY Hand is an under-actuated hand designed to be durable, inexpensive, and moderately dexterous, capable of performing tasks like fingertip grasping, power grasping, and some basic dexterous manipulation [111, 123]. The authors focused on these design parameters rather than attempting to meet general-purpose performance criterion for fine motor skills, such as in-hand manipulation, making the hand more accessible in monetary and skill costs. The work demonstrates a variety of grasp primitives covering a wide range of object shapes and sizes as well as demonstrating some basic in-hand manipulation. Although mechanically incapable of performing the complex tasks of high dexterity, anthropomorphic hand the iHY offers robust grasping and basic manipulation for a considerably lower cost.

6.4.1.3 Anthropomorphic Hands

Anthropomorphic Hands attempt to capture a portion of the performance and versatility demonstrated by the most advanced dexterous manipulator known; the human hand. The human hand has 27 DoFs including the wrist; this is a very large number of DoFs in a very small space. These robotic hands utilise a number of fingers (usually 4) and an opposable thumb. The existing designs have varying numbers of actuators and DoF, but for the most part they tend to be highly under-actuated. This is due to the high number of DoFs combined with the limited space available in the human hand form.

This complexity makes the hand both challenging to control and to construct. The latter of which makes them much more expensive tools that the other forms of robotic hand previously mentioned.

Anthropomorphic hands have advantages over other hands that give them higher potential for manipulation. Firstly the large number of DoF that makes these hands challenging to control also provide them with comparatively high levels of dexterity, which is a crucial component of the complex manipulation skills that we ultimately want our robotic systems to possess. Secondly, the human form of these hands makes them very useful for human centric robotics like tele-operation

and prosthetics.

Some anthropomorphic hands presented in the literature include the DLR Hand II (2002 [124]), Gifu hand II (2002 [114]), the highly biomimetic Xu Anthropomorphic hand (2016 [23]), and the Pisa/IIT Softhand II (2018 [116]). With others available commercially, such as the Shadow Dexterous Hand and Schunk SVH.

6.4.2 Tactile Grasping and Manipulation

The integration of tactile sensors into hands is a natural step in both tactile and hand development. Capitalising on this integration for skills such grasping and manipulation is still an open problem. In 2011, Romano et al. [168] presented an innovative study into a grasp control framework using touch. The hardware used was a pair of 5x3 capacitive tactile sensors and an accelerometer integrated with the two-fingered gripper of a PR2. The control system comprised of states that were transitioned between via hard-coded tactile signals.

After this more data driven methods have been employed. For example, an under-actuated, Robotiq gripper equipped with six array-based pressure sensors and a kernel logistic regression model, trained with tactile data from 192 grasps, was implement to predict grasp success with up to 89% accuracy [186]. Similarly, two 7x4 capacitive tactile arrays were integrated on the finger-pads of another Robotiq two-fingered gripper. Here 1,000 grasps were trained with a CNN, achieving a prediction accuracy of 88.4% [187].

Previous work into tactile dexterous manipulation with TacTip sensors has been conducted with GRAB Lab hands which have been integrated with the sensor technology. Firstly a cylinder was manipulated through rolling motion along a tactile trajectory with an M2 Gripper platform [33]. In another study object re-orientation was demonstrated with the under-actuated parallel GR2 gripper [175]. In both publications supervised learning was used to achieve and demonstrate the precise manipulation.

In a more recent study the TacTips have been integrated with the Shadow Modular Grasper [41]. This work presents a form of grasp modification, utilising the sensory feedback, for maximising surface contact and improving grasp stability. This Tactile version of the Shadow Grasper has three distal TacTip sensors, 9 fully actuated DoF.

6.4.3 Summary and Perceived Gap

As mentioned, the gap that we propose is in research and availability of a highly tactile, dexterous, and relatively inexpensive robotic hand. The literature highlights that existing hands like grippers are either too simple to perform dexterous manipulation tasks, or the likes of anthropomorphic hands, that have the superior dexterity with the drawback of complex control and construction. This also means that the hands are expensive to purchase.

The multi-fingered hands described above provide a good balance between dexterity and costs. In particular the iHY and the tactile Shadow Modular Grasper are the closest examples

of research that we found to address this gap. The iHY, which was designed to be durable, inexpensive, and moderately dexterous, provides great value for its low cost but is limited to under-actuation of its three digits. The tactile Shadow Modular Grasper on the other hand is robust, powerful, and deploys higher dexterity than most Non-anthropomorphic hands, although this incurs a higher commercial price and only has distal sensing capabilities. Ultimately, the perceived gap lies between these two hands.

Using the principles and fundamentals used to design the iHY as a launch pad, we aim to address the gap in robotic hands by designing a system that incorporates versatile tactile sensors, increased actuated freedoms, and is relatively inexpensive to construct.

6.5 Methods

In this section we discuss the goals that we hope to address with the design of the Tac-Manipulator and corresponding software. We focus on the integration of TacTip tactile technology into both of two phalanxes of the digits and how greater dexterity is provided.

6.5.1 Design of the Tactile Manipulator

6.5.1.1 Design Goals and Principles

The Tac-Manipulator is envisioned to be a simple robotic hand with the added tactile sensing performance and versatility of the TacTip. The aim of the work sets out with intention of producing a relatively inexpensive tool for exploration, and development of understanding, of tactile dexterous manipulation. The design of the hand will be focused on a set of parameters outlined below.

The design should...

- **maintain the low cost and rapid prototyping advantages of the TacTip:** A strong advantage of utilising the TacTip tech arises from the low cost involved in building and redesigning the sensors into different shapes and sizes. Designing the manipulator platform to conform with this costing principle will allow the for designs to be evolved through iterations on a limited budget. In addition, the platform will be affordable to build by others if the designs are open sourced.

- **provide highly versatile tactile sensing capabilities:** To explore tactile sensing within the in-hand tactile domain, high quality, versatility, and extent of sensor coverage will provide greater data quantity and value. To this end the authors aim to integrate their expertise and knowledge of the TacTip technology into every phalanx.

- **have full or near-full control of digits:** In many cases newly developed hardware derives inspiration and design elements from already existing and similar hardware.

Here is no exception, as many design principles and elements have been taken from very successful work in 3D printed hands by the GRAB Lab, specifically the model O design (open source derivative of the aforementioned iHY hand). The difference here is a focus on the potential of manipulation rather than grasping. Thus the design does not use the under-actuated principles adopted by the GRAB Lab and instead aims to provide the higher degree of actuation and control necessary for exploring dexterous manipulation.

- **be capable of robust and dynamic grasping:** The first aim of any hand is to be able to pick up and maintain a stable grasp of an object. Dexterous manipulation is a complex sub-state of grasping, in which a grasp state is changed, whilst maintaining grasp successes throughout that change. To this end the manipulator must be able to perform and maintain a grasp.

6.5.1.2 TacTip Optical Tactile Sensor

The tactile element of the proposed design is the TacTip optical tactile sensor. In prior publications the TacTip has been shown to be a robust, accurate, and cheap tool for tactile research [38], from which a clear research direction can be identified as the integration of the sensor on more complex platforms, such as the grab-labs M2 and GR2 grippers [33, 41, 175].

The advantages of using the TacTip sensor in the design of this tool include its low production cost, high robustness, compliant contact surface, adaptable shape, and the authors' expertise in the sensor hardware and software. A particular strength arises from being able to print the sensor tips in the desired shape for a finger integration; this simplifies integration and additionally provides a cheap solution to damaged tips as they can easily be reprinted and replaced. There are typical disadvantages to using optical tactile sensors, in particular the minimum size limitations of the technology make it difficult to integrate within the fingers, as certain functionality is dependent on profile, with smaller being better. An additional disadvantage of optical tactile sensors is that they are heavy; this factor must be considered in the design process.

To minimise the impact of the large sensor profiles on the performance of the design, a camera with a small physical footprint, short focal length, and wide angle visual field can be used. This compacts the whole sensor system. In this design, the reduction in profile is achieved with a ZeroCam (Figure 6.10). The ZeroCam is small and cheap, with a footprint of 10 mm $\times$ 25 mm (after modification), and a field of view at $\sim 120°$. The manual focus of the camera allows reduction of the focal length down to near 30 mm. In all, this allows minimisation of the digit depth profile to 40 mm. Although a necessary improvement, 40 mm is still a large profile for a phalanx and cost the digit some of the functionalities demonstrated by the iHY.

The iHY uses its low profile distal phalanxes, compliant joints, and nail feature to under-cut flat objects and flip them into a graspable position [111]. It is this functionality that the sensor profile compromises.

The TacTip' high acuity and compliant contact surface make it ideal for active sensing. This will aid in tasks such as grasp quality perception, grasp control, object perception, object manipulation, and tactile exploration. Increasing the quantity of available sensing surfaces will naturally add more information for completing these tasks, improving the results and enhancing the usability. To this end both phalanx of each digit are built around a TacTip sensor. With three digits consisting of two phalanges in each, six TacTip sensors are integrated into the hand. The ZeroCam are capable of capturing 480p frames at 90 fps, but are only usable via a Raspberry Pi interface. To avoid using six Raspberry Pis, multiplexors (IvMech IvPort V2) are used to link the cameras from a single digit to just one Pi. Using a multiplexor is a trade of frame rate for reduced hardware dependencies. The frame rate is dropped by just over half for each of the cameras as the feed is split between the two cameras on the one port. The resultant frame rate is ~30 fps for each camera, which is sufficient for the tasks that will be discussed here.

6.5.1.3 3D Printing and Rapid Prototyping

Producing the majority of the hand components via 3D printing allows for the production of both simple and complex parts at a relatively low cost in time and money when compared to other forms of one-off manufacturing. In the design of the hand, two 3D printing processes are used. These are fused deposition modelling (FDM) for structural and mechanical components and PolyJet multi material printing for the sensor tips. The thermoplastics from the FDM printer provide a good strength to weight ratio and adequate structure to withstand the mechanical forces involved in grasping and manipulation.

6.5.1.4 Grasp Primitives

The term grasp primitives describes preliminary grasping positions of the digits. These primitives result in different actions throughout the grasping phase. With multiple grasp primitives the manipulator has broader flexibility to solve a grasp. Achieving different grasp primitives is done through a rotational DoF at the base of two of the digits. This base rotation is a feature of the GRAB Lab model O that we have adopted for this design; it also exist in various forms, in other non-anthropomorphic multi-fingered hands. Such variations include hands with coupled rotation of opposing digits to independently rotating digits. The rotation provides the Tac-Manipulator with three grasp primitives. These can be moved between by changing the orientation (r) of the coupled digits, and are here identified as cylindrical, spherical, and opposed (Figure 6.9).

The cylindrical grasp ($r = 0$) moves all three digits in parallel planes with digit 1 passing between 2 and 3. This is grasp is well suited for long/tall objects where the length is greater than 8 cm (the distance between the base of digits 2 and 3). Some example objects for this grasp would be bottles and cans (from the side) and oblong objects like boxes.

The opposed grasp ($r = 1$) has digits 2 and 3 in parallel plans and digit 1 in a perpendicular plane. Digits 2 and 3 move into opposed contact during motion whilst digit 1 either stays clear, or

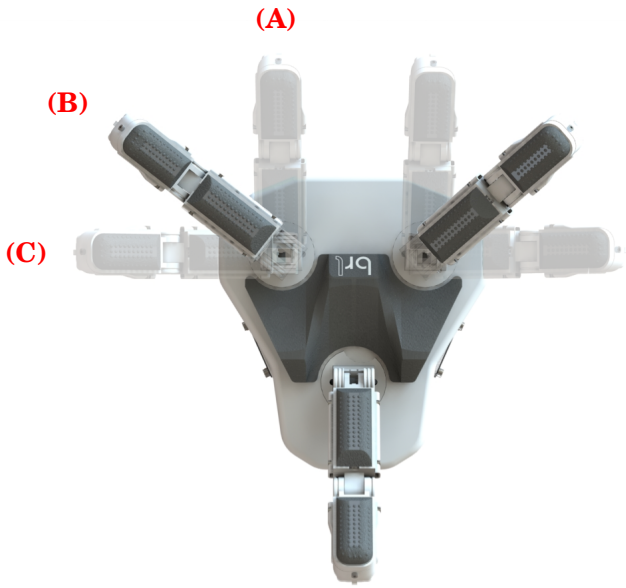

Figure 6.9: This figure demonstrates the grasp primitives of the hand: (A) Cylindrical; (B) Spherical; (C) Opposed

aids in supporting or manipulating the object. Used for objects smaller than what the cylindrical or spherical grasps can handle comfortably. Due to the surface to surface nature of this grasp objects like keys, coins, and small bolts are best to be grasped with this primitive.

The spherical grasp describes the range between the cylindrical and the opposed ($0 < r < 1$). Here all three digits move in planes offset from the other, with digits 2 and 3 mirrored, and move in towards the centre of the hand. A spherical grasp like this is best suited for objects that have some dimensional similarities or circular/spherical surfaces. For example balls, cylinders (from above), cubes unsuitable for grasping with the cylindrical grasp.

6.5.1.5 Digit

There were multiple challenges involved with designing the digits for this hand. The aim was to have independently controllable joints whilst using the minimal number of servos, with each phalanx having a TacTip sensor and sufficient movement capabilities for grasping and manipulation. Additionally the structural strength must withstand the loads applied to the fingers by servos and objects alike, and be light overall with low friction so that the servos can move the digit and apply the forces to objects sufficient for grasping and manipulation.

a) Joint Identities: For the rest of this publication, references to specific joints will be made using the naming convention used in anatomy. As the proposed digits have two phalanges we compare to the human thumb. The joint that links the proximal phalanx to the metacarpal bone in the hand is the metacarpophalangeal or MCP for short. The joint that connects distal and proximal phalanges is the interphalangeal or IP for short. The human thumb has an additional joint that

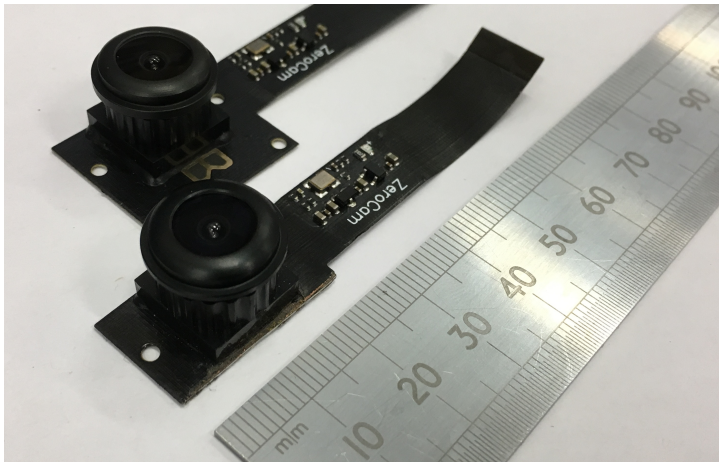

Figure 6.10: Photo of the ZeroCam camera used for the optical element of the integrated sensors. Un-modified camera at the top and modified camera at the bottom

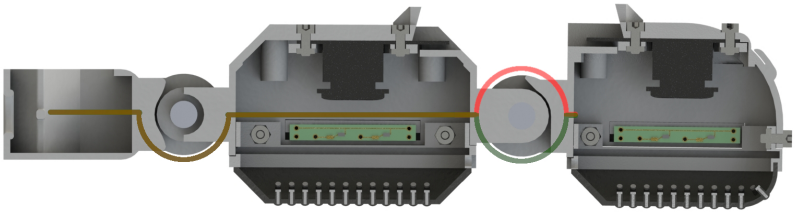

Figure 6.11: Side on cross section of the digit module

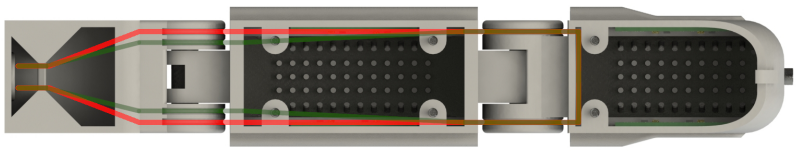

Figure 6.12: Top down cross section of the digit module

Figure 6.13: Both cross section have the tendon layout shown, with the lateral tendon (red) and the medial tendon (green). Figure 6.12 shows the parallel layout of the tendons that allows for unimpaired visual field whilst balancing lateral forces

the presented digits do not. This is the joint that connect the metacarpal bone to the carpal bones of the wrist, this is the carpometacarpal (CPC) joint.

b) Maximising Joint Control: One method for fully actuating a finger is to directly control the joint by embedding the servos into the joints. Another method is to use pairs of tendons, one to extend and one to flex (agonist and antagonist). Both of these methods allow for complete control of the targeted freedom. Direct control only requires a single servo for each joint nut which is

limited on the size of the motor, and thus the deliverable power. Additionally the hardware space required for the servos will consume space within the phalanges, which will be needed for the sensor integration. The other method, agonist and antagonist tendon pairs, requires two servos per joint to achieve the same control as a direct drive; extra servos increases costs and space requirements. On the other hand, using tendons means that the servos can be extrinsic to the fingers (and the hand if desired) providing more space to place the extra servos, and increase their size, therefore increasing power.

Due to the requirements of space within the phalanges, here we choose to use a tendon driven system. However the costs of four servos per digit are not in line with the goal of making the hand inexpensive. We solve this issue by using a combination of two different tendon paths that individually would create under-actuated motions, but when used together, in conjunction with a single passive return on the MCP, we can independently control the pose of the IP and MCP with only two servos. This layout can be seen in Figure 6.11.

The choice of this method of actuation was inspired by the combinations of tendons acting on different combinations of joints in the human hand. Specifically, the human thumb which has a total of five DoFs that are controlled by eight muscles (tendons), four extrinsic to the hand and four intrinsic to the hand, many of which display this principle. Of these four extrinsic muscles one flexes both the MCP and IP joints, one extends the MCP and the thumb at the CPC, one extends all three joints, and one for thumb abduction. And of the intrinsic muscles two abduct, one flexes the MCP joint, and one rotates and flexes the metacarpal into opposition.

c) Hyper-Mobile IP Joint: Using this tendon layout it is possible to have the range of the IP joint extend beyond straight. This ability is known as hyper-mobility in humans and can lead to injury if forcefully induced. Although here the ability provides a way of overcoming some of the limitations of the low DoF of the hand. For example with the hyper-mobile IP joint two or three distal sensors can be placed surface to surface maximising the contact area for grasping and sensing smaller objects. The hyper-mobility feature of the digits can be seen in the full extension of the digit shown in Figure 6.14.

d) TacTip Optical Tactile Sensor and Tactile Integration: Optical based tactile sensors tend to rely on cameras to extract the data from sensing surfaces, this requires an unimpeded field of view between camera and the surface. Creating this unimpeded space within a phalanx of a digit is challenging due to the limited profile and robustness required to make them functional. In many cases actuation components stop just above the Distal inter-phalangeal joint, but for proximal (and middle if it exists) the actuation for higher more distal joints either runs through or sits within the phalanx, be this mechanical components, cabling for a servo, or a tendon. As the digits shown here are driven by tendons we have solved the issue of having a tendon running through the visual feed of the sensor, by distributing them down the sides of the phalanx. This 'tram-line' tendon layout maintains the necessary torque to actuate the distal and proximal joint whilst balancing distribution of applied lateral torques on the digit Figure 6.12.

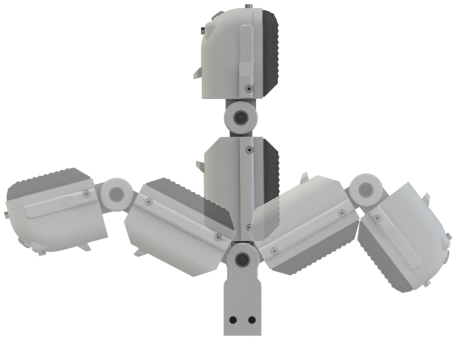

Figure 6.14: The digit module is shown here with its full extension (left), highlighting the 'hypermobile' IP joint. Full flexion of the digit (right) reaches ~90° between proximal and distal phalanges

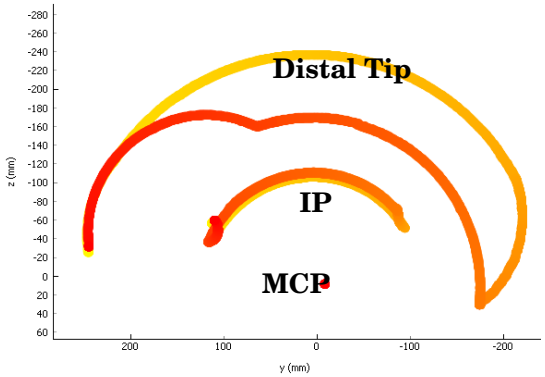

Figure 6.15: Tracking of joint positions through the finger work space. Colour on the plot represents time; with yellow being the start and red the end. Position data was collected from ArUco markers attached to the joint and the tip of the distal

In addition to the requirement of unimpeded field of view the cameras in optical tactile sensors require a minimum distance from the sensing surface to capture the required region and have enough focus to resolve the image to a level where data can be extracted. Although this profile has been minimised by using modified ZeroCams, the morphology of the digit is still compromised. For example, tasks like picking up a key require an undercutting, nail down style action only achievable with a very low profile between lateral and medial of the distal. This is demonstrated by GRAB Lab work for the DARPA challenge and is currently unachievable with this design.

e) Position Control: To control the MCP (α) and IP (β) joints independently the control of the servos pulling the lateral (θ) and medial (φ) tendons is coupled. The equations 6.1 and 6.2 calculate the servo positions for servos controlling medial and lateral tendons when moving either the MCP or IP joints. Where $\{\alpha \in \mathbb{R} : 0 \leq \alpha \leq 1\}$ and $\{\beta \in \mathbb{R} : 0 \leq \beta \leq 1\}$.

$$\theta = \theta_0 + d_\theta(\alpha.\Delta\text{MCP}) + D(\beta.\Delta\text{IP}) \tag{6.1}$$

$$\varphi = \varphi_0 + d_\varphi(\alpha.\Delta\text{IP}) + D(\beta.\Delta\text{MCP}) \tag{6.2}$$

The parameters θ_0 and φ_0 are the home or maximum extension encoder values of the servos θ and φ and the change in servo encoder position required for maximum flexion of each joint are defined as ΔIP and ΔMCP. The parameters d_θ and d_φ either negative or positive 1 and represent the direction of the servo and D is the negative or positive 1 depending on the order of the servos in the chain.

Table 6.2: Control Table for Tendon Layout

Action (Servo)		**Reaction (Joint)**	
lateral (θ)	**medial (φ)**	**IP**	**MCP**
pull	pull	static w.r.t. proximal	flex
release	release	static w.r.t. proximal	extend
pull	release	flex	static
release	pull	extend	static
pull	nothing	static w.r.t. hand	flex
nothing	pull	flex	flex

$$\alpha = \frac{(\theta - \theta_0) - (\varphi - \varphi_0)}{2 d_\theta \Delta \mathrm{MCP}} \tag{6.3}$$

$$\beta = \frac{(\varphi - \varphi_0) + (\theta - \theta_0)}{2 D \Delta \mathrm{IP}} \tag{6.4}$$

Equations 6.1 and 6.2 can be solved to maintain the same position values for α and β when either θ or φ is changed. This allows for coupled motions to be performed with the digit. Firstly, pulling the medial (φ) tendon only creates an under-actuated style flexion of the digit such that the digit curls with approximately one to one ratio of both IP and MCP joints. Also, when the lateral (θ) tendon is pulled alone the MCP joint moves whilst maintaining relative IP orientation with the hand.

f) Digit Workspace: Each digit operates within a 2D plan, which can be adjusted through the rotation of its base (Figure 6.14). Within this 2D plan the finger has a workspace defined by the joint limits. This workspace is mapped by tracking three ArUco markers, distributed across the MCP and IP joints and the tip of the distal phalanx (Figure 6.15). Due to the full control of joints enabled by the additional actuators, the distal tip maps out a large area that it can be controlled in. In contrast, if under-actuated the digit could access the same workspace but only passively. It is this active control within this workspace that provides the added dexterity that the design aimed for.

6.5.1.6 Additional Hardware Features

The hardware design and features discussed above are the key elements necessary to address the design goals for the system. In addition to these key elements, minor additions have been included in the design that do not contribute to the research goal of the design, but instead either solve minor issues with the design or make the manipulator easier to maintain.

Each digit is designed to be removable to allow the testing and implementation of different designs, in addition to the replacement of broken digits if such an incident occurs. To change

a digit the tendon must also be removed and in earlier designs the tendons were attached to the pulley by knots. The knots are difficult to remove in the tight space inside the manipulator. To improve removal and connection of tendons, a tension locking system is implemented to the tendons and the pulley. Where a brass insert is secured to the base of the tendon by a super-glued knot, this insert and the tendon fit into a slot in the side of the pulley. When spooled to tension the insert and tendon become laterally fixed to the pulley and cannot be removed until the tension is completely removed. With this, the fingers can be removed by simply undoing the fastening on the base of the finger and un-spooling the tendon.

The case around the centre of the hand provides protection to servos inside the hand whilst hiding the electronics. Removing the digits and tendons, as well as other maintenance, should be able to be done without completely dismantling the hand. Thus the case is constructed in two parts that snap hook together, allowing for the case to be removed and added quickly with no complex dismantling of the manipulator.

Having seven tightly packed dynamixal motors generates high temperatures that can cause the motors to shut into a protection mode under prolonged use. To address this, two 24 volt brush-less DC fans are incorporated into the body of the manipulator providing sufficient airflow to keep the servos operating.

Another addition to the manipulator is a 3D printed rubber palm pad. This is added to solve the fact that when the digits are at full flexion they fail to create a sealed grasp with the base plate of the hand. This creates a gap in grasp capabilities for objects smaller than 20 mm in diameter. Thus the palm pad conforms to the maximum flexion pose of the digits in the cylindrical grasp allowing much smaller objects to be grasped.

6.5.2 Software and Systems integration

The software design and implementation for this system is crucial for being able to both utilise and maximise the developed hardware. Providing the tactile sensing capabilities desired requires both the hardware integration and software capable of simultaneously collecting, interpreting, and distributing the tactile data of six TacTips sensors.

The additional control of the design's DoF comes at the cost of the morphological intelligent grasping that the under-actuation fingers, like those of the iHY, provide [111, 123]. To recover this lost functionality, the tactile data from the integrated sensors can be utilised to control the joints, mimicking the dynamics of under-actuated grasping. As stated, the aim is to design a system that will be capable of exploring tactile dexterous manipulation. To achieve this we require real-time closed loop control of the joints via tactile input.

As a prototype research tool the Tac-Manipulator should provide a platform for research and exploration. To this end we do not intend to provide all the software functionality that is potentially required for this, but to provide an initial framework that is both modular and expandable for pursuit of this goal.

An aspect for design of robotic hands that must not be overlooked, is that the software will be required to be integrated into other systems, particularly robotic arms, as automation of grasping and manipulation requires a platform that can deploy the hand as an end-effector.

6.5.2.1 Software Infrastructure

The software chosen to address the goals outlined above was the robot operating system (ROS) framework (version, Kinetic) of Python 2.7 libraries and scripts. ROS frameworks are flexible and designed to provide tools to support the integration of multiple system elements for the control of complex robotic systems. Python is a well documented language that supports the SDKs for Dynamixal motors in addition to being one of the available languages for programming ROS.
a) Raspberry Pi: As mentioned, each digit has two TacTip sensors, each with a camera. Both of these cameras are connected to a single raspberry pi via multiplexor. On-board the raspberry pis, frames are collected by sequentially alternating between the cameras. Each of these frames is processed to identify the centroids of each of the pin markers.

Pin marker positions are identified from the camera frames via the application of a binary threshold filter. This outputs a representation of the frame where features of an image that are above the threshold are represent as ones (white), and everything else is represented by a 0 (black). This new image is then further filtered, checking clusters of white pixels against a parametrised range of areas and eccentricities. This removes noise such as imperfection on the tip lens (dust, scratches) and a certain amount of external lighting. After this the remaining image shows only white clusters where the pin markers are in the original frame. The centres of these are the centroid's position (x pixels,y pixels) that make up the base data output of the TacTip. Lastly, this pin data is published to a ROS network, from which the control PC can read (subscribe) the data, process it further, and implement the closed loop control.
b) Tactile Sensing: For the tactile sensing software for this system we use the existing methods for interpreting TacTip pin data described above. The methods we use here infer a third dimension from the xy data [31]. This is achieved by performing a Voronoi tessellation on the pin data, generating cells that surround an associated pin. Due to the way that Voronoi tessellation forms these cells, their area is determined by both its associated marker and the neighbouring markers. This means that when contact on the sensor surface occurs, the pins move relative to each other and thus cell area changes. When the sensor is indented within the pin array, markers move away from each other, increasing the area of the cell. Regions of the sensor can bulge when large contacts are made elsewhere on the sensor surfaces; this cause the pins to move closer and thus decreases the area of the cells.

Using these cell areas as an inferred third dimension we can extrapolate a surface fit for the data. This represents the tactile sensors' compliant skin. This surface can be used to generate a prediction for contact location by identifying the peaks on the surface. Calculating the volume of the surface produces a proxy for the deformation of the sensor, this can be used to identify

contact and its extent.

These methods are constructed into a tactile library, from which the elements are wrapped in ROS bindings. This allows for the individual library functions to be processed and published on the network at the user's discretion, thus allowing for modular processing on features.

c) Hand: The mechanical operation of the manipulator functions through multiple levels. From bottom up these are servo, digit/rotation, and then hand, where the latter layers are an instantiation of one or more of the elements below. The servo layer is a library of function that connects and communicates directly to the dynamixal motors via the SDK and protocols, with commands for moving the servos at the encoder level along with commands for reading current pose and other status information the dynamixal servos provide. The second level creates a digit or rotation object that is a group of all the servos associated with that element. For example each digit has two servos each pulling one of two tendons, lateral or medial. Using the equations 6.1 through 6.4 with these servos moves the digits into desired positions. Lastly a hand object is instantiated as three digit and one rotation objects that all of the hands actuators can be controlled from.

d) Controller: The controller of the Tac-Manipulator combines the hand software with relevant tactile data for the purpose of closed loop control. This is achieved by instantiating the hand within ROS. This information is fed into controlling movements of the hand such as triggering state changes and modulating contact pressure.

6.5.2.2 Control

In this publication we aim to validate the grasping capabilities of the proposed design. To do this validation a tactile grasp controller is implemented in the system.

The grasp controller is a combination of a finite state machine with state transitions triggered by tactile perceptions and user inputs, and a proportional controller translating sensory data into position feedback. This system acts with shared autonomy with users deciding pre-grasps and when to close with the system automating the closing procedure. The detail of this are presented in Figure 6.16.

This closing procedure is chosen to start as a pinch, with the distal phalanges remaining perpendicular to the base of the hand through the move. This increases the chance that contact will occur flat on the distal sensors, improving sensing and contact area. Additionally this grasp style is best for grasps that only use the distal phalanges.

When contact occurs on one of the proximal phalanx sensors, a state shift is triggered switching the grasp strategy from a pinch grasp to a power grasp, ultimately caging the object. This is the same principle as deployed by the under-actuation of the iHY, where contact on the proximal causes the distal to cage. Although here this is a closed-loop process, actively triggering the state transition when sensing exceeds a threshold for contact, rather than the passive mechanical threshold of the iHY.

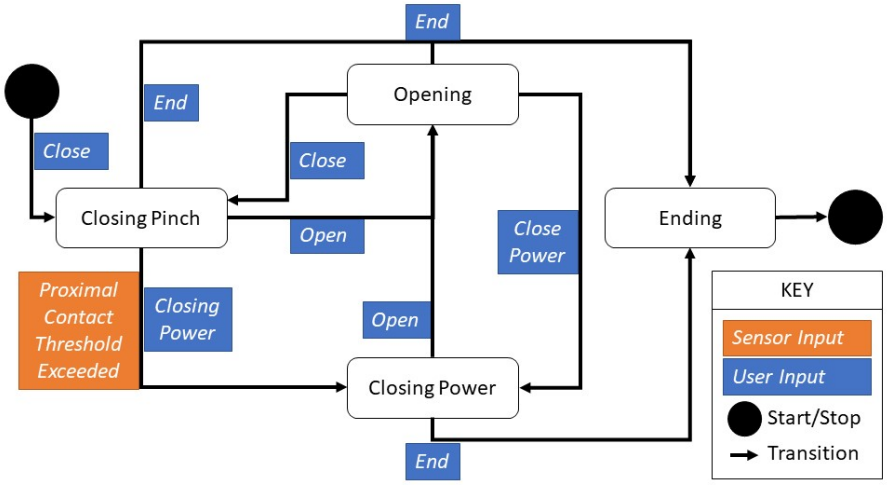

Figure 6.16: The grasp procedure that is used to grasp objects implements a closed loop control of pressure applied by the fingers. In addition to this the Tac-Manipulator can move between grasp strategies by commands sent by the user or by the sensory information. The state machine that describes this is shown above. Where ***Closing Pinch*** moves the fingers such that the distal remain perpendicular to the palm, allowing for precision grasps and ***Closing Power*** brings the fingers into cage the object for a power grasp.

Through the close procedure each joint position is iteratively updated towards the maximum allowed position (user defined). As the digit moves, the system constantly checks sensor outputs for contact. Upon which the controller switches into a proportional controller for the joint feeding back of the error in the volume output to the goal set-point, that is then converted into a change in joint angle.

For this stage in development we chose to have the user define pre-grasp and when to open and close. This is because automating pre-grasp choice is a grasp planning problem and best suited to vision techniques, thus out of the scope of this study. This can be implemented into the system for future studies if necessary. The user has four commands that can be used to control the system state, these are: ‘open’, for switching the hand to and open position if closed (maintains pre-grasp); ‘close’, initiating the main close procedure from an opening state; ‘close_power’, that forces a transitions to a power grasp regardless of contact triggers; and ‘end’, this moves the hand to the home position and ends the threading, shutting down the controller.

A note on the ‘close_power’ user command: as it can be called at any time while the system is in the closing_pinch state, it provides a powerful change in the motion of the hand. For example if called just before contact of a large cylindrical object it will begin to pull the object into the

proximal sensors for a more secure grasp. This action is an example of a feature that could be added to a tool-set for a system with automated grasp planer, or possibly learnt by a more data driven approach to controlling the hardware.

6.5.2.3 Calibration

As with many sensor systems there are subtle differences in the outputs. These differences can occur from discrepancies in how the camera sits on the 3D printed structure, in the 3D printed tips, poor consistency in tip manufacturing, and camera set-up.

Firstly, the robust detection of the pins by the software is paramount to the function of the sensing methods used here. Thus, we calibrate the parameters of the camera and pin identification layer for this task.

For the grasp controller, used for the validation of the presented designs grasping capabilities, the output of the Voronoi tessellation method, surface volume feature, is used to perceive contact and its extent. As this feature is output from all six sensors, into the controller, the values need to be calibrated against each other.

The calibration of the sensors is achieved by recording the volume output under different weights and fitting a multi-point calibration curve to the results. The weights used where 0 g, 5 g, 10 g, 20 g, 50 g, and 100 g. It should be noted that there is a known non-linearity between the TacTip data and applied forces, with additional non-linearity for different shapes under the same force. Although, for the purposes of this work the sensor output is only required to be relatively consistent over all the sensors. This is so that no proportional control is overly submissive or dominant, which would result in the system being unable to stabilise resulting in failed grasps.

6.5.3 Experimental Validation

6.5.3.1 Grasping Validation

Validating that the Tac-manipulator design provides the adequate grasping capabilities is crucial for justifying further exploration of the hand. To achieve this the hand is tested on a standard set of objects, YCB object set, for replicable research and benchmarking in manipulation. Firstly we explore what the hand is and is not capable of grasping (Figure 6.17), then a benchmarking procedure for grasping is implemented for further validation and comparison.

The benchmarking procedure is outlined by Calli *et al.* [11] and utilises the YCB object set. Within the work presented by Calli, procedures for multiple benchmarking tests covering a variety of different manipulation tasks are described; of these we use the 'YCB Gripper assessment protocol and benchmark' (basic GAB).

For this protocol four groups of objects are used from the YCB set: round, flat, tools, and articulated. The round objects are: soccer ball, softball, tennis ball, racquet-ball, golf ball, and four different sizes of marble. The flat objects are seven different sizes of washers and a credit

Figure 6.17: Objects from the YCB set that the hand can pick up (Left) and can not pick up (Right)

card. The Tools are: large marker pen, scissors, screwdriver, drill, hammer, and four different sizes of clamps. Lastly the articulated objects are a rope and a plastic chain.

The procedural set up uses a Cartesian grid for the placement of the objects and a 10 mm thick clear acrylic plate to raised the objects. The hand is mounted on a 6 axis robot arm (UR-5) above this grid.

The gripper robustness is tested by varying the object's location through four 'set points' (SP), detailed in Table 6.3. Objects are place upon the acrylic plate for SP1, SP2, and SP3 and upon the table for SP4.

Table 6.3: Object displacements for the Basic Gripper Assessment Benchmark.

	x(mm)	y(mm)	z(mm)
SP1	0	0	0
SP2	10	0	0
SP3	0	10	0
SP4	0	0	-10

Round objects are placed in upon the SP position so that their centroid are directly aligned, these objects can be stabilised with the washers. For the flat objects the same applies, with centroid of the washers being aligned with the SP. For the credit card and the tools the major axis should be parallel to either the x or y axis and maintained in that orientation for all four set points. The articulated object should be placed randomly within the circle of the grid.

The protocol constrains the task in the following ways: Firstly, the initial pre-grasp for each object can be chosen from anything the hand is capable of, but this choice must be maintained through all set points. Secondly, any grasping strategy or motion can be adopted for each of the objects, but again these must be maintained for each of the set points. Moving the object to the edge of the table or the planar object is not allowed.

The procedure is to place the object at SP1 and move the gripper to the object with the desired pre-grasp and move. The object is then grasped (or not) and lifted 150mm. If this is achieved with no visible movement of the object then 2 points are awarded, if movement occurs but the object

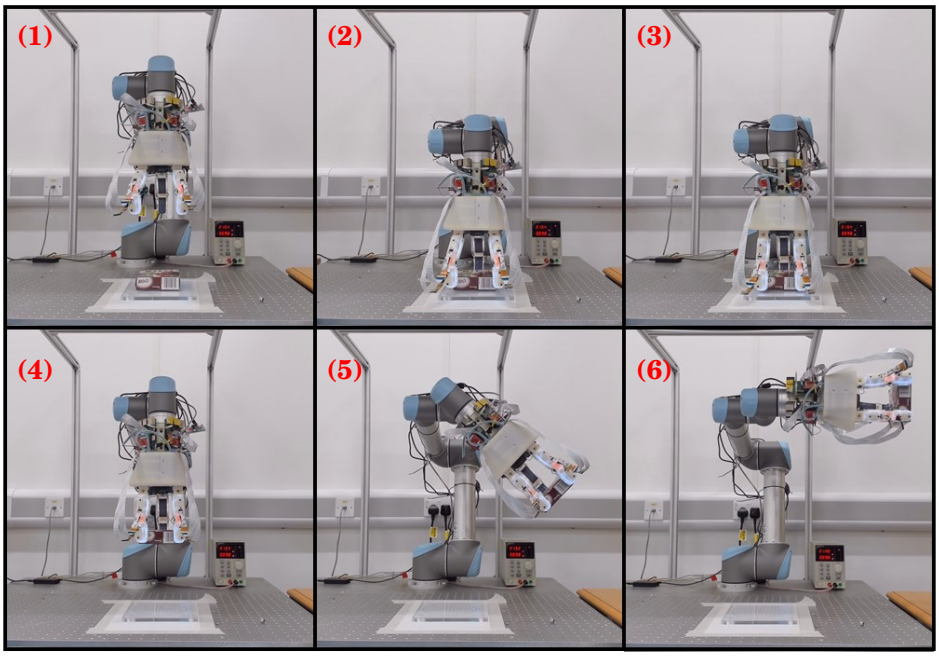

Figure 6.18: The panels above document the benchmarking procedure outlined by Calli *et al.* [11]. (1) A pre-grasp is chosen for use throughout the duration of the benchmark. (2) The hand is moved into position above the object. Again this position must be preserved throughout all set points. (3) The object is grasped. (4) The object is lifted 150 mm. If the object is successfully lifted and held for 3 seconds, 2 points are awarded, of which 1 is lost if any visible movement occurs. (5) The object is rotated through 90°. (6) As with the lift 2 point are awarded if the object is still held after 3 seconds (-1 for movement).

remains grasped only 1 point is awarded, if the object is dropped before being held for 3 seconds 0 point are awarded. After the Lift the object is rotated through 90° around the y axis, with the same scoring. This procedure is demonstrated in Figure 6.18.

For the articulated objects, the object must be picked up off the table with no part of the object being in contact with the table after 3 seconds. Once again the same grasp strategy and move should be used for all attempts. The grasp is repeated 20 times with a score of 0.5 for each successful grasp.

An extended set of objects is used to perform a further scoring of the hand. This set of objects was proposed by Jamone *et al.* for benchmarking the iCub Hand [12]. These objects are categorised into three sets. Cubic: Pudding Box, Foam Brick, Coloured Wooden Brick, and Dice. Cylindrical: Pringle's Can, Plastic Wine Glass, Large Cup, Medium Cup, and Small Cup. Complex: Plastic Pear, Plastic Strawberry, Plastic Bolt, and Plastic Nut. These are tested under the same protocol and scoring as the non-articulated object sets proposed by Calli.

By performing this benchmark, a comparison to other benchmarked hands becomes available. There are three hands in literature that have been benchmarked, we will use their results to discuss a comparison between them. These hands are the GRAB Lab Model T [119] and T-42 [110],

which are benchmarked within the Calli *et al.* [11], and the iCub anthropomorphic hand presented by Jamone *et al.* [12]. The Model T is a four fingered grasper, where each finger has two DoFs. The eight total DoF are controlled by a single servo creating a highly under-actuated grasper. This hand scored 118 out of the maximal 404. The Model T42 is has two wide opposing fingers each with two DoF. Each finger is controlled by one servo for under-actuated grasping. This is the best scoring hand of the three proposed with a score of 352 out of the total 404 available. Lastly of the three is the iCub anthropomorphic hand. This hand has four fingers and a thumb, in the traditional anthropomorphic layout. With 19 DoF and 9 actuators, this hand is the most dexterous of the three hands. This hand scored 173/404 on the basic GAB and 164/208 on the extended basic GAB.

6.5.3.2 Tactile Validation

The focus of this paper is predominately on the hardware developments of the hand and the validation of it grasping capabilities. But to be able explore tactile manipulation the system must demonstrate that it also has the tactile sensing capabilities to do so. To make this demonstration we collect all of the data being published on the ROS network for both quantitative and qualitative analysis of the design's sensing.

The main use of tactile sensing for this work is to provide feedback for the grasp controller, triggering transitions between grasp states and controlling the position of the fingers based on the extent of contact. The validation of this tactile feedback is reflected in that of the design's grasping capabilities, as the grasping demonstrated here is actively bound to the sensing.

We will present some of the resulting sensory data to provide a window into the available data that could be used to explore and develop tactile driven manipulation.

In addition to the material presented in this publication, there is a pool of research with TacTip technology. This pool demonstrates that the sensors can be used for slip detection [188], super-resolution acuity [146], and basic manipulation [28, 33, 175].

6.5.3.3 System Speed

The speed of the tactile sensing and motor control can prove a vital role in grasping and manipulation. If either operate to slowly, the system will not react fast enough to stimuli, causing failure in the grasp or damage to either the hand or the grasped object. The system communicates with the dynamixal servos that control the hand at the default baudrate of 57600 BPS (bits per second). This is fast enough to allow changes in servo command at less that a tenth of a second, whilst receiving information like torque.

With regards to the tactile sensing the raspberry pi collect frames at ~ 30 fps for each camera, and processes them to extract the pin position. This position data is transferred via a wireless ROS network resulting in a sensor frequency of ~ 25 Hz. As expected, further losses in frequency

occur with the additional processing of the Voronoi tessellation (~ 20 Hz), surface interpolation and volume processing (10-15 Hz).

The controller collects the data from the tactile ROS nodes in a loop that is faster than the data is sent from the pis. This means changes in sensor reading are reacted to as soon as they are published over the network. Thus, the closed loop control of the system bottle necks at the tactile sensing. However, there is room for optimisation of code, hardware, and system integration that will improve the speed. In the work presented here, these speeds are sufficient.

6.6 Results

In this section we present the findings from the grasping benchmarking perform with the Tac-Manipulator, aiming to validate that the hand has the adequate grasping capabilities for further work.

6.6.1 Basic GAB

As set out by the protocol detailed in Section 6.5.3, a pre-grasp, arm move, and a goal force are set for each object before performing the grasp and subsequent checks of success. The results of this test are recorded in Tables 6.4 and 6.5.

The total score of the basic GAB for the Tac-Manipulator is 206.5 out of a maximum 404, and for the extended basic GAB 178 out of a maximum 208. This is a total of 384.5 out of a maximum of 612, (62.8% of all points available).

The object groups that the design performed best on where the spherical objects, in addition to the cubic and cylindrical objects from the extended set. Nearly all of the objects in these groups could be stably grasped and rotated at all of the set points. The only exceptions are SP3 (y offset) and SP4 (z offset) for the dice from the cubic group, and the medium and small marbles from the spherical group. This is due to the small size of the objects (<16 mm), that when shifted in y moves the objects outside of the plan of the pinching fingers, or when moved in z, shifts the object under the closing arc of the fingers. Similarly for the small and medium clamps their small height (<20 mm) means that they cannot be grasped with a deflection in z. The set of clamps in the tools group and much of the objects in the complex group could be grasped and rotated, once again dropping points on the smaller dimension objects (Clamp M and S, Plastic Nut).

The screwdriver and the large marker were the two edge cases for the hand. This is reflected in the scores, being the two lowest scoring objects that could be grasped. The marker is at the very edge of the fingers' moving arc, thus under the exact centre of the hand, the fingers could make sufficient contact to grasp, raise and rotate, whereas SP2, 3, and 4 where all out of this range. The screwdriver handle on the other hand has a larger diameter than the marker, such that it can be grasped by the fingers when aligned with the x axis. The extra weight of the tool

Table 6.4: Scoring of the Tac-Manipulator in the Basic Gripper Assessment Benchmark. Set of objects and benchmarking procedure outlined by Calli *et al.* [11]. Total score is 206.5 out of 404, videos and data form the tests in this benchmark are available at *Luke_Cramphorn@bitbucket.org/Luke_Cramphorn/tac-manipulator_data*. *(SP - Set Point) (F.O. - Flat Objects) (A.O. - Articulated Objects)*

	Object	SP1	SP2	SP3	SP4
Round Objects	Soccer Ball	4	4	4	4
	Soft Ball	4	4	4	4
	Tennis Ball	4	4	4	4
	Racquet Ball	4	4	4	4
	Golf Ball	4	4	4	4
	Marble XL	4	4	4	4
	Marble L	4	4	4	4
	Marble M	4	4	0	0
	Marble S	4	4	0	0
	Score	128/144			
F.O.	Washer 1-7	0	0	0	
	Credit Card	0	0	0	
	Score	0/96			
Tools	Marker L	4	0	0	0
	Scissors	0	0	0	0
	Hammer	0	0	0	0
	Flat Screwdriver	3	4	0	0
	Drill	0	0	0	0
	Clamp XL	4	4	4	4
	Clamp L	4	4	4	4
	Clamp M	4	4	4	0
	Clamp S	4	4	4	0
	Score	67/144			
A.O.	Rope	10			
	Chain	1.5			
	Score	11.5/20			
Total		**206.5/404**			

requires using a power grasp to apply sufficient force to grasp and raise the screwdriver but the torsion created by the metal shaft creates a challenge for maintaining the object's stability.

With the articulated object the spherical grasp of the hand provides the best encompassing of the whole objects. For the rope, this grasp, in addition to the object's internal rigidity was sufficient to gain a perfect score. The chain on the other hand proved challenging to grasp with a sufficient encompassing of the links to raise the chain completely off the table in the specified 15 cm.

As mentioned the hand does not possesses the morphology necessary to perform the grasping strategies implemented in literature for picking up flat objects. The hand was tested on washer 1,

Table 6.5: Extended scoring of the Tac-Manipulator in the Basic Gripper Assessment Benchmark. Extended object set outlined by Jamone *et al.* for benchmarking the iCub Hand [12]. Total score is 178 out of 208, videos and data form the tests in this benchmark are available at *Luke_Cramphorn@bitbucket.org/Luke_Cramphorn/tac-manipulator_data*.

	Object	SP1	SP2	SP3	SP4
Cubic	Pudding Box	4	4	4	4
	Foam Brick	4	4	4	4
	Coloured Wood Block	4	4	4	4
	Dice	4	4	0	0
	Score	56/64			
Cylindrical	Pringle's Can	4	4	4	4
	Plastic Wine Glass	4	4	4	4
	Cup L	4	4	4	4
	Cup M	4	4	4	4
	Cup S	4	4	4	4
	Score	80/80			
Complex	Plastic Pear	4	4	4	2
	Plastic Strawberry	4	4	4	4
	Plastic Bolt	4	4	0	4
	Plastic Nut	0	0	0	0
	Score	42/64			
Total		**178/208**			

the largest and thickest of the flat objects, and as expected, was incapable of grasping it. To this end we did not perform the test on the rest of the flat object set. Additionally, the plastic nut in the extended set was also too flat and small for the hand to be able to grasp.

The Drill and the Hammer where not attempted during the test with the hand, due to their high weight, as it was expected that the hand has neither the power to grasp these objects nor the strength to completely avoid damage to the 3D printed fingers and sensors.

Overall the presented results for the YCB basic grasper assessment benchmark demonstrate that the proposed design of Tac-Manipulator can successfully grasp a wide range of objects (Figure 6.19). But objects with heights smaller than 10 mm and heavier than (~150 g) are outside the design's scope.

6.6.2 Grasp Procedure

The grasp controller designed for grasping objects, that was set out in Section 6.5.2.2, was successfully deployed during the above validation. The digits each performed the desired closed loop procedure, controlling the applied pressure in addition to switching between grasp strategies due to sensor and user cues. The motion of this process is documented in Figure 6.20.

Figure 6.19: Successfully grasped objects from the YCB benchmarking. Appearing in the same order as Tables 6.4 and 6.5

6.6.3 Tactile Sensing

Throughout the basic GAB, data outputs of all ROS topics where collected for each of the objects. This includes the sensory outputs from the Raspberry Pi's and the outputs of Voronoi feature processing.

The raw data from the sensors is passed from the Pi's to the control PC in the form of x and y coordinates of the centre of the pin markers. Here, as previously mentioned, we use a Voronoi tessellation method on this pin data to infer a third data dimension from the generated cell areas. This data is plotted from benchmarking test on the mini football object in Fig 6.21. This graph shows the deflection of the pin markers from their initial positions in both x and y directions. It also shows the area values produced by the Voronoi method form the shown pin data.

The data highlight the distinct separation of sensing of the object for each set point. There are four regions of deflection on the distal sensors, one for each of the set points, and three on

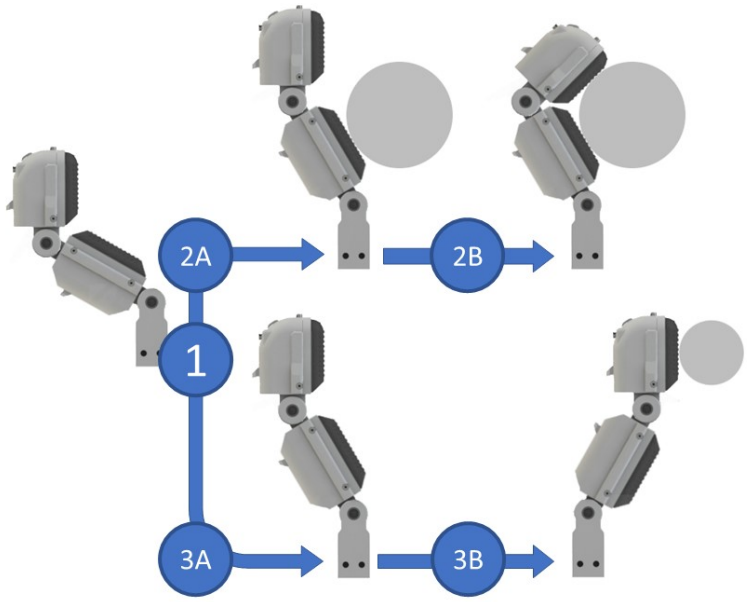

Figure 6.20: The process performed by the Tac-Manipulator to grasp objects follows a closed loop procedure that is demonstrated above. (1) The finger starts, pre-posed, with the Distal perpendicular to the palm. Upon command the system begins the close procedure, checking sensor values for contact at ~ $15Hz$. (2A) If a contact is detected on the Proximal phalanx sensor then the system switches grasp strategies, from a pinch to power. (2B) Using the sensor data from both phalanges as feedback in a proportional controller, the system adjusts digit pose such that the pressure applied to the object is close to a set point. (3A) If no contact is made on the proximal sensor the system continues with the pinch grasp strategy. (3B) Using the sensor data from the distal phalanx as feedback in a proportional controller, the system adjusts digit pose such that the pressure applied to the object is close to a set point.

the proximal as these sensors do not make contact during SP4 (z-deflection). At the start of the regions within the x deflection, there is a sudden change in the pin deflections that creates a peak before stabilising. This can be explained as the deflection first occurs due to the application of pressure (before shift) then as the object is raised off the table a shear occurs shifting all the deflections on the sensor. After grasping and raising the object, the rotation is applied to the hand. This can be seen within the pin deflections (predominately y) as pins shift together, creating what appears as a smooth bump within the data stream.

The Voronoi area data shows the relative change of the cell areas between no-contact and contact. As with the pin position data, the onset of contact is clearly visible.

The surface produced by interpolating this data, with the inferred third dimension, can be plotted as a visual aid for interpreting sensor output. As with the pin position and Voronoi area data presented in Figure 6.21, the surface visualisations clearly highlight the detection and the extent of contact Figure 6.22. In addition to this, the location and shape of the contact is easier to

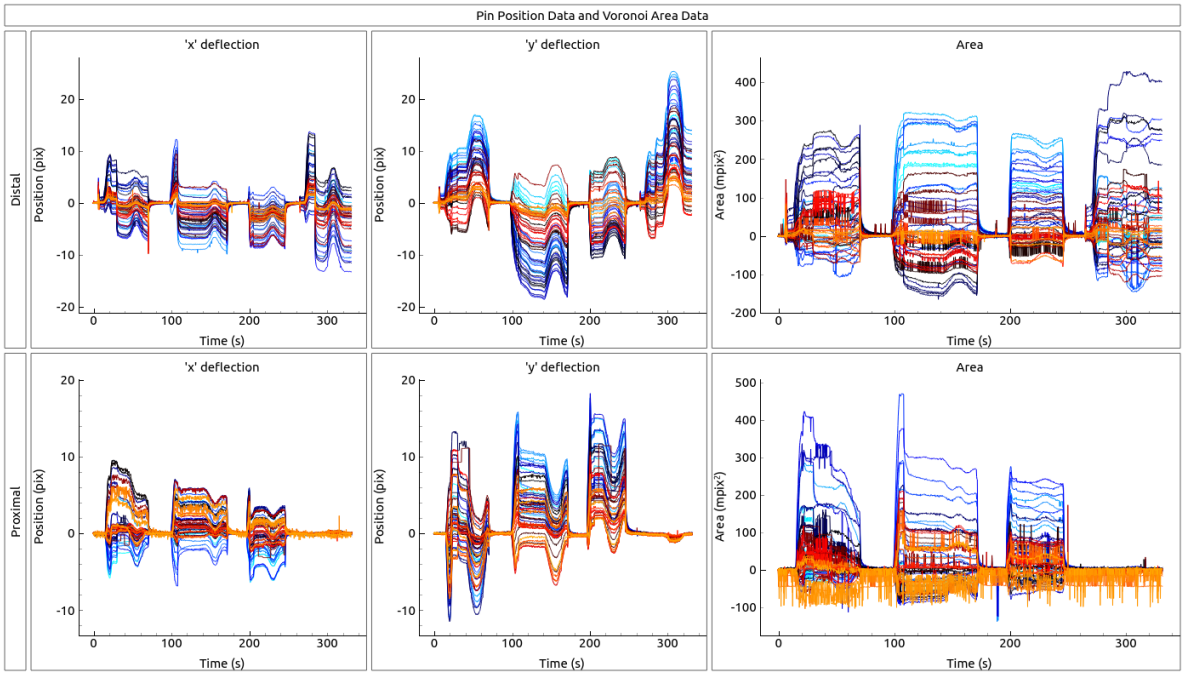

Figure 6.21: This figure shows the change in pin positions and associated inferred areas, over the course of the benchmarking test on the mini football object, for both the distal and proximal sensor on finger 1. The pin positions can be used within the Voronoi method to generate cells associated to each pin. When the sensor is contacted, the pins move relative to each other causing the areas of these cells to change. (Each colour represents a different pin ID)

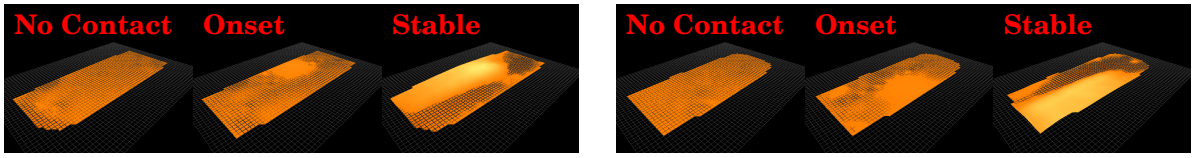

Figure 6.22: Using the Voronoi method we can infer a 3rd dimension to the standard 'xy' coordinates collected from the sensor. Here we show surface visualisations interpolated from this 3D data. Left Panel: Visualisations for; no contact; onset of contact; and stable contact, for the digit 1 proximal sensor. Right Panel: Visualisations for; no contact; onset of contact; and stable contact, for the digit 1 distal sensor. Visualisations are from data collected on the Mini Football from the YCB object set.

see on the visualisations than the presentation of pin positions.

To analyse the sensing collected during the benchmarking procedure, we provide examples of visualisations from three objects whilst being stably grasped.

The visualisation of the YCB mini football object shows data collected during set point 2 of the basic GAB procedure. As the largest object graspable within the set, the mini football is grasped with a power grasp, this allows the proximal sensors to come into contact with the object. Within the Figure 6.23 this contact can be seen as deformation on all sensors (with exception

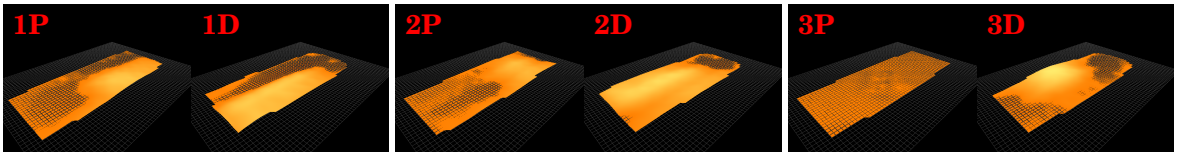

Figure 6.23: Visualisation of the stable grasp state on the YCB mini football object. The data for this visualisations was collected during the set point 2 of the basic GAB. We can clearly see the deformation of the surface as all sensors, bar digit 3 proximal, contact the large object. Interestingly, the offset in x can be seen in the sensor data, as the deformation is off-centre on digit 1, in addition to showing contact on both sensors on digit 2 and only the distal of digit 3.

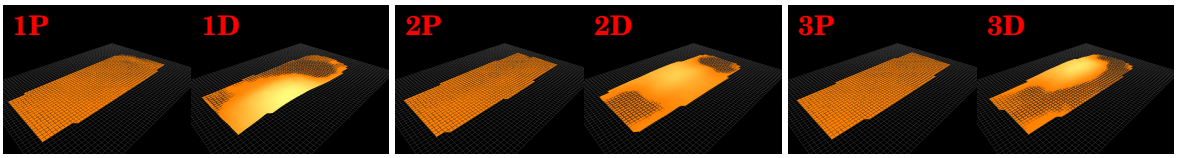

Figure 6.24: Visualisation of the stable grasp state on the YCB Raquetball object. The data for this visualisations was collected during the set point 1 of the basic GAB.

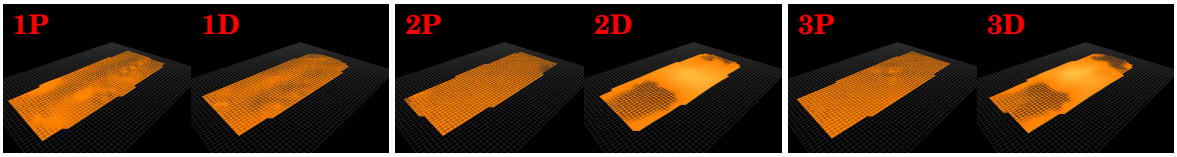

Figure 6.25: Visualisation of the stable grasp state on the YCB coloured block object. The data for this visualisations was collected during the set point 1 of the basic GAB. In contrast to the visualisations of the stable grasp sensor data from the mini football (Figure 6.23), it is clear that this much smaller object is grasped between the both distal of digit 2 and 3. During this grasp only digits 2 and 3 move as the pre-grasp is set to opposed.

digit 3 proximal). Interestingly, the offset in x can be seen in the sensor data, as the deformation is off-centre on digit 1, in addition to showing contact on both sensors on digit 2 and only the distal of digit 3.

In contrast to the mini football object the racquetball object is much smaller and can only be grasped with by the distal phalanges. The pre-grasp for this object is set to a spherical pose (r=0.5), this can be seen in the shape of the deformation on the sensors where a portion of the ball can be seen on each distal phalanx. Note the location of the contact is further up 1D than 2D and subsequently 3D. This is a result of the grasp being off centre, with digit 1 having closed less than the other fingers for this particular grasp (Figure6.24).

The last example of contact we present here is that of the coloured block object. This is one of the smaller objects that can be grasped by the proposed design. This is reflected in the use of the opposed pre-grasp (r=1) and the location of the contact visible upon 2D and 3D in Fig 6.25. The objects flat side also stand out by creating less indentation than the spherical racquetball.

The volume underneath the surface plots is a simple value that is a proxy to the deformation

Figure 6.26: This figure shows three graphs of data used for the control during the basic GAB on the mini football object. Top: The volume under the interpolated surfaces provides a simple value for determining the amount of contact. The graph shows the value of this output over the course of the test, for each of the sensor tips. Middle: The volume is passed in to a proportional controller, the feed back of which is plotted here. There are nine feedback values, one for each joint in power grasp, and 1 for each finger in the pinch grasp. Feedback is capped at +/- 0.02 to avoid rapid motion of the fingers if the controller overshoots. Feed-back below 0.01 has no effect on the system due to the limited resolution of the servos. Bottom: The last graph is a plot of joint the positions though the test, which are modified by the feedback and thus the amount of contact.

of the sensor. This is the value used as feedback into the grasp controller used for during the benchmarking tests. This sensory data along with the proportional feedback, and resulting joint positions are shown in Figure 6.26. This figure shows the data used for the control during the basic GAB on the mini football object. The volume graph shows the change in values through the test, for each of the sensor tips. The resulting data show the extent of the contact on each of the sensors, highlighting increase and decreases in surface deformation as the hand is rotated. The PID feedback graph shows the output value of the implement proportional controller, which is fed by the values in the volume graph. For the controller we have here used nine feedback values, one for each joint whilst in the power grasp, and one for each finger when in the pinch grasp. Note that as the hand does not power grasp the mini football for the final set point, thus the hand only uses the feedback for the pinch grasp (feedback 1L,2L,3L). The feedback is capped at +/- 0.02 to avoid rapid motion of the fingers if the controller overshoots. We found that feedback below 0.01 has no effect on the system as it results in commands lower than the resolution of the servos. Lastly we have included the plot of the joint positions that are controlled by the volume.

6.7 Discussion and Future Work

This paper presents a design of 3D printed hand with integrated 3D tactile sensors. The aim of the design is to address a gap in research by providing a relatively inexpensive, highly tactile hand with medium complexity and dexterity. This hand design's grasping capabilities have been tested on the basic grasp assessment benchmark, outlined for the Yale-CMU-Berkeley (YCB) object set [11] and additionally on an extended selection of objects used to test the iCub hand [12]. We have also presented sample outputs of the tactile data collected during the benchmarking procedure to highlight its richness, and justify its inclusion of it in this design.

6.7.1 Basic GAB

Following the basic grasper assessment benchmarking protocol provides the ability to asses, compare, and validate the grasping performance of robotic hands across the community. Comparing the scores of our design against other benchmarked hands provides a quantitative assessment of its abilities as well as better understanding of its weaknesses.

Our design scored 206.5 out of a maximum 404 on the basic GAB, performing better than the iCub hand (173/404) and the Model T (118/404) but it performed worse than the Model T42 (353/404). For the extended basic GAB out design scored 178 out of a maximum 208 performing marginal better than the iCub hand (164/208).

The Model T is a highly under-actuated gripper with four interlocking digits each equipped with flexible silicone IP joints. All of the fingers on this hand are driven by a single motor. The limited power that this lone motor can deliver results in the design being unable to grasp most of the heavier objects. In addition to this objects smaller than the racquet ball cannot be grasped, likely due to spilling out of the interlocking fingers. For this same reason all bar the credit card could not be grasped in the flat set, even with the nail down grasping strategy. On the other side of the coin, the hand performed well on the articulated set scoring 17 out of the available 20.

In comparison our design has multiple actuators per digit; this provides greater power per finger, although due to limitations created by the torsion spring, this advantage is limited to the screwdriver, softball, and mini-football (although span may have been a larger factor here). Our design deploys the ability to rotate the fingers into different pre grasps. This proves to be a major advantage and it allows the hand to grasp objects with opposed fingers, pinching smaller objects rather than spilling them through the interlocking fingers. Our design was not as effective at grasping the chain articulated object. This is may be due to four providing greater caging of the object.

The Tac-Manipulator scored much lower than the Model T42 (353/404). This under-actuated hand has two wide opposing fingers with flexible silicon IP joints. Each of these fingers are under-actuated and controlled by a single motor. The only objects in the set that this hand could not grasp at all were the hammer and the smallest washer, due to high weight and small size

respectively.

The most notable difference between the performance of the Tac-Manipulator and the Model T42 is that the latter can deploy techniques for picking up flat objects, scoring 84/96 compared to our 0/96. The Tac-Manipulator is unable to deploy this grasping strategy due to the distal phalanx profile being compromised by the tactile integration. Although both of these hands use Dynamixal MX-28 servos for control of the digits, the weight of the objects had a greater impact on the Tac-Manipulator's score. The 130 Nm torsion spring required to passively return the heavy tactile fingers whilst the hand faces palm down, cuts the torque that the motors can deliver upon the objects. This could possibly be addressed by using an additional servo (lower power than MX-28s) to actively return/release the MCP joint.

The iCub hand is a small anthropomorphic hand, around that of a child's, designed for the iCub robot. This hand is controlled by a human operator for the task, but due to its small size it cannot grasp a large number of the objects used in the benchmark. Weight and size of the object are the largest factors limiting the hand's grasping capabilities. Some of the objects that cannot be grasped are the heavy hammer and drill, large soccer ball and soft ball, and all the flat objects. This hand scored 173 out of the available 404 on the basic GAB and 164 of the available 208 on the extended set, introduced for the hands.

The iCub hand and our presented design both face challenges from the heavy and flat objects. The main differences between the two hands' grasping capabilities are due to the scale of the hand. Our design has a large finger span that allows it to grasp the larger spherical objects where the smaller iCub hand could not. However the iCub hand could pick up the plastic nut object from the complex set, where our design could not.

Overall the presented results for the YCB basic grasper assessment benchmark, and the comparison to other benchmarked hands, demonstrate that the proposed design of Tac-Manipulator can successfully grasp a wide range of objects, roughly bounded by objects with heights smaller than 10 mm and heavier than (~150 g). Although the performance of the presented hand is poorer than that of the Model T42, the greater DoF and the addition of tactile capabilities should allow the hand to be able to build upon the grasps it can achieve to perform more complex perception and manipulation than that of the Model T42.

6.7.2 YCB Object Set and Grasping Limitations

In addition to the benchmarking procedures that provide a comparison and quantitative analysis of the hand, we explored grasps on the whole object set to qualitatively analysis the grasping. Here we highlight features of objects that the design cannot grasp.

a) Small: The path of movement the digits move through, in the pinch state, is an arc that reaches a maximum distance from the palm when the digit is straight and perpendicular to the hand. As the digit continues to close from this point the distance decreases resulting in a region beneath the fingers path that cannpt be grasped without moving the hand. Moving the hand closer as

the fingers close ultimately maintaining the position of the distal tips in space would reduce this allowing for smaller objects to be grasped.

b) Heavy: Weight of objects is always an issue for robotic hands and grippers due to the limited power density of conventional motors. The maximum force Dynamixal motors, and therefore the payload of the Tac-Manipulator, is greatly eroded by the powerful torsion spring required to return the heavy sensorised digits whilst palm down. This erosion of deliverable force increases as the finger tends towards the maximum of the digit's range, due to the non-linearity of torsion springs. With the chosen tendon layout for the digits, the amount of force that can be applied can be increased by using a power grasp where both motors are pulling on the MCP joint, in comparison to the under-actuated pull of the pinch grasp. However this only marginally increases deliverable force and changes the state of the hand, the impact of which has yet to be explored.

c) Flat: Due to the deep profile required for the integrated sensors, the hand is unable to perform the 'nail down' grasping approach utilised by the Model T42 and iHY ([110, 123]) for undercutting and flipping flat objects into a stable state. Additionally, flat objects also exhibit the same properties outlined for small objects.

d) Borderline Objects: Some of the object in the set borderline the capabilities of the hand being graspable but not consistently. The large marker and the screwdrivers are some of these objects, with a diameter just large enough for the distal surface to come in contact with it in the pinch close. The contact is not constantly sufficient to provide enough frictional force to lift the objects.

6.7.3 Tactile Sensing and Sensors

With an existing body of research on the TacTip, we know that the sensors can be used for slip detection [188] and basic manipulation [28, 33, 175]. We believe that the TacTip hardware has been proven to be versatile and accurate, hence our integration of the sensors in this design.

The design demonstrates the integration of this sensor technology into each phalanx of the hand's fingers. This provides large coverage of tactile sensing on the hand allowing perception of objects in power grasps and tactile feedback for control purposes. We have successfully used the tactile sensing to trigger active state changes between grasping strategies that mimic the passive transitions of under-actuated grasper like the iHY [111].

In the presented work we have utilised the Voronoi tessellation methods of feature inference to determine the extent of contact and trigger state transitions within the grasp controller [31]. This allowed us to demonstrate the grasping of the hand by providing a simple value for closed-loop control of the hand and its DoFs.

We presented the data that is produced by the integrated sensors as the raw centroid positions of the pin markers and the as the pre-processed data using the Voronoi methods. The data shows a richness of information such as shear and deformation when being grasped, lifted, and rotated, in addition to shape a contact location that could be used for improved perception and control.

The sensing is limited to a single face of each phalanx. This introduces complications if the fingers were to come into contact with a stimulus where sensing is not present. Without the feedback the finger would aim to move into the object until motor torque is reached. Although this is unlikely to cause damage to the hand as the Dynamixal torque limit is low, it may cause complications in dynamic manipulations where contacts on objects are not perceived.

As mentioned earlier, the weight of the sensors is another concern for the design. The added weight of two TacTips to each finger requires that the spring providing the passive return is much stronger than would be required without the sensors. This decreases the amount of force the motors have left to apply to the objects. In the future a small motor with enough power to lift the finger against gravity could be used to solve this issue, as it could actively release to allow the other motors to use the full capabilities on the objects without any force erosion.

6.8 Conclusions and Future work

Overall the publication presents a validation of grasping and presentation of tactile capabilities. The scores of the benchmarking demonstrate that the presented design is capable of stably picking up and moving a variety of objects. Although, it also highlights limitations in its grasping capabilities that arise from the integration of the sensors. However we believe that the cost of functionality that is incurred by this integration is acceptable given that the sensors provide a depth of sensory information that can be used to both provide active control of the hand during grasping and to enable the exploration of tactile dexterous manipulation with the design.

The 3D printed design of the hand and the sensors allows for relatively low cost of production and with the TacTip technology and full control of both the IP and MCP joint the design addresses the gap of a relatively inexpensive, highly tactile hand with medium complexity and dexterity.

Future work will focus on exploring the dexterous capabilities of the hand and how the tactile sensing can be used to support and improve them. We will also aim to improve the design, specifically the grasping, sensing, and manipulation capabilities of the Tac-Manipulator.

6.9 Postface

6.9.1 Summary, Paper Analysis, and Closing Remarks

In this chapter we demonstrated tactile sensor integration on two robotics hands, the Shadow Modular Grasper, and a new design of 3D printed hand. The Shadow Modular Grasper integration was achieved by replacing the standard, non-sensor distal phalanx, with customised TacTips. This hand has the ability to rotate its three fingers independently, allowing for the rolling of the fingers whilst in contact with an object. Using the aforementioned Voronoi method, a centre-of-pressure feature is extracted and calibrated to roll and pitch. This is then fed into the hands controller to perform roll and pitch adjustments of the distal phalanges, maximising contact area.

The second hand/sensor integration was on the Tac-Manipulator, a 3D printed hand designed with six integrated sensors, one for each phalanx. The goal of the design was to provide a tool that makes tactile dexterous manipulation accessible. Within the work, the grasping capabilities of the design were tested against a benchmarking procedure and the outputs of the tactile sensing are presented. Overall the work showed that the design has adequate grasping capabilities and tactile outputs to pursue the exploration of more complex tactile focused manipulation.

The paper presented in this chapter is the introduction to the new hand design. It covers the hardware and software developments and demonstrates the core functionality that is required for further work. The paper does not explore any manipulation or advanced use of the tactile sensing as it was not within the introductory scope of the paper. The next steps would be to begin testing the system with the algorithms and experiments, and ultimately, the exploration of tactile manipulation.

This chapter poses the question 'Can the integration of tactile sensing into multi-fingered system provide data to improve dexterous capabilities?': With regards to this, the presented material demonstrates tactile sensing informing control of digit reorientation to maximise surface contact and the changing of grasp strategy in a simple grasp controller. These both demonstrate dexterous capabilities supported or driven by the tactile sensing. However the scope of this question has not been met here as tactile manipulation is a complex and challenging problem. More research is needed to understand dexterous manipulation and how much of a role tactile will play in the solutions. The hope is that the work in this chapter and the thesis will provide another brick in the foundations for which the ultimate goal of robotic dexterous in-hand manipulation will be built upon.

CHAPTER 7

DISCUSSIONS, CONCLUSIONS, AND FUTURE WORK

In this thesis, a series of studies have been presented that provide answers to four research questions. These questions set out to address an overall research aim, where each is the focus of a chapter of this thesis. Here we will summarise and discuss the material presented in this thesis, focusing on how findings from all of the chapters fit into the overall thesis research aim, and what conclusions can be drawn from this. Finally we will discuss and suggest a future direction for the work.

7.1 Discussion

In this thesis I set out the research aim 'to develop hardware and methods for the purpose of improving understanding, and conducting exploration, of tactile perception and tactile manipulation'. To address this I have presented a collection of research on developing and utilising tactile sensing. Starting this thesis with a literature review that presents aspects of tactile sensing, manipulation, and biomimetics and highlighting that these fields together are both relevant and necessary considerations when trying to achieve dexterous manipulation. To further address this aim I proceeded with four chapters, each presenting an aspect of work that contributes towards the research aim.

Making reflections on the work presented in this thesis is crucial for critically analysing the progress made towards the proposed research aim. It is also an important exercise for understanding the strengths and limitations of contributions made throughout my doctoral studies, allowing me to provide an expert opinion on the direction for continued work on the topic.

7.1.1 TacTip Hardware

The tactile sensor that is used throughout this work is the TacTip. Chapter 3 discusses the original sensor hardware developed by Chorley *et al.* in 2009 [143] and presents an analysis of the sensor technology. From this, I introduce sensor redevelopments that reduce the cost and time required to prototype the sensor. This was achieved by introducing a combination of multi-material 3D printing methods and modular sensor tips. These developments to the sensor hardware made it possible to implement a pin marker layout that is better suited for identification in computer vision software. But ultimately the changes allow for increased complexity in the construction of the sensor tips. Leading to the development and testing of a biomimetic artificial fingerprint that demonstrated that spatial tactile perception can be improved on small spatial scales (≤2.5 mm) by the inclusion of papillary ridges by up to 140-170% when compared with a sensor tip without them [30]. In addition to this, a variety of fingertip designs have been created with these methods, including TacTip integrations on the Model-M2 [33], GR2 [175], Shadow Modular Grasper [41], and the Tac-Manipulator presented in Chapter 6 6. Overall, the work in this thesis has demonstrated that the TacTip, being 3D printed in multiple materials, proves to be a flexible and versatile hardware for tactile sensing.

Benefits of the new TacTip Design The TacTip V2 provides some benefits over the original sensor and other tactile sensors. In comparison to the original sensor the new manufacturing technique of 3D printing allows for faster prototyping, more complex geometries, and low one-off cost. The modularity of the tips provides quick and easy replacement of damage tip in addition to swapping between alternative tip designs.

When compared to other sensor technology the new TacTip has the benefit of being cheap and modifiable. both of which are valuable attributes for a research tool. The camera based methods of tactile sensing employed by the TacTip means that the sensor has relatively high resolution [8]. This use of a camera also moves the electronics away from the contact surface, this both improves robustness and allows for the very compliant skin that characteristics the tactile interactions of the TacTip.

Limitations of the new TacTip Design With regards to the original sensor, the new design is not an improvement on all fronts. There are strong points that the original sensor has benefits that future versions of the TacTip should attempt to recover. There are three points that are crucial to remark upon, and all of which are differences between the 3D printed sensor skin and the original moulded silicone skin. Firstly, lower robustness of the Tango Black + 3D printed rubber means that sensor tips will tear easier. Secondly, silicone is both more flexible and more elastic than the new tips. This means that the new system has added levels of hysteresis. Lastly, the silicone was very near to opaque and thus blocked out the noise of external lighting. However

the new skin is participially translucent, allowing noise that can interfere with the sensors in certain conditions.

As with the original sensor, the camera limits the size and shape of the complete sensor. In particular the field of view and focus of the camera has to be able to capture and resolve the pin marker in the sensor; thus it must be placed at a distance from the sensing element making the profile of the TacTip larger than alternative technologies like capacitive and resistive tactile sensors.

7.1.2 Active Manipulation

Chapter 4 shows an early venture into tactile manipulation. Implementing the sensor as an end-effector on a 6 DoF robot arm with algorithms for active perception [27, 166], modified with a control policy to adjust position that creates an action on a stimulus. This action is a basic manipulation in the form of rolling, where only tactile feedback is used to perform a trajectory following task [28]. In this, subtleties were indicated under large (20 mm) disturbances of the cylinder location during testing with respect to the system's ability to react to the sudden change in perceived object location. This reaction was found to depend on the Bayesian update rule for the location belief during perceptual decision making. If the prior beliefs for estimating location are set equal to the posterior beliefs for the previous estimate, the system was not able to perceive sudden changes of location. This was because the prior beliefs had become sufficiently peaked late in the trial that new sensory evidence for location was ignored. This could be addressed with a maximum likelihood procedure applied to just the present contact data, although this solution reduces the accuracy of the tactile manipulation. An intermediate solution was proposed, in which the prior beliefs are diminished by a power law relative to the posterior beliefs, giving moderately accurate performance that can respond to sudden changes in location. This presents as a trade-off between responsiveness to unknown change and manipulation accuracy. These methods for rolling manipulations were expanded onto simple hand platform of the GRAB Lab Model-M2 [33]. By performing the manipulation with lower physical constraints and a variety of stimuli, the work showed the versatility of the methods. Performing manipulations within the context of hands demonstrates an important step towards exploring dexterous tactile manipulation. Although presenting only a simple manipulation, the work demonstrates that tactile sensors can provide sufficient feedback to perform them. This highlights the potential for their role in more dexterous and complex manipulations.

7.1.3 Visualisation and Feature inference

The demonstration of methods for directly inferring tip displacement, contact location, shear direction, and magnitude from the TacTip tactile sensor were presented in Chapter 5. This work has highlighted that the use of Voronoi tessellation on the data set allows transduction of a 3^{rd} dimension to the data, whilst providing a visualisation that enhances human interpretation

of the sensor output. These methods showed that without the use of black box classification or regression techniques it is possible to extract useful information from the sensor data. The work focused on the inference of shear direction, which was validated against arm telemetry and showed predications to an average of $\sim 2.3°$. It is likely that this error in shear direction would be lower for classifier methods previously used with the TacTip; it is clear that the lack of training required allows the shear to be interpreted under different pressures. I believe that the generality of this method will be of benefit for future work where the collection of large datasets for black box methods is either challenging or not possible. Due to this, the methods are implemented and utilised for closed loop control of the integrated Shadow Modular Grasper and the Tac-Manipulator design presented in Chapter 6.

7.1.4 Tactile Hands

The integration of tactile sensors into robotic hand platforms is a crucial step in advancing capabilities to explore tactile perception and manipulation. Work in this direction was presented in Chapter 6, where tactile sensors where integrated with the shadow modular grasper and new design of 3D printed hand.

The shadow modular integrated with the sensors combines the ability to rotate its three fingers independently, with a centre of pressure feature from the Voronoi method allowing the controller to perform roll and pitch adjustments of the distal phalanges, maximising contact area.

We also presented the Tac-Manipulator, a 3D printed hand designed with six integrated sensors. The grasping capabilities of this design were tested against a benchmarking procedure and the outputs of the tactile sensing are presented, demonstrating both adequate grasping capabilities and tactile outputs to pursue the exploration of more complex tactile focused manipulation.

Benefits of the new Tac-Manipulator Design The extra degrees of freedom employed by the Tac-Manipulator provide it with more control over the pose of the digits both in and out of a grasp. This should allow the hand to be able to perform more dexterous action upon grasped objects in the form of in hand manipulation. Additionally, each digit has coverage of high-resolution tactile sensors on the contact side of both phalanges. This gives the system a large amount of tactile information that can be used for many perceptual task that other hands are not equipped for. This also allows for the deployment of closed-loop grasping that can mimic the adaptivity of under-actuation.

Limitations of the new Tac-Manipulator Design The current design of the Tac-Manipulator has some limitations that may need to be addressed moving forward. Firstly, the TacTip technology modifies the profile of the distal phalanx in such away that the undercutting grasp strategy utilised by other hands for picking up flatter objects is not possible. This reflected in the score

achieved in the benchmarking procedure. Lastly, the integrated TacTip sensor add extra weight to the digits. This weight means that a much stronger passive return mechanism is required to hold the fingers in the standby position upside down. Ultimately, this erodes the maximum force that the motors can deliver and thus the payload of the hand.

7.2 Conclusions

This thesis set out to address the overall research aim of...

'To develop hardware and methods for the purpose of improving understanding, and conducting exploration, of tactile perception and tactile manipulation.'

For which four research questions were proposed and answered within each of the chapters. To summarise these findings, the questions are revisited and the answers summarised.

- **Question 1:** 'Can developments and improvements in the TacTip hardware lead to gains in its tactile sensing capabilities and new directions in which the sensor can be utilised?'

  In Chapter 3, I set out to answer this question by developing and improving the TacTip hardware. This lead to gains in tactile sensing capabilities, notably due to the addition of a biomimetic fingerprint. These modifications provided new directions in which the sensor can be utilised as the 3D printing process allows for greater versatility in the form of the sensor, due to the simplified manufacturing process. This proved most valuable for designing sensor integration for the hands briefly presented in Chapter 4 and for the design documented in Chapter 6.

- **Question 2:** 'Can tactile sensing be used to provide the necessary information and feedback for performing basic manipulation of an object based solely on the state of contact?'

  Chapter 4 presents the basic manipulation of rolling a cylinder using, solely, the tactile perception of the state of contact. This was demonstrated with both a simple single DoF roller and a sensor mounted on a 6 DoF arm, and a simple tactile robotic gripper. This answers the posed question for a rolling manipulation, but further work is needed to answer this for other forms of manipulation, basic or complex.

- **Question 3:** 'What key features can be identified from tactile data without training black-box methods like classifiers or regressors and will this enable greater versatility and generality of tactile sensing?'

  The methods demonstrated in Chapter 5 showed that inference of shear direction, shear magnitude, contact location, and tip displacement could be achieved without the use of

black-box methods. In particular, shear direction was found to be inferable irrespective of contact depth and required no training. I also showed that shear magnitude and the displacement of the sensor tip could be inferred with only simple calibrations. These methods show improved versatility and generality of sensing, in comparison to the methods utilised in Chapter 4, by being able to extract useful features, irrespective of the contact state. Further work to validate the extent of these improvements is still necessary for deeper understanding.

- **Question 4:** 'Can the integration of tactile sensing into multi fingered system provide data to improve dexterous capabilities?'

  The material in Chapter 6 demonstrates the use of tactile sensing to inform control. Both reorientation of digits to maximise surface contact and the triggered change of grasp strategy in a simple grasp controller were presented. In general this provides an answer to the question; yes, the tactile sensing provided by the integration allowed for feedback that drove dexterous actions. But it is important to note that tactile manipulation is a complex and challenging problem. To fully answer this question more research is need to understand dexterous manipulation and how much of a role tactile will play in the solutions.

These questions were proposed to guide the research towards the overall aim. The answers to these questions allow us to conclude whether the outlined aim has been addressed by this thesis.

As highlighted in the answers for questions 1 and 4, tactile hardware has been developed in the form of a modified sensor and a tactile hand design. From these developments I presented improved understanding on the effects of fingerprints on tactile perception and presented a tool for the exploration of tactile dexterous manipulation.

As mentioned in the answer to question 2, I also developed methods for the basic manipulation of rolling a cylinder using, solely, the tactile perception of the state of contact. Continued exploration for which was conducted upon a simple hand system in the form of the Model-M2. Although this answered the posed question, it highlights many more with regards to more complex tactile manipulation. To address these, I have developed the tactile hand hardware presented in Chapter 6, aiming to provide a platform to explore more complex tactile manipulation.

In answering question 3 it can be seen that methods have been developed which allow for the perception by direct inference of key tactile features. This provided versatility and generality that allowed for the exploration of tactile manipulation by reorienting the digits of the Shadow Modular Grasper and for control and perception of force in a grasp controller implemented on the Tac-Manipulator.

Lastly, answering question 4 produced two robotic hands with tactile integrations. This work introduced both new hardware and methods that have allowed the exploration of tactile perception and to touch on the exploration of tactile manipulation. This work has greatly enhanced my own understanding of tactile hands and the challenges and potentials associated with them.

From this I conclude that the research aims set out for this thesis have been addressed. Although upon reflection only the surface of tactile manipulation has been scratched within the presented material. I would argue that tactile sensing will play a crucial role in achieving complex dexterous tactile manipulation. This is supported by the work I have presented, as it has demonstrated accurate location perception, feature perception, simple manipulations, and grasp adaptation which are all components of the bigger challenge that complex dexterous tactile manipulation presents.

7.2.1 Future Work

There a are few directions that I would propose for continuation and future work. Firstly the TacTip sensor technology has strengths and weaknesses, some of which are a trade off that may or may not be unavoidable. It has proven to be a cheap, versatile, flexible sensor but suffers from hysteresis, noise, and large size. The development of the integrated TacTips for the Tac-Manipulator has already demonstrated that the scale of the sensor can be drastically reduced (when compared to the standard TacTip). Although these versions still have a cumbersome profile that impairs grasping. I propose that there should be future developments of the sensor hardware that explore pushing the limits of the sensor's scale and profile as this will improve its integration with hands. Additionally exploration of possible alternative materials used for the skin and the flesh should be performed to minimise the impacts of hysteresis and noise within the sensor system.

The Voronoi method of inferring a third dimension for the data provided a powerful interpretation of that TacTip data that has allowed for closed loop control of the sensor without the need for complex training or modelling. Although the work presented in this thesis only explored a few of the noted identifiable features, such as deformation, shear direction, and centre of pressure. The work could be explored further by validating the accuracy of the contact location feature or identifying whether distinct features like shape, corners, or edges can be directly inferred.

The hand design presented in Chapter 6 has been designed to have greater control of its degrees of freedom with a full complement of TacTip tactile sensors. The work presented here only demonstrates the grasping and tactile capabilities of the hand, providing the tool for exploring in-hand tactile manipulation. Due to this, there is work required on exploring how the integrated tactile sensor can be utilised to enable and improve the hand in a manipulation workspace. The hand itself is an initial functional prototype, the digits, sensors tips, and camera of which are modular; thus further development of the hand is possible and may be required to fully explore its capabilities .

Lastly, the design methodology of inexpensive and 3D printed hardware, make the sensors and the hand ideal for open-sourcing. This has been attempted with the original TacTip sensor, but has not been attempted with the new multi-material designs. Open-sourcing the design will allow for other groups who are interested in exploring tactile sensing and manipulation, but lack

the expertise or time to produce their own or the funding to purchase the expensive sensors or sensor equipped hands. However, some modifications of the hardware will be necessary to make them accessible and usable to the wider community.

7.3 Closing Statement

It is my hope that the developments and exploration of tactile sensing in this thesis demonstrate some incremental addition to the scientific understanding of the field. It is possible that in the not too distant future we could see breakthroughs in tactile sensing and artificial intelligence that begin to address the challenges of dexterous manipulation.

In a world where robots are equipped with a complete sense of touch and the learning and control algorithms to maximise them, we can expect to see robots actively playing a role in many more areas of our society. There are some important areas of robotics that continued research on these topic could revolutionise. Firstly, with these abilities robots will perform much better in human environments, being able to interact with both the environments and humans safely. One potential use of these robots would be in the care of our elderly, taking pressure off our over-stretched healthcare system and preserving the independence of our ageing population. Another could be deployment of robotics into unknown environments where sensing and interacting with the environment in necessary for it to complete tasks without maps or models. Specifically areas where risk is high for humans, for instance search and rescue in collapsed buildings or clean-up efforts following environmental disasters. In the long term I suspect tactile sensing will become as accessible and important to robotics as computer vision.

BIBLIOGRAPHY

[1] R. S. Dahiya, G. Metta, M. Valle, and G. Sandini, "Tactile sensing-from humans to humanoids," *IEEE Transactions on Robotics*, vol. 26, no. 1, pp. 1–20, 2010.

[2] J. M. Wolfe, K. R. Kluender, D. M. Levi, L. M. Bartoshuk, R. S. Herz, R. L. Klatzky, S. J. Lederman, and D. M. Merfeld, *Sensation & perception*.
Sinauer Sunderland, MA, 2006.

[3] E. R. Kandel, J. H. Schwartz, T. M. Jessell, D. of Biochemistry, M. B. T. Jessell, S. Siegelbaum, and A. J. Hudspeth, *Principles of neural science*, vol. 4.
McGraw-hill New York, 2000.

[4] J. R. Phillips and K. O. Johnson, "Tactile spatial resolution. III. A continuum mechanics model of skin predicting mechanoreceptor responses to bars, edges, and gratings," *Journal of neurophysiology*, vol. 46, no. 6, pp. 1204–1225, 1981.

[5] R. S. Johansson, U. Landstro, and R. Lundstro, "Responses of mechanoreceptive afferent units in the glabrous skin of the human hand to sinusoidal skin displacements.," *Brain Research*, vol. 244, no. 1, pp. 17–25, 1982.

[6] Å. Vallbo and R. S. Johansson, "Properties of cutaneous mechanoreceptors in the human hand related to touch sensation.," *Human neurobiology*, vol. 3, no. 1, pp. 3–14, 1984.

[7] D. Purves, G. J. Augustine, D. Fitzpatrick, W. C. Hall, A.-S. LaMantia, J. O. McNamara, and L. E. White, "Neuroscience. 4th," *Sunderland, Mass.: Sinauer. xvii*, vol. 857, p. 944, 2008.

[8] Z. Kappassov, J. A. Corrales, and V. Perdereau, "Tactile sensing in dexterous robot hands - Review," *Robotics and Autonomous Systems*, vol. 74, pp. 195–220, 2015.

[9] Smooth-On, "Vytaflex 60 Datasheet." https://www.smooth-on.com/products/vytaflex-60/.
09/11/18.

[10] Camodels, "Stratasys TangoBlack+ Datasheet." https://www.camodels.co.uk/media/1268/connex-tango-black-plus.pdf.
09/11/2018.

[11] B. Calli, A. Walsman, S. Member, A. Singh, S. Member, S. Srinivasa, S. Member, P. Abbeel, S. Member, M. Dollar, and S. Member, *Benchmarking in Manipulation Research : The YCB Object and Model Set and Benchmarking Protocols*.
2015.

[12] L. Jamone, A. Bernardino, and J. Santos-Victor, "Benchmarking the Grasping Capabilities of the iCub Hand With the YCB Object and Model Set," *IEEE Robotics and Automation Letters*, vol. 1, no. 1, pp. 288–294, 2016.

[13] M. J. Pearson, B. Mitchinson, J. Welsby, T. Pipe, and T. J. Prescott, "SCRATCHbot: Active tactile sensing in a whiskered mobile robot," in *Lecture Notes in Computer Science (including subseries Lecture Notes in Artificial Intelligence and Lecture Notes in Bioinformatics)*, vol. 6226 LNAI, pp. 93–103, Springer, Berlin, Heidelberg, 2010.

[14] R. J. Wood, B. Finio, M. Karpelson, K. Ma, N. O. Pérez-Arancibia, P. S. Sreetharan, H. Tanaka, and J. P. Whitney, "Progress on 'pico' air vehicles," in *Springer Tracts in Advanced Robotics*, vol. 100, pp. 3–19, 2012.

[15] G. Sandini, G. Metta, D. Vernon, L. Natale, and F. Nori, "The iCub humanoid robot," in *Proceedings of the 8th Workshop on Performance Metrics for Intelligent Systems - PerMIS '08*, (New York, New York, USA), p. 50, ACM Press, 2010.

[16] University of Calgary, "Sensory Cortical Homunculus." http://www.ucalgary.ca/pip369/mod7/touch/neural2.
05/10/2019.

[17] B. R. Komisaruk, N. Wise, E. Frangos, W. C. Liu, K. Allen, and S. Brody, "Women's clitoris, vagina, and cervix mapped on the sensory cortex: fMRI evidence," *Journal of Sexual Medicine*, vol. 8, pp. 2822–2830, oct 2011.

[18] F. Mancini, A. Bauleo, J. Cole, F. Lui, C. A. Porro, P. Haggard, and G. D. Iannetti, "Whole-body mapping of spatial acuity for pain and touch," *Annals of Neurology*, vol. 75, pp. 917–924, jun 2014.

[19] Robotiq, "Adaptive Gripper Datasheet Hand-E 2F-85 2F-140." https://blog.robotiq.com/hubfs/Product-sheets/Product-sheet-Adaptive-Grippers-EN.pdf, 2018.
2019-02-15.

[20] Thinkbot Solutions, "Robotiq Gripper Image Source." https://www.thinkbotsolutions.com/shop/robotiq-2-finger-85.
05/10/2019.

[21] Righthand Labs, "ReFlex Robotic Gripper." https://www.labs.righthandrobotics.com/reflexhand. 2019-02-15.

[22] Righthand Labs, "Righthand Labs Reflex Image." https://www.labs.righthandrobotics.com/reflexhand. 05/10/19.

[23] Z. Xu and E. Todorov, "Design of a highly biomimetic anthropomorphic robotic hand towards artificial limb regeneration," *Proceedings - IEEE International Conference on Robotics and Automation*, vol. 2016-June, pp. 3485–3492, 2016.

[24] D. Guinard, Y. Usson, C. Guillermet, and R. Saxod, "Merkel complexes of human digital skin: Three-dimensional imaging with confocal laser microscopy and double immunofluorescence," *Journal of Comparative Neurology*, vol. 398, no. 1, pp. 98–104, 1998.

[25] M. A. Goodrich and A. C. Schultz, "Human-Robot Interaction: A Survey," *Foundations and Trends® in Human-Computer Interaction*, vol. 1, no. 3, pp. 203–275, 2008.

[26] D. Feil-Seifer and M. J. Matarić, "Defining socially assistive robotics," in *Proceedings of the 2005 IEEE 9th International Conference on Rehabilitation Robotics*, vol. 2005, pp. 465–468, IEEE, 2005.

[27] N. F. Lepora, U. Martinez-Hernandez, and T. J. Prescott, "Active Bayesian Perception for Simultaneous Object Localization and Identification," in *Robotics: Science and Systems IX*, 2013.

[28] L. Cramphorn, B. Ward-Cherrier, and N. F. Lepora, "Tactile manipulation with biomimetic active touch," in *Proceedings - IEEE International Conference on Robotics and Automation*, vol. 2016-June, pp. 123–129, IEEE, may 2016.

[29] L. Cramphorn, B. Ward-Cherrier, and N. F. Lepora, "Addition of a Biomimetic Fingerprint on an Artificial Fingertip Enhances Tactile Spatial Acuity," *IEEE Robotics and Automation Letters*, vol. 2, no. 3, pp. 1336–1343, 2017.

[30] L. Cramphorn, B. Ward-Cherrier, and N. F. Lepora, "A Biomimetic Fingerprint Improves Spatial Tactile Perception," pp. 418–423, Springer, Cham, 2016.

[31] L. Cramphorn, J. Lloyd, and N. F. Lepora, "Voronoi Features for Tactile Sensing: Direct Inference of Pressure, Shear, and Contact Locations," in *IEEE International Conference on Intelligent Robots and Systems*, pp. 2752–2757, IEEE, may 2018.

[32] L. Cramphorn, J. James, N. Pestell, A. Church, and N. F. Lepora, "The Tac-Manipulator: A tactile robotic hand with the tools for manipulation at its fingertips," *Not Submitted*, 2019.

[33] B. Ward-Cherrier, L. Cramphorn, and N. F. Lepora, "Tactile Manipulation With a TacThumb Integrated on the Open-Hand M2 Gripper," *IEEE Robotics and Automation Letters*, vol. 1, no. 1, pp. 169–175, 2016.

[34] B. Ward-Cherrier, L. Cramphorn, and N. F. Lepora, "Exploiting symmetry to generalize biomimetic touch," in *Lecture Notes in Computer Science (including subseries Lecture Notes in Artificial Intelligence and Lecture Notes in Bioinformatics)*, vol. 9793, pp. 540–544, 2016.

[35] N. Pestell, B. Ward-Cherrier, L. Cramphorn, and N. F. Lepora, "Tactile exploration by contour following using a biomimetic fingertip," in *Lecture Notes in Computer Science (including subseries Lecture Notes in Artificial Intelligence and Lecture Notes in Bioinformatics)*, vol. 9793, pp. 485–489, 2016.

[36] N. F. Lepora, K. Aquilina, and L. Cramphorn, "Exploratory Tactile Servoing With Active Touch," *IEEE Robotics and Automation Letters*, vol. 2, no. 2, pp. 1156–1163, 2017.

[37] B. Ward-Cherrier, L. Cramphorn, and N. F. Lepora, "Exploiting Sensor Symmetry for Generalized Tactile Perception in Biomimetic Touch," *IEEE Robotics and Automation Letters*, vol. 2, no. 2, pp. 1218–1225, 2017.

[38] B. Ward-Cherrier, N. Pestell, L. Cramphorn, B. Winstone, M. E. Giannaccini, J. Rossiter, and N. F. Lepora, "The TacTip Family: Soft Optical Tactile Sensors with 3D-Printed Biomimetic Morphologies," *Soft Robotics*, p. soro.2017.0052, 2018.

[39] N. Lepora, M. Pearson, and L. Cramphorn, "TacWhiskers: Biomimetic optical tactile whiskered robots," *IEEE International Conference on Intelligent Robots and Systems (IROS)*, 2018.

[40] N. F. Lepora, N. Burnus, Y. Tao, and L. Cramphorn, "Active Touch with a Biomimetic 3D-Printed Whiskered Robot," in *Conference on Biomimetic and Biohybrid Systems*, pp. 263–275, Springer, Cham, 2018.

[41] N. Pestell, L. Cramphorn, F. Papadopoulos, and N. F. Lepora, "A Sense of Touch for the Shadow Modular Grasper," *IEEE Robotics and Automation Letters*, vol. 4, pp. 2220–2226, apr 2019.

[42] W. Moyle, C. J. Jones, J. E. Murfield, L. Thalib, E. R. Beattie, D. K. Shum, S. T. O'Dwyer, M. C. Mervin, and B. M. Draper, "Use of a Robotic Seal as a Therapeutic Tool to Improve Dementia Symptoms: A Cluster-Randomized Controlled Trial," *Journal of the American Medical Directors Association*, vol. 18, pp. 766–773, sep 2017.

[43] C. Kunz, C. Murphy, R. Camilli, H. Singh, J. Bailey, R. Eustice, M. Jakuba, K. I. Nakamura, C. Roman, T. Sato, R. A. Sohn, and C. Willis, "Deep sea underwater robotic exploration in the ice-covered arctic ocean with AUVs," *2008 IEEE/RSJ International Conference on Intelligent Robots and Systems, IROS*, pp. 3654–3660, 2008.

[44] Boston Dynamics, "Atlas Humanoid." https://www.bostondynamics.com/atlas, 2018. 2019-03-11.

[45] J. F. Vincent, O. A. Bogatyreva, N. R. Bogatyrev, A. Bowyer, and A. K. Pahl, "Biomimetics: Its practice and theory," 2006.

[46] O. H. Schmitt, "Some interesting and useful biomimetic transforms," in *Third Int. Biophysics Congress*, vol. 1069, p. 197, 1969.

[47] Y. Bar-Cohen and C. Breazeal, "Biologically inspired intelligent robots," vol. 5051, p. 14, International Society for Optics and Photonics, jul 2003.

[48] N. F. Lepora, P. F. M. J. Verschure, and T. J. Prescott, "The state-of-the-art in biomimetics," *Lecture Notes in Computer Science (including subseries Lecture Notes in Artificial Intelligence and Lecture Notes in Bioinformatics)*, vol. 7375 LNAI, pp. 367–368, 2013.

[49] R. Wood, S. Avadhanula, M. Menon, and R. Fearing, "Microrobotics using composite materials: the micromechanical flying insect thorax," pp. 1842–1849, 2004.

[50] W. Choi, G. M. Whitesides, M. Wang, X. Chen, R. F. Shepherd, A. D. Mazzeo, S. A. Morin, A. A. Stokes, and F. Ilievski, "Multigait soft robot," *Proceedings of the National Academy of Sciences*, vol. 108, no. 51, pp. 20400–20403, 2011.

[51] T. Hirai, K; Hirose, M; Haikawa, Y; Takenaka, "Development of a honda humanoid robot.pdf," pp. 1321–1326, 1998.

[52] E. Mattar, "A survey of bio-inspired robotics hands implementation: New directions in dexterous manipulation," *Robotics and Autonomous Systems*, vol. 61, no. 5, pp. 517–544, 2013.

[53] E. Sahin, "Swarm Robotics: From Sources of Inspiration to Domains of Application," pp. 10–20, Springer, Berlin, Heidelberg, 2010.

[54] D. F. Specht, "Probabilistic neural networks," *Neural Networks*, vol. 3, pp. 109–118, jan 1990.

[55] R. Pfeifer, M. Lungarella, and F. Iida, "Self-organization, embodiment, and biologically inspired robotics," nov 2007.

[56] R. Pfeifer and G. Gomez, "Morphological computation - Connecting brain, body, and environment," in *Lecture Notes in Computer Science (including subseries Lecture Notes in Artificial Intelligence and Lecture Notes in Bioinformatics)*, vol. 5436, pp. 66–83, Springer, Berlin, Heidelberg, 2009.

[57] H. Hauser, A. J. Ijspeert, R. M. Füchslin, R. Pfeifer, and W. Maass, "Towards a theoretical foundation for morphological computation with compliant bodies," *Biological Cybernetics*, vol. 105, pp. 355–370, dec 2011.

[58] V. C. Müller and M. Hoffmann, "What Is Morphological Computation? On How the Body Contributes to Cognition and Control," *Artificial Life*, vol. 23, no. 1, pp. 1–24, 2017.

[59] R. S. Johansson and G. Westling, "Roles of glabrous skin receptors and sensorimotor memory in automatic control of precision grip when lifting rougher or more slippery objects," *Experimental Brain Research*, vol. 56, pp. 550–564, oct 1984.

[60] W. Penfield and E. Boldrey, "Somatic motor and sensory representation in the cerebral cortex of man as studied by electrical stimulation," *Brain*, vol. 60, pp. 389–443, 1937.

[61] L. S. Löken, J. Wessberg, I. Morrison, F. McGlone, and H. Olausson, "Coding of pleasant touch by unmyelinated afferents in humans," *Nature Neuroscience*, vol. 12, pp. 547–548, may 2009.

[62] K. O. Johnson and J. R. Phillips, "Tactile spatial resolution. I. Two-point discrimination, gap detection, grating resolution, and letter recognition," *Journal of Neurophysiology*, vol. 46, pp. 1177–1192, dec 1981.

[63] J. C. Craig, "Grating orientation as a measure of tactile spatial acuity," *Somatosensory and Motor Research*, vol. 16, pp. 197–206, jan 1999.

[64] R. W. Van Boven and K. O. Johnson, "The limit of tactile spatial resolution in humans: Grating orientation discrimination at the lip, tongue, and finger," *Neurology*, vol. 44, pp. 2361–2361, dec 1994.

[65] G. J. Gerling, "SA-I mechanoreceptor position in fingertip skin may impact sensitivity to edge stimuli," *Applied Bionics and Biomechanics*, vol. 7, no. 1, pp. 19–29, 2010.

[66] M. Tremblay and M. Cutkosky, "Estimating friction using incipient slip sensing during a manipulation task," in *[1993] Proceedings IEEE International Conference on Robotics and Automation*, pp. 429–434, IEEE, 1993.

[67] A.-s. Augurelle, A. M. Smith, T. Lejeune, and J.-l. Thonnard, "Importance of Cutaneous Feedback in Maintaining a Secure Grip During Manipulation of Hand-Held Objects," *Journal of Neurophysiology*, vol. 89, no. 2, pp. 665–671, 2003.

[68] J. Scheibert, S. Leurent, A. Prevost, and G. Debrégeas, "The role of fingerprints in the coding of tactile information probed with a biomimetic sensor," *Science*, vol. 323, no. 5920, pp. 1503–1506, 2009.

[69] J. Fraden and J. G. King, "Handbook of Modern Sensors: Physics, Designs, and Applications, 2nd ed.," *American Journal of Physics*, vol. 66, no. 4, pp. 357–359, 2004.

[70] T. Someya, "Bionic skins using flexible organic devices," in *European Solid-State Device Research Conference*, pp. 38–41, IEEE, jan 2014.

[71] H. K. Lee, J. Chung, S. I. Chang, and E. Yoon, "Normal and shear force measurement using a flexible polymer tactile sensor with embedded multiple capacitors," *Journal of Microelectromechanical Systems*, vol. 17, pp. 934–942, aug 2008.

[72] M. R. Cutkosky, R. D. Howe, and W. R. Provancher, "Force and Tactile Sensors," in *Springer Handbook of Robotics*, pp. 455–476, Berlin, Heidelberg: Springer Berlin Heidelberg, 2008.

[73] C. A. Jara, J. Pomares, F. A. Candelas, and F. Torres, "Control framework for dexterous manipulation using dynamic visual servoing and tactile sensors' feedback," *Sensors (Switzerland)*, vol. 14, pp. 1787–1804, jan 2014.

[74] A. Schmitz, P. Maiolino, M. Maggiali, L. Natale, G. Cannata, and G. Metta, "Methods and technologies for the implementation of large-scale robot tactile sensors," *IEEE Transactions on Robotics*, vol. 27, pp. 389–400, jun 2011.

[75] J. R. Flanagan and A. M. Wing, "Modulation of grip force with load force during point-to-point arm movements," *Experimental Brain Research*, vol. 95, pp. 131–143, jul 1993.

[76] D. Göger, N. Gorges, and H. Wörn, "Tactile sensing for an anthropomorphic robotic hand: Hardware and signal processing," in *Proceedings - IEEE International Conference on Robotics and Automation*, pp. 895–901, 2009.

[77] S. Schulz, C. Pylatiuk, A. Kargov, R. Oberle, and G. Bretthauer, "Progress in the development of anthropomorphic fluidic hands for a humanoid robot," in *4th IEEE/RAS International Conference on Humanoid Robots, 2004.*, vol. 2, pp. 566–575, IEEE, 2004.

[78] Syntouch, "BioTac." http://www.syntouchinc.com/en/sensor-technology/. 09/11/18.

[79] N. Wettels and G. E. Loeb, "Haptic feature extraction from a biomimetic tactile sensor: Force, contact location and curvature," in *2011 IEEE International Conference on Robotics and Biomimetics, ROBIO 2011*, pp. 2471–2478, IEEE, dec 2011.

[80] Y. Tenzer, L. P. Jentoft, and R. D. Howe, "The feel of MEMS barometers: Inexpensive and easily customized tactile array sensors," *IEEE Robotics and Automation Magazine*, vol. 21, no. 3, pp. 89–95, 2014.

[81] T. Zhang, H. Liu, L. Jiang, S. Fan, and J. Yang, "Development of a flexible 3-D tactile sensor system for anthropomorphic artificial hand," *IEEE Sensors Journal*, vol. 13, pp. 510–518, feb 2013.

[82] S. Begej, "Planar and Finger-Shaped Optical Tactile Sensors for Robotic Applications," *IEEE Journal on Robotics and Automation*, vol. 4, no. 5, pp. 472–484, 1988.

[83] M. Mehdian, S. M. Vaezi-Nejad, and I. Shams, "Optical tactile sensor for robots," *International Journal of Electronics*, vol. 76, no. 5, pp. 821–827, 1994.

[84] D. Hristu, N. Ferrier, and R. Brockett, "The performance of a deformable-membrane tactile sensor: basic results on geometrically-defined tasks," in *Proceedings 2000 ICRA. Millennium Conference. IEEE International Conference on Robotics and Automation. Symposia Proceedings (Cat. No.00CH37065)*, vol. 1, pp. 508–513, IEEE, 2000.

[85] K. Kamiyama, H. Kajimoto, N. Kawakami, and S. Tachi, "Evaluation of a vision-based tactile sensor," in *Robotics and Automation, 2004. Proceedings. ICRA '04. 2004 IEEE International Conference on*, vol. 2, pp. 1542–1547 Vol.2, IEEE, 2004.

[86] P. Lang, "Optical Tactile Sensors for Medical Palpation Pencilla Lang," 2004.

[87] R. Li and E. H. Adelson, "Sensing and Recognizing Surface Textures Using a GelSight Sensor," in *2013 IEEE Conference on Computer Vision and Pattern Recognition*, pp. 1241–1247, jun 2013.

[88] E. Donlon, S. Dong, M. Liu, J. Li, E. Adelson, and A. Rodriguez, "GelSlim: A High-Resolution, Compact, Robust, and Calibrated Tactile-sensing Finger," 2018.

[89] L. Zou, C. Ge, Z. J. Wang, E. Cretu, and X. Li, "Novel tactile sensor technology and smart tactile sensing systems: A review," nov 2017.

[90] J. A. Fishel and G. E. Loeb, "Bayesian exploration for intelligent identification of textures," *Frontiers in Neurorobotics*, no. JUNE, pp. 1–20, 2012.

[91] M. Schöpfer, M. Pardowitz, R. Haschke, and H. Ritter, "Identifying relevant tactile features for object identification," *Springer Tracts in Advanced Robotics*, vol. 76, no. STAR, pp. 417–430, 2012.

[92] M. Madry, L. Bo, D. Kragic, and D. Fox, "ST-HMP: Unsupervised Spatio-Temporal feature learning for tactile data," *Proceedings - IEEE International Conference on Robotics and Automation*, pp. 2262–2269, 2014.

[93] K. S. Sohn, J. Chung, M. Y. Cho, S. Timilsina, W. B. Park, M. Pyo, N. Shin, K. Sohn, and J. S. Kim, "An extremely simple macroscale electronic skin realized by deep machine learning," *Scientific Reports*, vol. 7, no. 1, 2017.

[94] W. Yuan, C. Zhu, A. Owens, M. A. Srinivasan, and E. H. Adelson, "Shape-independent hardness estimation using deep learning and a GelSight tactile sensor," in *Proceedings - IEEE International Conference on Robotics and Automation*, pp. 951–958, IEEE, may 2017.

[95] A. J. Spiers, M. V. Liarokapis, B. Calli, and A. M. Dollar, "Single-Grasp Object Classification and Feature Extraction with Simple Robot Hands and Tactile Sensors," *IEEE Transactions on Haptics*, vol. 9, pp. 207–220, apr 2016.

[96] T. Bhattacharjee, J. M. Rehg, and C. C. Kemp, "Haptic classification and recognition of objects using a tactile sensing forearm," *IEEE International Conference on Intelligent Robots and Systems*, pp. 4090–4097, 2012.

[97] D. Xu, G. E. Loeb, and J. A. Fishel, "Tactile identification of objects using Bayesian exploration," in *Proceedings - IEEE International Conference on Robotics and Automation*, pp. 3056–3061, IEEE, may 2013.

[98] P. Dallaire, P. Giguère, D. Émond, and B. Chaib-Draa, "Autonomous tactile perception: A combined improved sensing and Bayesian nonparametric approach," *Robotics and Autonomous Systems*, vol. 62, pp. 422–435, apr 2014.

[99] N. F. Lepora, U. Martinez-Hernandez, H. Barron-Gonzalez, M. Evans, G. Metta, and T. J. Prescott, "Embodied hyperacuity from Bayesian perception: Shape and position discrimination with an iCub fingertip sensor," in *IEEE International Conference on Intelligent Robots and Systems*, pp. 4638–4643, 2012.

[100] U. Martinez-Hernandez, G. Metta, T. J. Dodd, T. J. Prescott, L. Natale, and N. F. Lepora, "Active contour following to explore object shape with robot touch," in *2013 World Haptics Conference, WHC 2013*, pp. 341–346, IEEE, apr 2013.

[101] S. S. Baishya and B. Bäuml, "Robust material classification with a tactile skin using deep learning," in *IEEE International Conference on Intelligent Robots and Systems*, vol. 2016-Novem, pp. 8–15, IEEE, oct 2016.

[102] A. Schmitz, Y. Bansho, K. Noda, H. Iwata, T. Ogata, and S. Sugano, "Tactile object recognition using deep learning and dropout," in *IEEE-RAS International Conference on Humanoid Robots*, vol. 2015-Febru, pp. 1044–1050, IEEE, nov 2015.

[103] R. R. Ma and A. M. Dollar, "On dexterity and dexterous manipulation," *IEEE 15th International Conference on Advanced Robotics: New Boundaries for Robotics, ICAR 2011*, pp. 1–7, 2011.

[104] A. Okamura, N. Smaby, and M. Cutkosky, "An overview of dexterous manipulation," *Proceedings 2000 ICRA. Millennium Conference. IEEE International Conference on Robotics and Automation. Symposia Proceedings (Cat. No.00CH37065)*, vol. 1, pp. 255–262.

[105] A. Bicchi, "Hands for dexterous manipulation and robust grasping: A difficult road toward simplicity," *IEEE Transactions on Robotics and Automation*, vol. 16, no. 6, pp. 652–662, 2000.

[106] Z. Li, J. Canny, and S. Sastry, "On motion planning for dexterous manipulation. I. The problem formulation," in *Proceedings, 1989 International Conference on Robotics and Automation*, pp. 775–780, IEEE Comput. Soc. Press, 1989.

[107] R. S. Johansson and J. R. Flanagan, "Coding and use of tactile signals from the fingertips in object manipulation tasks," *Nature Reviews Neuroscience*, vol. 10, pp. 345–359, may 2009.

[108] N. Rojas, R. R. Ma, and A. M. Dollar, "The GR2 Gripper: An Underactuated Hand for Open-Loop In-Hand Planar Manipulation," *IEEE Transactions on Robotics*, vol. 32, no. 3, pp. 763–770, 2016.

[109] ROBOTIS, "Hand RH-P12-RN." http://www.robotis.us/robotis-hand-rh-p12-rn/. 2019-02-15.

[110] L. U. Odhner, R. R. Ma, and A. M. Dollar, "Open-loop precision grasping with underactuated hands inspired by a human manipulation strategy," *IEEE Transactions on Automation Science and Engineering*, vol. 10, no. 3, pp. 625–633, 2013.

[111] R. Kohout, R. D. Howe, A. M. Dollar, L. U. Odhner, L. P. Jentoft, M. R. Claffee, N. Corson, Y. Tenzer, R. R. Ma, and M. Buehler, "A compliant, underactuated hand for robust manipulation," *The International Journal of Robotics Research*, vol. 33, no. 5, pp. 736–752, 2014.

[112] Yale, "OpenHand Project." https://www.eng.yale.edu/grablab/openhand/. 2019-01-31.

[113] Shadow Robot Company, "Shadow Dexterous Hand Technical Specification." https://www.shadowrobot.com/wp-content/uploads/shadow_dexterous_hand_technical_specification_E_20150827.pdf, 2015.
2019-02-15.

[114] H. Kawasaki, T. Komatsu, and K. Uchiyama, "Dexterous anthropomorphic robot hand with distributed tactile sensor: Gifu hand II," *IEEE/ASME Transactions on Mechatronics*, vol. 7, no. 3, pp. 296–303, 2002.

[115] M. G. Catalano, G. Grioli, E. Farnioli, A. Serio, C. Piazza, and A. Bicchi, "Adaptive synergies for the design and control of the Pisa/IIT SoftHand," *International Journal of Robotics Research*, vol. 33, no. 5, pp. 768–782, 2014.

[116] C. D. Santina, C. Piazza, G. Grioli, M. G. Catalano, and A. Bicchi, "Toward Dexterous Manipulation With Augmented Adaptive Synergies: The Pisa/IIT SoftHand 2," *IEEE Transactions on Robotics*, vol. PP, pp. 1–16, 2018.

[117] R. Deimel and O. Brock, "A novel type of compliant and underactuated robotic hand for dexterous grasping," *International Journal of Robotics Research*, vol. 35, no. 1-3, pp. 161–185, 2016.

[118] M. R. Williams and W. Walter, "Development of a prototype over-actuated biomimetic prosthetic hand," *PLoS ONE*, vol. 10, p. e0118817, mar 2015.

[119] A. M. Dollar and R. D. Howe, "The highly adaptive SDM hand: Design and performance evaluation," in *International Journal of Robotics Research*, vol. 29, pp. 585–597, 2010.

[120] Shadow Robot Company, "Agile Grasper Documentation." https://agile-grasper.readthedocs.io/en/latest/.
2019-01-31.

[121] Barrett, "Barrett Hand Technical Specification." https://web.barrett.com/files/BarrettHandSpecs.pdf.
2019-10-16.

[122] Kinova, "Grippers KG-2 and KG-3, Accessories for robotic arms." https://www.kinovarobotics.com/en/products/accessories/grippers.
2019-02-21.

[123] L. U. Odhner, R. R. Ma, and A. M. Dollar, "Exploring Dexterous Manipulation Workspaces with the iHY Hand," *Journal of the Robotics Society of Japan*, vol. 32, no. 4, pp. 318–322, 2014.

[124] J. Butterfass, M. Grebenstein, H. Liu, and G. Hirzinger, "DLR-Hand II: next generation of a dextrous robot hand," pp. 109–114, 2002.

[125] OpenAI, M. Andrychowicz, B. Baker, M. Chociej, R. Jozefowicz, B. McGrew, J. Pachocki, A. Petron, M. Plappert, G. Powell, A. Ray, J. Schneider, S. Sidor, J. Tobin, P. Welinder, L. Weng, and W. Zaremba, "Learning Dexterous In-Hand Manipulation," 2018.

[126] SCHUNK, "5-Fingerhand SVH." https://schunk.com/gb_en/gripping-systems/series/schunk-5-fingerhand-svh/.
2019-04-02.

[127] A. B. Swanson, I. B. Matev, and G. de Groot, "The strength of the hand," *Applied Ergonomics*, vol. 3, no. 4, p. 241, 2005.

[128] Eaton Hand, "Interesting facts about hands." http://www.eatonhand.com/hw/facts.htm.
2019-02-21.

[129] TeachMeAnatomy, "The Upper Limb." https://teachmeanatomy.info/upper-limb/.
2019-02-22.

[130] R. Fearing, "Implementing a force strategy for object re-orientation," pp. 96–102, 1986.

[131] D. Rus, "In-Hand Dexterous Manipulation of 3D Objects," *The International Journal of Robotics Research*, vol. 18, pp. 355–381, 1999.

[132] A. Bicchi and R. Sorrentino, "Dexterous manipulation through rolling," pp. 452–457, 1995.

[133] J. Shi, J. Z. Woodruff, P. B. Umbanhowar, and K. M. Lynch, "Dynamic In-Hand Sliding Manipulation," *IEEE Transactions on Robotics*, vol. 33, no. 4, pp. 778–795, 2017.

[134] N. Chavan-Dafle and A. Rodriguez, "Sampling-based Planning of In-Hand Manipulation with External Pushes," 2017.

[135] N. C. Dafle, A. Rodriguez, R. Paolini, B. Tang, S. S. Srinivasa, M. Erdmann, M. T. Mason, I. Lundberg, H. Staab, and T. Fuhlbrigge, "Extrinsic dexterity: In-hand manipulation with external forces," in *Proceedings - IEEE International Conference oBristoln Robotics and Automation*, pp. 1578–1585, IEEE, may 2014.

[136] L. Han and J. C. Trinkle, "Dextrous manipulation by rolling and finger gaiting," in *Proceedings - IEEE International Conference on Robotics and Automation*, vol. 1, pp. 730–735, IEEE, 1998.

[137] V. Kumar, A. Gupta, E. Todorov, and S. Levine, "Learning Dexterous Manipulation Policies from Experience and Imitation," 2016.

[138] C. Ott, O. Eiberger, W. Friedl, B. Bäuml, U. Hillenbrand, C. Borst, A. Albu-Schäffer, B. Brunner, H. Hirschmüller, S. Kielhöfer, R. Konietschke, M. Suppa, T. Wimböck, F. Zacharias, and G. Hirzinger, "A humanoid two-arm system for dexterous manipulation," *Proceedings of the 2006 6th IEEE-RAS International Conference on Humanoid Robots, HUMANOIDS*, pp. 276–283, 2006.

[139] H. Yousef, M. Boukallel, and K. Althoefer, "Tactile sensing for dexterous in-hand manipulation in robotics - A review," 2011.

[140] H. Van Hoof, T. Hermans, G. Neumann, and J. Peters, "Learning robot in-hand manipulation with tactile features," in *IEEE-RAS International Conference on Humanoid Robots*, vol. 2015-Decem, pp. 121–127, IEEE, nov 2015.

[141] M. Li, Y. Bekiroglu, D. Kragic, and A. Billard, "Learning of grasp adaptation through experience and tactile sensing," in *IEEE International Conference on Intelligent Robots and Systems*, pp. 3339–3346, IEEE, sep 2014.

[142] M. Li, H. Yin, K. Tahara, and A. Billard, "Learning object-level impedance control for robust grasping and dexterous manipulation," in *Proceedings - IEEE International Conference on Robotics and Automation*, pp. 6784–6791, IEEE, may 2014.

[143] C. Chorley, C. Melhuish, T. Pipe, and J. Rossiter, "Development of a Tactile Sensor Based on Biologically Inspired Edge Encoding," in *International Conference on Advanced Robotics*, pp. 1–6, IEEE, 2009.

[144] B. Winstone, G. Griffiths, C. Melhuish, T. Pipe, and J. Rossiter, "TACTIP - Tactile fingertip device, challenges in reduction of size to ready for robot hand integration," in *2012 IEEE International Conference on Robotics and Biomimetics, ROBIO 2012 - Conference Digest*, pp. 160–166, IEEE, 2012.

[145] T. Assaf, C. Roke, J. Rossiter, T. Pipe, and C. Melhuish, "Seeing by touch: Evaluation of a soft biologically-inspired artificial fingertip in real-time active touch," *Sensors (Switzerland)*, vol. 14, no. 2, pp. 2561–2577, 2014.

[146] N. F. Lepora and B. Ward-Cherrier, "Superresolution with an optical tactile sensor," in *IEEE International Conference on Intelligent Robots and Systems*, vol. 2015-Decem, pp. 2686–2691, IEEE, 2015.

[147] Techsil, "RTV27905 CLEAR GEL." https://www.techsil.co.uk/media/pdf/TDS/TESI19128-tds.pdf.
09/11/18.

[148] Mircrosoft, "LifeCam Cinema Datasheet." https://www.microsoft.com/accessories/en-gb/products/webcams/lifecam-cinema/h5d-00014#specsColumns-testCarousel.
09/11/2018.

[149] K. Shimoga and A. Goldenberg, "Soft materials for robotic fingers," in *Proceedings 1992 IEEE International Conference on Robotics and Automation*, pp. 1300–1305, IEEE Comput. Soc. Press, 1992.

[150] EnvisionTEC, "Perfactory Family Archives." https://envisiontec.com/3d-printers/perfactory-family/.
2019-03-12.

[151] C. M. Oddo, M. Controzzi, L. Beccai, C. Cipriani, and M. C. Carrozza, "Roughness encoding for discrimination of surfaces in artificial active-touch," *IEEE Transactions on Robotics*, vol. 27, no. 3, pp. 522–533, 2011.

[152] B. Winstone, G. Griffiths, T. Pipe, C. Melhuish, and J. Rossiter, "TACTIP - Tactile fingertip device, texture analysis through optical tracking of skin features," in *Lecture Notes in Computer Science (including subseries Lecture Notes in Artificial Intelligence and Lecture Notes in Bioinformatics)*, vol. 8064 LNAI, pp. 323–334, Springer, 2013.

[153] S. Salehi, J. J. Cabibihan, and S. G. Sam, "Artificial skin ridges enhance local tactile shape discrimination," *Sensors*, vol. 11, no. 9, pp. 8626–8642, 2011.

[154] G. J. Gerling and G. W. Thomas, "The effect of fingertip microstructures on tactile edge perception," in *Proceedings - 1st Joint Eurohaptics Conference and Symposium on Haptic Interfaces for Virtual Environment and Teleoperator Systems; World Haptics Conference, WHC 2005*, pp. 63–72, 2005.

[155] N. Cauna, "Nature and functions of the papillary ridges of the digital skin," *The Anatomical Record*, vol. 119, no. 4, pp. 449–468, 1954.

[156] L. A. Jones and S. J. Lederman, *Human Hand Function Abstract and Keywords*.
No. November 2012, Oxford University Press, 2006.

[157] U. Martinez-Hernandez, "Tactile Sensors," *Scholarpedia*, vol. 10, no. 4, p. 32398, 2015.

[158] N. F. Lepora, U. Martinez-Hernandez, M. Evans, L. Natale, G. Metta, and T. J. Prescott, "Tactile Superresolution and Biomimetic Hyperacuity," *IEEE Transactions on Robotics*, vol. 31, no. 3, pp. 605–618, 2015.

[159] N. F. Lepora and B. Ward-Cherrier, "Tactile Quality Control with Biomimetic Active Touch," in *IEEE Robotics and Automation Letters*, vol. 1, pp. 646–652, 2016.

[160] A. W. Goodwin and H. E. Wheat, "Sensory Signals in Neural Populations Underlying Tactile Perception and Manipulation," *Annual Review of Neuroscience*, vol. 27, pp. 53–77, jul 2004.

[161] R. Bajcsy, "Active perception.," tech. rep., 1988.

[162] J. Gibson, "Kick the bar chart habit," *Nature Methods*, 1966.

[163] T. J. Prescott, M. E. Diamond, and A. M. Wing, "Active touch sensing," *Philosophical Transactions of the Royal Society B: Biological Sciences*, vol. 366, no. 1581, pp. 2989–2995, 2011.

[164] N. F. Lepora, "Active tactile perception," *Scholarpedia*, vol. 10, no. 3, p. 32364, 2015.

[165] Z. Su, J. A. Fishel, T. Yamamoto, and G. E. Loeb, "Use of tactile feedback to control exploratory movements to characterize object compliance," *Frontiers in Neurorobotics*, vol. 6, no. JULY, pp. 1–9, 2012.

[166] N. F. Lepora, U. Martinez-Hernandez, and T. J. Prescott, "Active touch for robust perception under position uncertainty," in *Proceedings - IEEE International Conference on Robotics and Automation*, pp. 3020–3025, IEEE, 2013.

[167] Z. Pezzementi, E. Plaku, C. Reyda, and G. D. Hager, "Tactile-object recognition from appearance information," *IEEE Transactions on Robotics*, vol. 27, no. 3, pp. 473–487, 2011.

[168] J. M. Romano, K. Hsiao, G. Niemeyer, S. Chitta, and K. J. Kuchenbecker, "Human-inspired robotic grasp control with tactile sensing," *IEEE Transactions on Robotics*, vol. 27, no. 6, pp. 1067–1079, 2011.

[169] H. Liu, K. C. Nguyen, V. Perdereau, J. Bimbo, J. Back, M. Godden, L. D. Seneviratne, and K. Althoefer, "Finger contact sensing and the application in dexterous hand manipulation," *Autonomous Robots*, vol. 39, no. 1, pp. 25–41, 2015.

[170] H. Zhang and N. N. Chen, "Control of contact via tactile sensing," *IEEE Transactions on Robotics and Automation*, vol. 16, no. 5, pp. 482–495, 2000.

[171] M. C. Koval, N. S. Pollard, and S. S. Srinivasa, "Pose estimation for planar contact manipulation with manifold particle filters," *International Journal of Robotics Research*, vol. 34, no. 7, pp. 922–945, 2015.

[172] E. Knoop and J. Rossiter, "Dual-mode compliant optical tactile sensor," in *Proceedings - IEEE International Conference on Robotics and Automation*, pp. 1006–1011, 2013.

[173] N. F. Lepora, J. C. Sullivan, B. Mitchinson, M. Pearson, K. Gurney, and T. J. Prescott, "Brain-inspired Bayesian perception for biomimetic robot touch," in *Proceedings - IEEE International Conference on Robotics and Automation*, pp. 5111–5116, IEEE, 2012.

[174] N. F. Lepora, C. W. Fox, M. H. Evans, M. E. Diamond, K. Gurney, and T. J. Prescott, "Optimal decision-making in mammals: Insights from a robot study of rodent texture discrimination," *Journal of the Royal Society Interface*, vol. 9, no. 72, pp. 1517–1528, 2012.

[175] B. Ward-Cherrier, N. Rojas, and N. F. Lepora, "Model-Free Precise in-Hand Manipulation with a 3D-Printed Tactile Gripper," *IEEE Robotics and Automation Letters*, vol. 2, pp. 2056–2063, oct 2017.

[176] R. Li, R. Platt, W. Yuan, A. Ten Pas, N. Roscup, M. A. Srinivasan, and E. Adelson, "Localization and manipulation of small parts using GelSight tactile sensing," in *IEEE International Conference on Intelligent Robots and Systems*, pp. 3988–3993, 2014.

[177] J. Back, P. Dasgupta, L. Seneviratne, K. Althoefer, and H. Liu, "Feasibility study- novel optical soft tactile array sensing for minimally invasive surgery," in *IEEE International Conference on Intelligent Robots and Systems*, vol. 2015-Decem, pp. 1528–1533, 2015.

[178] F. Aurenhammer, "Voronoi diagrams—a survey of a fundamental geometric data structure," *ACM Computing Surveys*, vol. 23, no. 3, pp. 345–405, 1991.

[179] G. H. Büscher, R. Kõiva, C. Schürmann, R. Haschke, and H. J. Ritter, "Flexible and stretchable fabric-based tactile sensor," *Robotics and Autonomous Systems*, vol. 63, no. P3, pp. 244–252, 2015.

[180] B. Delhaye, P. Lefèvre, and J. L. Thonnard, "Dynamics of fingertip contact during the onset of tangential slip," *Journal of the Royal Society Interface*, vol. 11, no. 100, pp. 20140698–20140698, 2014.

[181] R. Koiva, M. Zenker, C. Schurmann, R. Haschke, and H. J. Ritter, "A highly sensitive 3D-shaped tactile sensor," *2013 IEEE/ASME International Conference on Advanced Intelligent Mechatronics: Mechatronics for Human Wellbeing, AIM 2013*, pp. 1084–1089, 2013.

[182] J. Bimbo, S. Luo, K. Althoefer, and H. Liu, "In-Hand Object Pose Estimation Using Covariance-Based Tactile To Geometry Matching," *IEEE Robotics and Automation Letters*, vol. 1, no. 1, pp. 570–577, 2016.

[183] G. Cannata, S. Denei, and F. Mastrogiovanni, "A framework for representing interaction tasks based on tactile data," in *Proceedings - IEEE International Workshop on Robot and Human Interactive Communication*, pp. 698–703, 2010.

[184] B. Winstone, C. Melhuish, T. Pipe, M. Callaway, and S. Dogramadzi, "Toward Bio-Inspired Tactile Sensing Capsule Endoscopy for Detection of Submucosal Tumors," *IEEE Sensors Journal*, vol. 17, no. 3, pp. 848–857, 2017.

[185] M. A. Erdmann and M. T. Mason, "An Exploration of Sensorless Manipulation," *IEEE Journal on Robotics and Automation*, vol. 4, no. 4, pp. 369–379, 1988.

[186] E. Hyttinen, D. Kragic, and R. Detry, "Learning the tactile signatures of prototypical object parts for robust part-based grasping of novel objects," in *Proceedings - IEEE International Conference on Robotics and Automation*, vol. 2015-June, pp. 4927–4932, IEEE, may 2015.

[187] J. Kwiatkowski, D. Cockburn, and V. Duchaine, "Grasp stability assessment through the fusion of proprioception and tactile signals using convolutional neural networks," in *Intelligent Robots and Systems (IROS), 2017 IEEE/RSJ International Conference on*, pp. 286–292, IEEE, sep 2017.

[188] J. W. James, N. Pestell, and N. F. Lepora, "Slip Detection With a Biomimetic Tactile Sensor," *IEEE Robotics and Automation Letters*, vol. 3, pp. 3340–3346, oct 2018.